UNIVERSITA' DEGLI STUDI DI NAPOLI

"FEDERICO II"

Scuola politecnica e delle scienze di base

Area didattica Scienze Matematiche, Fisiche e Naturali

Dottorato di Ricerca in Biologia

(**XXX CICLO**)

Effetti del p,p-DDE sullo stress ossidativo in tessuti di ratto e cellule in coltura. Studio della variazione della dinamica mitocondriale *in vitro*.

Effects of p,p-DDE on the oxidative stress in rat tissues and in cell cultures. Study of the mitochondrial dynamics variations *in vitro*.

Coordinatore :

Prof. Salvatore Cozzolino

Dottorando:

Dr. Migliaccio Vincenzo

Tutore:

Prof.ssa Rosaria Scudiero

Anno accademico 2016-2017

INDEX

Summary

Introduction. Exposure to environmental contaminants is one of the most associated risk factors for health damage. The most well-known and harmful synthetic molecules introduced in the environment are the pesticides. Acts to reduce the infectious risk on plants, animals and humans, the pesticides can cause a variety of toxic effects due to ingestion, contact direct with skin or by their entry into the body through the respiratory tract. The toxicity of these substances also depends by their ability to persist in the environment. In fact, the persistent substances are subject to bioaccumulation and biomagnification phenomena in the food chain. For example, Dichlorodiphenyltrichloroethane (DDT) and its metabolites go against to these processes.

Aim of project. The purpose of this work was done to evaluate the effects of the Dichlorodiphenyldichloroethylene (p,p-DDE), the first metabolite of p,p-DDT, in male *Wistar* rats for 4 weeks of treatment at a dose of 10 mg / Kg b.w. Since p,p-DDE is a lipophilic organic pesticide, its effects were also monitored in association with a diet rich in saturated fatty acids. Four experimental groups were studied: N (Normal Diet); D (High-Fat Diet, 45% saturated); N + DDE (Normal Diet + p,p-DDE 10 mg / Kg b.w.); D + DDE (High-Fat Diet, 45% saturated, + p,p-DDE 10 mg / Kg b.w). The analyzes were conducted *in vivo* on three different organs (testis, kidney and liver) and *in vitro* on the experimental model of human hepatocarcinoma cell (Huh7).

Results. ***In vivo***

Testis: Morphological alteration in some tubules, in their distal part, in D group; release of non-differentiated cells in both groups in presence of p,p-DDE; positives spermatogonia to cleaved caspase 3 in group D were found; spermatogonia, spermatocytes and spermatidis positives to cleaved caspase 3 in presence of the pesticide were observed. Probably, the activation of the apoptotic pathway is started by mitochondria. This hypothesis was formulated because in both DDE-treated groups there is an increase of Bak and BAX proteins (regulated by p53 incremented levels) when there is a need to activate cell death. Down-regulation of MTs, particularly significant in the N + DDE group. Activation of the antioxidant enzymes (SOD1 / 2, GPX1) especially in the N + DDE group, indicating a major effect of DDE on the oxidative stress generation in absence of saturated fats. Increased cell proliferation in all groups, most significant in the N + DDE group, probably to mitigate the negative effects on testis due to the apoptotic stimuli.

Kidney: Morphological alteration on the tubule-proximal component in presence of saturated fats accumulated in the cells; epithelial-tubular erosion in N + DDE with some damage on the glomerular component; peritubular collagen deposition in presence of p, p-DDE and recruitment of macrophages; activation of the antioxidant system in the enzyme component analyzed (SOD1 / 2 and GPX1) and up-regulation of reticular chaperones (Grp78 and Grp75); Up-regulation of MT and nuclear translocation particularly in the presence of pesticides to protect DNA from oxidative stress and ensure the transport of useful metals during the transcriptional processes.

Liver: Accumulation of fatty acids in Group D and cellular vacuolization in the presence of pesticide were observed; mitochondrial superoxide anion production in all experimental groups vs. N; accumulation of lipid peroxides in presence of p,p-DDE (D + DDE, N + DDE); mitochondrial decoupling and up-regulation of the antioxidant system (SOD1 / 2, GPX1); increase of mitochondrial BAX and release of cytochrome c from mitochondria in the p,p-DDE treated groups; activation of caspase 3, bulging of the endoplasmic reticulum cisterns and increased levels of Grp78; MT down-regulation associated to their nuclear translocation in all experimental groups vs N; recruitment of macrophages in the tissue to eliminate cells death.

Results. ***In vitro***

Huh7. Cells treated with pesticide exhibit increased levels of mitochondrial superoxide anion and hydrogen peroxide. Decrease of mitochondrial membrane potential and ATP synthesis were observed, indicating that p,p-DDE play a role in the mitochondrial disease generation. Additionally, mitochondria vary in their dynamics by fragmenting and assuming donut morphology. Marker of apoptosis were measured by western blotting analyses indicating activation of mitochondrial apoptotic pathway after 24h of exposition to pesticide.

Conclusions: Our results indicate that p, p-DDE generates both *in vivo* and *in vitro* oxidative stress. *In vivo*, at the dose and time used, buffer systems are activated to control tissue physiology; *In vitro*, mitochondrial damage activates cellular apoptosis (similarly to what was observed in the liver of rat model).

Riassunto

Introduzione. L'esposizione ai contaminanti ambientali è uno dei fattori di rischio maggiormente associato a danni per la salute. Le più note e dannose molecole di sintesi, immesse nell'ambiente dall'uomo, sono i pesticidi. Atti alla scopo di ridurre il rischio infettivo generato da vettori di infezione di piante, animali ed uomo, i pesticidi possono generare una serie di effetti tossici dovuti all'ingestione, al contatto con la pelle o al loro ingresso nell'organismo tramite le vie respiratorie. La tossicità della sostanza dipende altresì dalla sua capacità di persistere nell'ambiente. Infatti, le sostanze maggiormente persistenti sono soggette ad accumulo e biomagnificazione nella catena alimentare. Lo sono ad esempio i policlorobifenili (PCBs) a cui appartiene il Diclorodifeniltricloroetano (p,p-DDT) con tutti i suoi metaboliti.

Scopo del lavoro. Lo scopo di questo lavoro è stato proprio quello di valutare gli effetti del Diclorodifenildicloroetene (p,p-DDE) in ratti maschi di 2 mesi, per 4 settimane di trattamento alla dose di 10mg/Kg p.c. Essendo il p,p-DDE un pesticida organico di natura lipofila, è stato monitorato il suo effetto in associazione e non ad una dieta ricca in grassi saturi. Quattro sono stati i gruppi sperimentali studiati: N (Dieta normale); D(dieta ad alto contenuto in grassi, 45% saturi); N+DDE (dieta normale + p,p-DDE 10mg/Kg p.c.); D+DDE (dieta ad alto contenuto in grassi, 45% saturi, + p,p-DDE 10mg/Kg p.c.). Le analisi sono state condotte *in vivo* su tre organi (Testicolo, Rene e Fegato) ed *in vitro* sul modello sperimentale di epatocarcinoma umano (Huh7).

Risultati. *In vivo*

Testicolo: Alterazione morfologica a carico di alcuni tubuli, nella loro parte distale, nel gruppo D; rilascio di cellule non differenziate nei gruppi in presenza di p,p-DDE; spermatogoni positivi alla caspasi 3 nel gruppo D; spermatogoni, spermatociti e spermatidi postivi alla caspasi 3 in presenza del pesticida. Probabilmente, l'attivazione della via apoptotica è innescata dai mitocondri in quanto in presenza di DDE si osserva aumento delle proteine Bak e BAX (regolate dall'aumento dei livelli di p53) quando c'è necessità di innescare la morte cellulare. Down-regulation delle MT, in maniera particolarmente significativa nel gruppo N+DDE. Attivazione del sistema antiossidante in tutte le sue componenti analizzate (SOD1/2, GPX1) in particolar modo nel gruppo N+DDE, indicando un effetto maggioritario del DDE sullo stress ossidativo in assenza di grassi saturi. Aumento della proliferazione cellulare in tutti i gruppi, maggiormente significativa nel gruppo N+DDE, probabilmente per contrastare il fenomeno apoptotico.

Rene: Alterazione morfologica a carico della componente tubulo-prossimale in presenza di grassi saturi per accumulo di grasso; sfaldamento epitelio-tubulare in N+DDE con qualche danno alla componete dei glomeruli; deposizione peritubulare di collageno in presenza di p,p-DDE e reclutamento di macrofagi; attivazione del sistema antiossidante nella componente enzimatica analizzata (SOD1/2 e GPX1) e up-regolazione di chaperones reticolari (Grp78 e Grp75); Up-regulation delle MT e traslocazione nucleare in particolar modo in presenza del pesticida per proteggere il DNA dallo stress ossidativo e garantire il trasporto di metalli utili durante i processi di trascrizione.

Fegato: Accumulo di grasso nel gruppo D e vacuolizzazione cellulare in presenza del pesticida; produzione mitocondriale di anione superossido in tutti i gruppi sperimentali vs N; accumulo di perossidi lipidici in presenza di p,p-DDE (D+DDE, N+DDE); disaccoppiamento mitocondriale e up-regolazione del sistema antiossidante (SOD1/2, GPX1); aumento di BAX mitocondriale e rilascio di citocromo c dai mitocondri nei gruppi trattati con pesticida; attivazione della caspasi 3, bulging delle creste del reticolo endoplasmatico ed aumento dei livelli di Grp78; Down-regulation delle MT con traslocazione nucleare in tutti i gruppi trattati, probabilmente per proteggere il DNA dallo stress ossidativo; reclutamento di macrofagi nel tessuto per eliminare le cellule in fase di morte programmata.

Risultati. *In vitro*

Huh7. Le cellule trattate con il pesticida esibiscono aumentati livelli di anione superossido mitocondriale e perossido di idrogeno. La diminuzione del potenziale di membrana e dell'ATP prodotte indicano un ruolo del p,p-DDE nella generazione del danno mitocondriale. Accanto a ciò, i mitocondri variano la loro dinamica frammentandosi e assumendo morfologia a ciambella e viene attivato il pathway apoptotico mediato dalla via mitocondriale dopo 24 h di esposizione al pesticida.

Conclusioni: Tali risultati indicano che il p,p-DDE genera sia *in vivo* che *in vitro* stress ossidativo. *In vivo*, alla dose e tempo utilizzati, sono attivati sistemi tampone per controllare la fisiologia tissutale; *in vitro*, il danno mitocondriale attiva l'apoptosi cellulare similmente a quanto osservato a livello epatico nel modello sperimentale di ratto.

INTRODUCTION

Polychlorinated biphenyls, known also as PCBs, are a class of organic chlorine compounds with chemical formula $C_{12}H_{10-x}Cl_x$. At this class of chemicals, are also associated the organochlorinated insecticides such as DDT and its metabolites. Technically, DDT is a white powder consisting of a mixture of three different isomers, the largest of which is represented by p, p-DDT (p,p'-DDT (85%), o,p'-DDT (15%), and o,o'-DDT (trace amounts))[1]. Already in 1943, the DDT was used as insecticide. It has been used for the control of different disease vectors (anopheles mosquitoes, phlebotomies, fleas) that which carry different parasites that cause pathologies such as malaria, yellow fever and typhus[2]. Its utilization was extended in the agriculture, to control parasites of plants, because DDT has a wide spectrum of activity for the insects[3]. Today, its utilization is restricted to equatorial counties to control disease vectors and where malaria is still endemic[4]. In North America, Asia and Europe DDT in 1979, because its toxicity was been demonstrate. DDT and its metabolites, in particular p,p-DDE, are included in the environmental persistent organic pollutants (POPs) with androgen antagonist activity[5]. They undergo to bioaccumulation and biomagnification phenomena causing different problems for the organisms that experiments their presence in the environmental matrix. Exposure to these substances may occur in different way. Firstly, during the synthesis is possible undergo to acute effects due to high dose exposition. The most common exposition, however, is the result residual levels on the environmental water particulate, in water sediments, and in the foods[6]. The International Agency for Research on Cancer (IARC), introduces DDT in the potentially carcinogenic compounds for human[7]. In fact, in relationship to the dose of exposition, was found a correlation to different lymphomas, increase risk to leukemia and probable correlation to lung cancer and respiratory deficit in case-controls studies[8]. Other studies, correlate p,p-DDE (a metabolite very persistent of p,p-DDT) with an increase tendency to liver cancer development in female and male mice[9]. In addition, some studies in vitro conducted in presence of p,p-DDE correlate this metabolite of p,p-DDT with chromosomal aberrations and with inhibition of gap-junctional intercellular communication generating metabolic injury and dysfunctions[10]. Since p,p-DDT and its metabolites cause oxidative stress in different organism, such as marines species[11] rodent culture cells[12] and animals[13] in my studies conducted on male Wistar rats, I evaluate the effects of the p,p-DDE oral administration (10mg/Kg b.w. daily), using a short treatment period (4 weeks). My investigation was done on three different tissue:

- Testis, to evaluate the effects on the reproductive system;
- Kidney, that with the homeostasis of salts, water and macronutrients allows an excellent state of health ;
- Liver, as a central organ of the metabolism.

The effects of p,p-DDE were monitored in two ways. Initially, I evaluated the responses activate by the cells to mitigate the possible negative effects generate in presence of this pesticide as observed by other researchers *in vivo* and *in vitro* as indicate previously. In parallel to that, were monitored some of toxic effects using morphological analyses for all organs. In addition, different pathways were monitored in different ways for each tissue:

apoptosis (particularly studied in the liver and testis), inflammation (monitoring macrophages infiltration in the liver and kidney) and probably fibrotic effect on kidney.

Finally, the last part of this research was obtained on culture cells.

- Huh7 cells were treated with p,p-DDE to better understand what is the toxic mechanism activate in the hepatocytes.

The results obtained *in vitro* were compared to the results obtained on liver *in vivo*. In fact, culture cells of human hepatocellular carcinoma, were treated using a dose of pesticide that induce mitochondrial oxidative damage, condition observed in the liver in presence of p,p-DDE.

This manuscript consists of works in preparation and works already published, as described below:

<u>In preparation</u>

1) **Toxicity induced by the organochlorine pesticide p,p-DDE in *Wistar* rat testis. Apoptotic stimuli and compensatory mechanisms activated in conditions of stress.**

2) **High fat diet and p,p-DDE: characterization of the endogenous sources used to contrast the kidney injury.**

3) **The involvement of Metallothionein in cellular response to p,p-DDE administration in rat tissues.**

4) **Potential protective role of the mitochondrial channel UCP2 to regulate ROS accumulation and oxidative damages in male *Wistar* rat Liver.**

5) **p,p-DDE causes oxidative stress in *Wistar* rat Liver: preliminary studies conducted in *Huh7* cells.**

<u>Already published</u>

1) **Diet impact on Mitochondrial Bioenergetics and Dynamics.**

2) **Skeletal muscle mitochondrial bioenergetics and morphology in high fat diet induced obesity and insulin resistance: Focus on dietary fat source.**

Toxicity induced by the organochlorine pesticide p,p-DDE in *Wistar* rat testis. Apoptotic stimuli and compensatory mechanisms activated in stress conditions.

Summary

Polychlorinated biphenyls (PCBs) are hydrophobic chemicals more used in the past for different environmental aspects. Dichlorodiphenyltrichloroethane (DDT) is an organochlorinated insecticide, belongs to PCBs compounds, that was largely used during the post global war period in the world, to control the principals parasite vectors[14]. Today, it is particularly used in equatorial countries where are endemics the malaria cases[15]. More studies conducted during the last 30 years demonstrate that this pesticide, and its metabolites such as Dichlorodiphenydichloroethene (DDE), have dangerous implications in terms of reproductive capacity in different species, such as birds and reptiles[16,17,18]; embryology development[19] and generation of acute or chronic damages depending to dose and time of exposition[20]. In our studies, conducted on adult male *Wistar* rats, we evaluate the effect of DDE at the dose of 10mg/kg b.w. in association or not with saturated fatty acids. For this reason, we performed four experimental groups: normal diet group, high fat diet group, normal diet group with DDE and high fat diet group with DDE. Our results indicate morphological alteration of the seminiferous tubules, up-regulation of the principals antioxidant enzymes SOD1 and GPX1 and activation of apoptotic pathway in presence of DDE. These data demonstrate that a chronic oral administration of DDE may determinate toxicant effect that as indicate in literature, after long time of exposition, lead to cellular death and loss of organ function[21].

Introduction

Polychlorinated biphenyls PCBs are chemical compounds used in a serious of industrial processes, such as plasticizers in paints and cements, additives in flexible PVC coatings of electrical cables and electronic components, pesticide extenders and reactive flame retardants[22]. An important group of these chemical compounds enclose synthetic insecticides such as the DDT an ancestral insecticide used in the last century[23] and today used for the control of malaria cases in the center of World. In general, these compounds are very stable and have a long persistent time. They undergo to degradation thanks to aerobic and anaerobic reactions catalyzed by organisms or substances presents in the environment[24]. Different studies conducted to clarify the effects on the organisms distributed in the World, demonstrate correlation between toxicity and risk for health. In particular, in the 1994, L S Birnbaum has been described the effect of PCBs as endocrine disruptors[25]. In fact, these studies highlight the ability of these substances on the modulation capacity of several different hormones activities[26]. Our studies want to highlight the effects of the administration of DDE *in vivo*, first metabolite of DDT, on rat testis. These studies are intended to assess whether chronic pesticide administration may cause functional and morphological alterations for the seminal cells.

Materials and methods

Experimental model. Our *in vivo* study was conducted on Testis of male *Wistar* rats to identify the effects of DDE, used at the dose of 10mg/Kg b.w., on different pathways activated in the cells. Since DDE is a liposoluble molecule associated in particular to the fats stored in the foods[27], we tested its effects also in combination with a diet rich in saturated fatty acids. For these reasons, we performed four different experimental groups: N (Normal diet, 15,47 KJ/g), N+DDE (Normal diet 15,47 KJ/g + DDE), D (High fat diet, 19,23 KJ/g), D+DDE (High fat diet, 19,23 KJ/g + DDE). All rats were housed individually, acclimatized in a temperature-controlled room (24° C) and subjected to a circadian light-dark cycle (12 hours light / 12 hours dark). The experiments were conducted after four weeks of treatment and the dose mentioned above was chosen on the basis of previous data showing that the oral administration for 4 or 6 weeks did not affect physical development, sexual maturation, and serum metabolic parameters in male adult or pubertal rats[28]. After treatment, the rats were sacrificed with decapitation subsequently anesthetization by an intraperitoneal injection of chloral hydrate (40mg/100g of body weight). Diets composition was shown in table 1.

Hemallume & Eosin. Morphological alterations were analyzed with Hematoxylin & Eosin stain. Tissue sections were deparaffinized in xylene and hydrated in alcohol solutions arriving to water. (100°, 95°, 75°, 50°, H_2O). Nuclear contrast was obtained with hematoxylin for 3-5 minutes and differentiated in running water. Cytoplasm and others cell parts were detected with 0,5% Eosin for 1 minute, acidified with glacial acetic acid (three drops of glacial acetic acid/100mL Eosin 0,5%). The slides were washed in distillated water. Eosin color excess was removed with alcohol 75°. Finally, the sections were dehydrated in alcohol, clarified in xylene and the slides were mounted using balsam and coverslip.

Western blotting. Different proteins and enzyme were checked with western blotting analysis. Total protein extract was obtained using RIPA Buffer solution (150mM sodium chloride, 1.0% Triton X-100, 0.5% sodium deoxycholate, 0.1% sodium dodecyl sulfate, 50mM Tris, pH 8) and a cocktail of protease inhibitors (Aprotinin, Pepstatin, Leupeptin, Sodium orthovanadate, Phenylmethylsulfonyl fluoride, Sigma Aldrich) by using a polytron (KINEMATICA Polytron™ Model PT10-35 GT/PT 3100D Homogenizer, Fisher Scientific), and centrifuged at 12,000g for 15 min. Proteins were quantified with Bradford method and 30µg of proteins were charged in polyacrylamide gels at 13% for proteins that have low molecular weight and gels at 10% for high molecular weight proteins. The electrophoresis was made together a pre-stained protein marker (Color Burst Electrophoresis Marker m.w. 8,000-220,000 Da, Sigma Aldrich) in presence of SDS. After running, the proteins were transferred on nitrocellulose membranes (Immobilon-P, Millipore, Switzerland) at 350mA for 60 minutes. Membrane blocking was made in blocking buffer (1×TBS/ 1% Tween-20, 5% milk) for 60 minutes at room temperature and incubated O.N at 4°C with the antibodies of interest in 1×TBS/ 1% Tween-20, 2% milk.

Primary antibodies
SOD1: Thermo Scientific PA5-27240, rabbit polyclonal antibody, 1:500;
GPX1: Thermo Scientific PA5-30593, rabbit polyclonal antibody, 1:1000;
MT: Thermo Scientific MA1-25479, mouse monoclonal antibody, 1:500;

Grp78: Santa Cruz Biotechnology (N-20):SC-1050, goat polyclonal antibody, 1:200;
P53: Cell Signaling 1C12 mouse monoclonal antibody, 1:500;
BAK: Santa Cruz Biotechnology (G-23): sc-832 rabbit polyclonal antibody, 1:200;
BAX: Santa Cruz Biotechnology (P-19): sc-526 rabbit polyclonal antibody, 1:200;
cl-Casp3: Cell Signaling (D175) (5A1E) rabbit monoclonal antibody, 1:300;
PCNA: Cell Signaling (D3H8P) rabbit monoclonal antibody, 1:500;

The second day, membranes were washed 4×15 minutes with TBST solution and incubate with the relative secondary antibodies labeled with horseradish peroxidase in 1×TBS/ 1% Tween-20, 5% milk.

Secondary antibodies
Anti-mouse: Santa Cruz Biotechnology, goat-anti mouse, IgG-HRP: SC-2005, 1:5000;
Anti-rabbit: Santa Cruz Biotechnology, donkey-anti rabbit, IgG-HRP: SC-2313, 1:5000;
Anti-goat: Santa Cruz Biotechnology, donkey-anti goat, IgG-HRP: SC-2020, 1:5000;

Finally, membranes were washed 4×15 minutes with TBST solution and the bands were quantified using C-DiGit Chemiluminescent Western Blot Scanner (LI-COR).

Immunohistochemistry. IHC analysis was conducted to verify cl-casp3 immunolocalization on the tissue sections. To check the antigen, it was used "Novolink Polymer Detection Kit", Leica. The slides were prepared and the sections were deparaffinized in absolute xylene. Then, the sections were rehydrated in ethanol decreasing solutions (100°, 95°, 75°, 50°) and, in the end, placed in distillated water. After rehydration, few drops of peroxidase block solution and then protein block solution were added on each section for 5 minutes. They were used respectively to block the endogenous peroxidase activity and to limit non-specific interaction between primary antibody and antigen. Therefore, it was added on the sections a solution of anti-cleaved-caspase3 (primary antibody), 1:300 in PBS, O.N. at 4°C. The next day, the slides were washed in PBS solution to eliminate the primary antibody unbound with the antigen and on each section were added few drops of Novolink Polymer for 30 minutes (secondary antibody associated with a dextran polymer on which there are associated a series units of horseradish peroxidase. Again, the slides were washed in PBS and the reaction was produced with DAB chromogen and substrate solutions and monitored with microscope. Finally, the sections were contrasted with Hematoxylin to color the nuclei in blue and then, dehydrated in ethanol increasing solutions (50°, 75°, 95°, 100°, absolute xylene) and mounted with coverslip. The images were obtained with optic microscope associated to Zeiss Axiovision image program.

Real-Time PCR. MT mRNA was quantified with qReal-Time PCR. The analyses make using the Applied Biosystem 7500 Real-Time PCR System and the Power SYBR® Green PCR Master Mix (Life Technologies) following the procedure recommended by the manufacturer. Samples amplification was conducted at 20 µL (final Volume) for each reaction. Each reaction containing 12 µL of real-time PCR Master Mix, 1 µL of forward and reverse primers (10 µM), 2 µL of cDNA diluted 1:1 and 4 µL of nuclease free water. Reactions were conducted firstly with an initial step at 95 °C for 1 minute, followed by 40 cycles of 95 °C for 15 s at and 60 °C for 40 s. A melting curve analysis of PCR products was

performed from 60 to 95 °C in order to ensure gene-specific amplification. All data were conducted also to beta-Actin that was used as a normalize gene expression levels in each sample[29]. Changes in the gene expression in the samples were obtained in according to standard $2^{-\Delta\Delta Ct}$ method described by Livak and Schmittgen[30]. The primers used are follow described:

forward, 5'-CCCTGCTGCTGTAAAGGCG-3';
reverse, 5'-GTGCAAAGAAGATCACTGGGG-3'

Statistical analysis. All data were shown as mean ± standard error of the mean (SEM). Statistical analyses were carried out with Graph pad software. Differences between mean values obtained to control and treated group were analyzed by one-way analysis of variance (ANOVA) followed by Bonferroni post-test for RT-PCR experiments and t-test for the Western blotting analyses. The differences were considered significant when P value was "$p < 0,05$".

Results

Morphological analysis.

Morphological analysis indicates some alterations for each experimental group respect to control animals. In D group we found cell-free holes or vacuoles at level of the seminiferous tubules (Image 1, D group). This condition could indicate toxic effect due to by saturated fatty acids. In presence of p,p-DDE, in combination or not with high fat diet, we demonstrate alterations in regard to the cellular differentiation. In fact, we found release of undifferentiated cells in the lumen of seminiferous tubule (Image 1, DDE-treated groups). These results could be related to previous results obtained on testis homogenate that indicate reduction of Testosterone levels produced, in particular after p,p-DDE administration[31] (Table 2).

Antioxidant system: WB analysis. In our experimental conditions, we also monitored the antioxidant system enzymes. This choice was done because also in the other organs analyzed during my PhD research, especially in the presence of DDE, the up-regulation of antioxidant enzymes were observed. In particular way, I focused my attention on the Cu/Zn-SOD/SOD1 and Mn-SOD/SOD2 (respectively implicated in the anion superoxide dismutation) and GPX1 (used for the elimination of the hydrogen peroxide pre-generated by SODs activity). The results obtained indicate that SOD2 was not modulates in the testis. In contrast to this, SOD1 was up-regulated in all treated groups vs controls (Image 2, A). In fact, I identify increase of SOD1 already in presence of saturated fatty acids, indicating probably pro-oxidant effect of saturated fatty acids. In presence of DDE, there was an important difference if the pesticide was associated or not to fatty acids. In D+DDE group, in fact, I found significant increase of SOD1, respect to controls and hyperlipidic diet alone-treated animals. This increment is probably due to by DDE administration. However, in the N+DDE group I found the greatest increment of SOD1 respect to the others group. This data suggest that the DDE has pro-oxidant effect in the Testis. GPX1 appears modulated only in N+DDE group (Image 2, A), where was identified the greatest amount of SOD1. In our opinion, when the

DDE is associated to a normal diet, has more toxicity. Therefore, the up-regulation of the both antioxidant enzymes indirectly reports genesis and consequent ROS accumulation at cellular level.

Stress signals and pro-apoptotic effect of p,p-DDE. Many proteins are modulated under stress conditions. Some of these are involved in the restore of physiological conditions and in the activation of death signals to eliminate damaged cells. In this work, I evaluated the amount of Grp78 / BIP1 (as a reticular chaperon implicates in the protein folding) and p53 (as stress response protein) by WB. The results observed indicate that in presence of fatty acids alone (D group) there is a slight significant increase of Grp78 respect to control animals (Image 2B). Regarding p53, I did not observed differences between the both groups above mentioned (Image 2B). This data could indicate that in presence of saturated fatty acids, there was an additional request of GRP78 / BIP1 to correctly regulate proteins folding. In presence of DDE, I identify in p,p-DDE-treated groups, the same effect on these proteins analyzed. There was increase of the both Grp78 and p53 in significant way vs N and D groups (Image 2B). This analysis was conducted because Grp78 is described as a good marker to evaluate ER-tress response[32]. In addition to this, p53 seems directly associated to the apoptotic pathway activation regulating BAX[33]. This pro-apoptotic channel, associated to another member known as BAK, is involved in the mitochondrial outer membrane permeabilization, cytochrome-c release and activation of apoptosis. Therefore, I also evaluate the amount of BAK and BAX by WB on total protein extract. Regarding BAK, the results obtained shown up-regulation only in presence of DDE in significant way respect to control animals (Image 2B). Again, in according to p53 levels, the greatest increment of BAX was found in presence of pesticide. Differences between D+DDE and N+DDE were observed for the both proteins BAK and BAX analyzed. In according to our experiments, several studies demonstrate that BAX is directly involved in the germ cell density regulating apoptosis[34]. To confirm this data, I performed IHC analysis on paraffin-embedded sections to evaluate if in presence of high fat diet and pesticide there was increase of cells number positive to cleaved caspase 3 antibody (Image 3). In this case, we have not a quantitative analyses to say exactly in what treated group there is more casp-3 activated, but in line with the results obtained previously in particular in presence of DDE, we found a lot of positive cells to cleaved caspase 3. In addition we have also identified some Leydig cells positives to cl-casp3 antibody (Image 4) in presence of DDE. As described in literature, caspase 3 is essential during Leydig cells apoptosis and it is also associated to apoptosis of germ cells resulting from intratesticular Testosterone reduction[35,36].

Metallothionein expression and synthesis. Another protein examined in this paper is the Metallothionein 1 (MT1), because it is modulated in conditions of cellular stress. In different papers was described the negative effect of DDT on the MT expression and protein synthesis. In our study, in presence of saturated fatty acids alone (D group), we identify MT down regulation (Image 5A). In D+DDE group we observed similar response compared to D group (Image 5A), indicating that p,p-DDE has not effect in association to high fat diet. Finally, in N+DDE group we demonstrate the greatest reduction of the MT levels (mRNA and protein) as described in literature[37,38](Image 5A).

Discussions

In our experimental conditions, we demonstrate correlation between pesticide and stress responses activated in the testis. In presence of fatty acids, without p,p-DDE, we found slight up-regulation of the proteins and enzymes to control the lipotoxic effect of diet. In this group, previous experimental data, indicated that were not differences in regarding of mitochondrial oxygen consumption compared with control animals. For this reason, we hypothesized that in presence of high fat diet there is a good control of cellular metabolism. A few cells positives to cl-Casp3 will be probably eliminate and substituted with a new cellular population thanks of proliferation, as indicate by PCNA increase (Image 2B). Also in presence of p,p-DDE we identify up-regulation of the proteins analyzed. P53 and Grp78 were up-regulated in the same way. We found increase of these proteins respect to N and D groups but without differences between D+DDE and N+DDE groups. These results confirm that in the testis are activated different molecular pathways in presence of DDE. Firstly, Grp78 could be necessary to optimally regulate the ER-protein folding in condition of stress. In fact, a lot of proteins are up-regulated in response to p,p-DDE administration (SOD1, BAK, BAX and for Grp78). Then, p53 may regulates apoptosis, cellular growth and division[39]. Simultaneously, in the same experimental groups, we identify increase of cl-casp3 cellular positivity and increase of PCNA indicating cellular proliferation. These data suggest a possible mechanism activated in presence of p,p-DDE, probably to maintain a balance between dead and newborn cells.

Conclusions

The results obtained in our experimental conditions, in association to previous studies on testis mitochondria, indicate that p,p-DDE is directly implicates in the mitochondrial impairment and in the apoptotic pathway activation. In particular in the N+DDE group, this condition is clearly represented through the greatest up-regulation of BAX, BAK and cl-casp3 respect to the other groups. On the contrary, cellular proliferation could be used to ensure a good cell turn-over , hypothesis confirmed by PCNA levels. For this reason, we concluded saying that low dose of p,p-DDE during for weeks activate apoptosis and proliferation. The antioxidant enzymes explicate their function to control the oxidative damage. Caspase 3 activation, that also interest some Leydig cells in presence of pesticide, could explicate our previous results obtained on Testosterone reduction that may be the cause of the undifferentiated cell release in the lumen of seminiferous tubules.

High fat diet and p,p-DDE: characterization of the endogenous sources used to contrast the kidney injury.

Summary

Chemical compounds, such as pesticides, were improperly used in the past and also actually to control different sectors such as industrial, sanitary and agriculture with important implications for our health. For all chemicals, before its utilization, many studies are conduced to give a threshold value of use to ensure maximum effectiveness of the product with the lowest risk to environmental and human health. This concept is very important because in this way is possible to avoid contaminations and damages for the ecosystem. In the past, the vast utilization of many substances has led to toxic effects due to, for example, by their accumulation in soil, water and atmosphere. Examples are the polychlorinated biphenyls compounds (PCBs), that are also used against insects. The best known is DTT (Dichlorodiphenyltrichloroethane), hydrophobic insecticide largely used in the past in different parts of world. Today it is used in many equatorial countries to contain the development of malaria cases. Its insecticide propriety was discovered by Paul Herman Müller in 1939.[40] A serious problems for these compound is the persistence during time, especially for their metabolites, and the bioaccumulation capacity in the tissue rich in fats generating biomagnification in the food chain[41]. In our studies conducted on male *Wistar* rats I evaluated the negative effects on Kidney generated in presence of DDE (Dichlorodiphenyldichloroethylene), a persistent metabolite of DDT.[42] To characterize its toxic power, DDE administration was protracted for a short treatment period (four weeks) and at low dose (10mg/Kg b.w.). In addition, to simulate a possible condition present in our developed societies, we evaluate the effects of this pesticide also in association with a diet rich in saturated fatty acids. Therefore, four experimental group were performed: N (control diet), D (high fat diet) and others two groups in presence of DDE associated to the diets previous described (N+DDE and D+DDE groups). Our results indicate morphological changing in all treated groups; up-regulation of the antioxidant enzymes SOD1, SOD2 and GPX1 analyzed; synthesis of the both chaperones Grp78 and Grp75. In addition, increase of CD68 directly associated to phagocytic cells in the tissue, was observed. Finally, CRBP-1 increase in presence of pesticide, in particular without fatty acids, indicate a possible involvement of DDE in the progression to Kidney fibrosis. Since p,p-DDE is a liposoluble compound, future experiments could be traced to confirm cellular stress monitoring lipid peroxides and apoptosis.

Introduction

DDE is one of the principals metabolites of DDT, an ancestral organochlorinated insecticide. It was largely used during the last century for the control of the principal diseases vectors such as mosquitoes, phlebotomies and others vector of parasites[43]. Banned in Europe in 1978[44], today the DDT is essentially used for the control of malaria cases in the equatorial countries.[45] The most important propriety of DDT and metabolites is the bioaccumulation capacity in the animal**,** such as fish, and in the human tissue rich in fatty acids[46]. In this way, as indicate by Pocock and Vost (1974)[47], DDT and its metabolites enter in contact with the

human body in particular through the foods, arriving into the blood with chylomicrons. Their metabolism, in fact, starts with the intestinal absorption[48] and then, they are organized into the core of the nascent-chylomicrons with others hydrophobic compounds contained into the foods. The remnant-chylomicrons can be absorbed only from the hepatocytes that firstly experiment the effects of the liposoluble compounds arrived with foods. Therefore, the hepatocytes may produce another class of lipoproteins known as VLDL (Very Low Density Lipoproteins). When are formed, these lipoproteins will contain a whole range of hydrophobic compounds and a large amount of molecules that arrive at liver from the small intestine. For this reason, the Liver can partially release toxic compounds by re-immobilizing them in circles with the VLDL[49]. In the same way of nascent-chylomicrons, VLDL are degraded into the blood to LDL (Low Density Lipoproteins). This class of lipoproteins may be absorbed by all cells of the tissues. For this reason, if there were chemicals in the VLDL core, such as DDE, it generated toxicity also in the cells that absorb the LDL. In this mechanism play an important role the Kidney because in association to liver is implicate in the DDE excretion from the body with urine formation[50]. For this reason I evaluate the effects on Kidney generate in presence of this pesticide in association with saturated fatty acids (as a vehicle of liposoluble compounds) and in normal diet condition. This study aims to highlight the pesticide-induced response mechanisms, particularly in relation to the systems designed to counteract the potential oxidative damages, well-known associated to the organochlorinated insecticides[51].

Materials and Methods

Experimental model. Our study in vivo was conducted on Kidney of male Wistar rats to identify the effects of DDE, used at the concentration of 10mg/Kg b.w., on different pathways activated by response induced in presence of this pesticide. Since DDE is a liposoluble chemical, we used also a diet rich in saturated fatty acids to verify if in their presence there was synergic effects of fats and DDE. For these reasons, we performed four experimental groups: N (Normal diet, 15,47 KJ/g), N+DDE (Normal diet 15,47 KJ/g + DDE), D (High fat diet, 19,23 KJ/g), D+DDE (High fat diet, 19,23 KJ/g + DDE). All rats were housed individually, acclimatized in a temperature-controlled room (24° C) and subjected to a circadian light-dark cycle (12 hours light / 12 hours dark). The experiments were conducted after four weeks of treatment and the dose mentioned above was chosen on the basis of previous data showing that the oral administration of such dose for 4 or 6 weeks did not affect physical development, sexual maturation, and serum metabolic parameters in male adult or pubertal rats, respectively (Yuji Makita et al, 2003). After treatment, the rats were sacrificed with decapitation subsequently anesthetization by an intraperitoneal injection of chloral hydrate (40mg/100g of body weight). Diets composition are described in Table 1.

Hematoxylin & Eosin. Morphological alterations were analyzed with Hematoxylin & eosin stain. Tissue sections were deparaffinized in xylene and rehydrated in a decreasing ethanol solutions arriving to water (100°, 95°, 75°, 50°, H_2O). Nuclear contrast was obtained with Hematoxylin for 3-5 minutes and differentiated by washing in running water. Cytoplasm and others cell parts were detected with Eosin 0,5% for 1 minute, acidified with three drops of acetic acid. The slides were washed in distillated water and Eosin color excess was removed

in ethanol 75°. Finally, the sections were dehydrated in ethanol, clarified in xylene and mounted with balsam and coverslip.

Picrosirius Red. To view collagen deposited in the kidney, we used Picrosirius Red. This technique allows to colour the collagen in dark red. The protocol used was described follow:

- Deparaffinization in pure xylene
- Rehydration in alcohol solutions to water (100°, 95°, 75°, 50°, H_2O)
- Nuclear stain with Mayer's Emallume solution for 10 minutes
- Nuclear colour stabilization in tap water
- 1 hour in Picrosirius red solution (1g Red80 in 10mL of picric acid to arrive 100ml with distilled water) (Sigma Aldrich chemicals)
- Wash the slides in distilled water
- Wash red excess in acidified water (10mL of acetic acid to arrive 100mL with distilled water)
- Slide dehydration in alcohol solutions (50°, 75°, 95°, 100°, to arrive in pure xylene)
- Mount the slide with balsam and coverslip

Western blotting. Different proteins and enzyme were checked with western blotting analysis. Total protein extract was quantified with Bradford method and 30µg of proteins were charged in polyacrylamide gels at 13% or 10% depending by protein mass. The electrophoresis was done together with a pre-stained protein marker (Color Burst Electrophoresis Marker m.w. 8,000-220,000 Da, Sigma Aldrich) in presence of SDS. After running, marker and proteins were transferred on nitrocellulose membranes (Immobilon-P, Millipore, Switzerland) at 350mA for 60 minutes. Membrane were blocked in TBST/milk (1×TBS/ 1% Tween-20, 5% milk) for 60 minutes at room temperature and incubated O.N at 4°C with the antibodies of interest in 1xTBS/1% Tween-20, 2% milk.

Primary Antibodies
SOD2: Thermo Scientific PA5-30604, rabbit polyclonal antibody, 1:500;
SOD1: Thermo Scientific PA5-27240, rabbit polyclonal antibody, 1:500;
GPX1: Thermo Scientific PA5-30593, rabbit polyclonal antibody, 1:1000;
CRBP1: Santa Cruz Biotechnology(FL-135):SC-30106, rabbit polyclonal antibody, 1:200;
CD68: Santa Cruz Biotechnology (ED1): SC-59103, mouse monoclonal antibody, 1:100;
GRP78: Santa Cruz Biotechnology (N-20): SC-1050, goat polyclonal antibody, 1:200;
GRP75: Santa Cruz Biotechnology (H-155): SC-13967, rabbit polyclonal antibody, 1:200;
β-Actin: Santa Cruz Biotechnology (C4): SC-47778, mouse monoclonal antibody, 1:200;
C0XIV: Santa Cruz Biotechnology (H-84): SC-292052, rabbit polyclonal antibody, 1:200;

The second day, membranes were washed 4×15 minutes with TBST solution and incubate with the relative secondary antibodies labeled with horseradish peroxidase.

Secondary Antibodies
Anti-mouse: Santa Cruz Biotechnology, goat-anti mouse, IgG-HRP: SC-2005, 1:5000;
Anti-rabbit: Santa Cruz Biotechnology, donkey-anti rabbit, IgG-HRP: SC-2313, 1:5000;
Anti-goat: Santa Cruz Biotechnology, donkey-anti goat, IgG-HRP: SC-2020, 1:5000;

Finally, membranes were washed 4×15 minutes with TBST solution and the bands were quantified using C-DiGit Chemiluminescent Western Blot Scanner (LI-COR).

Mitochondrial extraction. Kidney fragments were washed and homogenized in 220mM Mannitol, 70mM sucrose, 20mM HEPES, 2mM EDTA and 0,1% fatty acid-free BSA, pH 7,4 (1:10, w/v) with a Potter Elvehjem homogenizer (Heidolph, Kelheim, Germany) set to 500 rpm (4 strokes/min). The homogenate obtained was filtrated and centrifuged at 900g for 10 minutes. The pellet was discarded and the supernatant, that contain mitochondria, was rapidly centrifuged at 11,000g for 15 min. Pellet contains total sub cellular mitochondrial fraction. Mitochondrial suspension was washed for three times in 80mM LiCl, 50mM HEPES, 5mM Tris P, 1mM EGTA, and 0,1% fatty acid-free BSA, pH 7.4, and resuspended in the same solution. To permit longer protein conservation, protease inhibitors were added (Sigma Aldrich chemicals).

Immunolocalization. Kidney, after sacrifice, was washed in cold ice NaCL 0,9% and fixed in bouin for 12 hours, dehydrated in alcohol and included in paraffin. After slides preparation, the sections were deparaffinized with xylene 100% for 4 minutes and hydrated. Novolink Polymer Detection Systems (RE7280-CE, Leica Biosystems) was used for the Immunohistochemical analysis. This kit is based on a novel Compact Polymer technology and the reaction was conducted as indicate by manufactory. Primary antibody (CD68 sc-59103, mouse monoclonal antibody, 1:200) was incubated overnight at 4°C. Nuclear contrast was obtained in Hematoxylin. Finally, the sections were dehydrated in ethanol, clarified in xylene and the slides were mounted.

Results

Hematoxylin & eosin stain (Image 1). In the kidney we did not observe serious alterations in treated animals compared with controls, but in some part of tissue there were some morphological change. We identify white patches in some proximal tubule cells of rats treated with saturated fatty acids (D and D+DDE groups). Probably, in presence of fatty acids, a part of lipids arrive in ectopic sites and are stored as lipid drops in the cytosol generating lipotoxicity (black circles). In the N+DDE group we found some tubules where the epithelial component was compromised. In fact, as indicate with a black rectangle, there is release of cells in the lumen of the tubules. In the end, in N+DDE group, we found some glomeruli that have the vascular component particularly condensed (red arrow).

Antioxidant enzymes (Image 2). The antioxidant enzymes were analyzed by WB. We investigated on SOD1/2 and GPX1 that are directly implicate in the hydrogen peroxide production (principally from mitochondria) and its degradation to water by GPXs. In regard to SOD1 and SOD2 appear clear that in all treated groups there is up-regulation of these

enzymes. In presence of saturated fatty acids alone (D group) there is a significant up-regulation of SODs respect vs N. In the both groups in presence of DDE (D+DDE and N+DDE) we found significant increment of these enzymes respect to N and D groups but without differences between them. The lost protein analyzed was GPX1 that eliminate the hydrogen peroxide using glutathione. WB data indicate an important role of fatty acids in the up-regulation of GPX1. In fact, in the both groups treated with saturated fatty acids (D and D+DDE), GPX1 is up-regulated in the greatest way. Also in the N+DDE group we found up-regulation of GPX1 but not in the same way described for the groups treated with fats. These analyses conducted on the antioxidant enzymes could indicate a possible role of treatments in the mitochondria superoxide accumulation that is directly controlled in situ by SODs. In fact, the activity of SOD2 (mitochondrial isoform) and SOD1 (cytosolic isoform) convert the superoxide anion in H_2O_2 which is less dangerous and easily eliminated by peroxidase and catalase activity.

ER chaperones: GRP75, GRP78 (Image 3). Two different chaperones were analyzed by WB: Grp75 and Grp78. The both proteins function as reticulum chaperon and play different roles during cellular proliferation, ageing and cellular death[52]. The results obtained in our research demonstrate a different trend for the proteins analyzed. Grp78 is up-regulated in the same way in all treated groups respect to control animals. In regard to Grp75, we observed significant increase in D group vs N but this trend is more represented in presence of DDE. These results could indicate that Grp78 is up-regulate in all conditions to facilitate the correct folding of the proteins synthesized in response to kidney stress[53]. Grp75 appears to be involved in different mechanisms in the cells. In particular new important research have been demonstrate that Grp75 functions as a bridge between mitochondria and endoplasmic reticulum which is essential for the efficient calcium transfer from the ER to mitochondria [54],[55]. As indicate by Qiukai E. et al., 2013[56], the over expression of Grp75 is important to prevent the damages caused by oxidative stress in the liver. Since liver and kidney play a common role in the detoxification and elimination of harmful substances outside of the body, the result obtained in the kidney in regard to Grp75 could indicate an adaptive mechanism to contain the oxidative damage caused by the ROS probable produced in particular in presence of DDE, as suggest by ER-chaperones synthesis and up-regulation of antioxidant enzymes.

Picrosirius red indicate a possible role of DDE in the progression to renal fibrosis (Image 4). With this technique we evaluated if under our experimental conditions, respect to controls, there were collagen deposits in the extra tubular matrix of kidney. The results obtained indicate in both groups in presence of DDE increase of collagen deposition around some tubules. In D group we did not observe significant morphological variation in regard to this qualitative parameter indicating that only this pesticide functions as a potential mediator of kidney fibrosis.

CRBP-1: myofibrobalstic marker in the renal fibrosis. As indicate by Katrien Van Beneden et al., 2008[57], a good parameter to identify renal fibrosis is the amount of CRBP-1 in the total protein extract by WB. This protein is expressed specifically by myofibroblastic cells in the tissue[58]. In our experimental condition it was demonstrate by WB that CRBP-1 was increased in both groups treated with DDE respect to control animals. In D group we

found only a tendency to its increment that not appear significantly increased respect to control group. In the N+DDE was found the greater increment of CRBP-1 in according to Picrosirius red stain through which was clear observed collagen deposition. These results could indicate that DDE has a direct role in the progression to fibrosis in particular when it is not associated to high fat diet. Probably, in presence of saturated fatty acids, a part of DDE remains sequestrated in inert form accumulated in the adipose tissue generating loss effects compared to group in normal diet condition.

CD68 as a marker of immune cells in the tissue (Image 5). CD68 was used in our research to investigate if in condition of stress generated in presence of saturated fatty acids and DDE, there was a recruitment of phagocytic cells such as monocytes / macrophages that may activate inflammation and phagocytosis of death cells[59]. In particular we evaluate by western blotting and Immunohistochemical analyses the amount of CD68 in the total protein extract and its localization in the tissue. In the N group we identify a basal positivity to CD68. In D group increase of CD68 was confirmed by WB data. However, the greater increment of CD68 was demonstrate in the both groups treated with DDE. As indicate by WB data, in the kidney there was recruitment of phagocytic cells that probably play a role in the elimination of death cells induced predominantly in presence of p,p-DDE . In particular we have also verified that in the DDE-treated groups, $CD68^+$ is localized around of some tubules and glomeruli (image 5, D+DDE and N+DDE groups).

Discussions

This study have been shown the possible mechanisms activated in the Kidney by fats and hydrophobic chemicals present into the foods. The results obtained in this model *in vivo* indicate important modifications of the enzymes and proteins directly or indirectly involved in the control of cellular stress. In presence of fatty acids alone (D group) we found immune cells recruitment in the kidney and up-regulation of principals antioxidant enzymes SOD1, SOD2 and GPX-1. In addition to that, up-regulation of both chaperones Grp75 and Grp78 analyzed was observed. They explicate protective roles during the cellular stress. In presence of DDE, we demonstrate that there are some differences depending from diet type. In fact, in regard of GPX1, in the N+DDE group we found less up-regulation of this enzyme respect to D+DDE group. This enzyme could have a key role in the control of the oxidative stress progression in our experimental conditions. In fact, we have indirectly hypothesized that in both group in presence of DDE there is a probably ROS accumulation, because SOD1 and SOD2 were up-regulated in the same way in these experimental groups. Always in indirectly way, since SOD1/2 were up-regulated also in D group but in minor way respect to DDE conditions, we can hypothesized that in D group the antioxidant system well controls ROS accumulation. In fact, the hydrogen peroxide produced by SOD1/2 is converted to water by GPX1 activity, that appear strongly up-regulated in presence of fats. At the same way, in D+DDE group the amount of GPX1 analyzed was more respect to N+DDE. Probably in presence of fatty acids is activated a preferential pathway in which is particularly involved GPX1. In absence of fats, the DDE stimulate less the up-regulation of GPX1 and the ROS could accumulate predominantly. In addition to that, we did not observe synergic effect of high fat diet and DDE for any enzyme or protein analyzed. For this reason we can assume

that in presence of fats, a part of DDE remain in inert form associate to fatty acids stored into the lipids accumulate in the adipose tissue. On the contrary, without fatty acids, the DDE explicate its toxic power and determines the major morphological tissue alteration, as previously described and induces fibrotic effect.

Conclusions

In conclusion we demonstrate that in presence of saturated fatty acids the cells put in place different mechanisms to control the damages caused by stress. In presence of DDE the additional increment of antioxidant enzymes, chaperones, and recruitment of phagocytic cells indicate that this pesticide, especially if is not associated with high fat diet, results in a significant modulation of pathways activated against the toxic effects. For this reason we can conclude that DDE, at the dose and time used, activate modulation of surviving signals to contrast in part its toxicity, but, in association to normal diet, causes also alteration of nephrons components and probable progression to kidney fibrosis. On the base of these results, future studies to confirm renal injury and fibrosis will be focused on collagen deposition by IHC and western blotting of collagen IV and alpha-SMA (associated to Kidney fibrosis[60]). Again, verify the DDE deposition in the tissue to clarify if in presence of fatty acids it is stored in inert form into the lipid matrix. Finally, the accumulation of pro-oxidant species and the analysis of caspase activation will be made to confirm the oxidative stress and the apoptotic pathway activation in consequence to the treatments.

The involvement of Metallothionein in cellular response to p,p-DDE administration in rat tissues.

Introduction

The 1,1'-(2,2,2-Trichloroethane-1,1-diyl) bis (4-chlorobenzene) (known as Dichlorodiphenyltrichloroethane, DDT) is a synthetic organochlorine, low-cost pesticide widely used in the past years against malaria (Paul Herman Muller, Nobel Prize 1948). It exerts its toxicity on the central nervous system altering the functionality of ion channels; many *in vivo* and *in vitro* studies have demonstrated adverse effects also on vertebrates including humans, affecting lipid and glucose metabolism and inducing cellular oxidative stress[61]. Hepatoxicity, nephrotoxicity and hormonal disorders induced by DDT and its metabolites have been also established[62]. Though having been banned in rich industrialized countries from '70s, it is still used in developing areas of Africa and Asia, where malaria, dengue and other diseases transmitted by mosquitoes are endemic[63]. Highly lipophilic and chemically stable, DDT persists in environment and accumulates in food chain[64]. In food, maximum residues levels of DDT and its metabolites from 0.02 (for vegetables) to 5 (for meat) ppm are allowed[65]. For this reason, detectable blood levels of dichlorodiphenyldichloroethylene (DDE), the major metabolite of DDT, has been found in human populations of different geographical areas, including North America and Europe[66]. Metallothionein (MT), a metal-binding, low molecular mass protein rich in cysteine residues[67] exhibits a powerful free radical scavenging activity. It has been demonstrated that MTs are able to reduce peroxidative damages in liver (Ahmad et al., 2000)[68], to protect neurons from peroxynitrite-induced oxidative stress in Parkinson's disease (Sharma and Ebadi, 2003)[69] and to prevent hydroxyl radical-generated DNA degradation (Abel et al., 1989; Chiaverini and De Ley, 2010)[70,71]. Redox changes in cells are also responsible of MTs translocation from cytoplasm to nucleus[72]. It has been proposed the existence of a specific cargo system that anchors MT in the cytosol; oxidative stimuli and the consequent increase in ROS induce the oxidation of the cytosolic partner and the nuclear localization of MT (Takahashi et al., 2005)[73]. Once in the nucleus, MT protects DNA from damage and apoptosis[74,75,76;] in addition, the requirement for zinc for several metallo-enzymes and transcription factors suggests the involvement of nuclear Zn-MT in the regulation of gene expression during progression of the cell cycle[77]. The aim of this work was to verify the involvement of MT in cellular response to DDE contamination in vivo, using rat tissues as model study. In particular, we decided to investigate MT expression and synthesis in liver and kidney of Wistar rats fed with DDE-contaminated food. The effect of DDE-administration on MT amount and localization was investigated giving the pesticide alone or in combination with a high content of lard in the diet, that promotes DDE accumulation in deposits of lipid material and increases oxidative stress in the cells.

Materials and Methods

Animals and treatments. This study was performed in strict accordance with the criteria established by the National Institutes of Health. The protocol was approved by the Committee on the Ethics of Animal Experiments of the University of Naples Federico II. All surgeries were performed under chloral hydrate anesthesia, and all efforts were made to

minimize suffering. Male *Wistar* rats aged 60 days (Charles River Italia, Calco, Como, Italy) were caged singly in a temperature-controlled room at 24°C with a 12 h light–dark cycle. The rats were divided into 4 groups (8 rats each), and in each group the mean body weight was approximately 370 g. For 4 weeks, two groups (N and N+DDE) received a standard diet (10% fat J/J, 15.47 KJ/g), and the other two groups (HF and HF+DDE) received a high fat diet rich in lard (45% fat J/J, 19.23KJ/g). Concurrently, all rats were exposed to DDE (10 mg/kg body mass, N+DDE and HF+DDE groups) or vehicle (corn oil, N and HF groups) via gavage every days. DDE dose was chosen on the basis of previous data showing that the oral administration of such dose for 4 or 6 weeks did not affect physical development, sexual maturation, and serum metabolic parameters in male adult or pubertal rats, respectively (Yuji Makita et al, 2003). Diet compositions are shown in Table 1. Throughout the experimental period, body weights and food intakes were monitored daily to calculate the body-weight gain and the gross energy intake. Spilled food was collected and compensated in readjusting the calculation of food intake. At the end of the experimental treatments, the rats were anesthetized by i.p. injection of chloral hydrate (40 mg/100 g body mass) and decapitated with a guillotine. The tissues were quickly removed, weighed and processed for both morphological and molecular analysis. Tissues slices were also immediately frozen in liquid nitrogen and stored at −80°C.

Immunohistochemistry. Small pieces of liver and kidney were fixed in Bouin's fluid, embedded in Paraffin according to routine protocols and cut into 4–5 μm sections. Novolink Polymer Detection Systems (RE7280-CE, Leica Biosystems) was used for the analysis. After antigen retrieval and quenching of endogenous peroxidase, sections were incubated overnight at 4°C with the MT mouse monoclonal antibody (1:400) (ThermoFisher Scientific). Immunostaining was performed using 3,3′-diaminobenzidine substrate/solution (DAB 1 mg/ml; Kit) as the chromogen. To test the specificity of the reactions, the incubation of the sections were performed with either non-immune serum (1:10 and 1:20) or bovine serum albumin (BSA; Sigma Aldrich) omitting the primary antibody. Images of sections were acquired using a Zeiss Axiovision microscope fitted with a TV camera.

Protein extraction. For the total protein extraction, liver and kidney slices were homogenated in RIPA buffer (150mM sodium chloride, 1.0% Triton X-100, 0.5% sodium deoxycholate, 0.1% sodium dodecyl sulfate, 50mM Tris, pH 8) and a cocktail of protease inhibitors (Aprotinin, Pepstatin, Leupeptin, Sodium orthovanadate, Phenylmethylsulfonyl fluoride, Sigma Aldrich) by using a polytron (KINEMATICA Polytron™ Model PT10-35 GT/PT 3100D Homogenizer, Fisher Scientific), and centrifuged at 12,000g for 15 min. The pellet was discarded and the freshly supernatant used for western blotting analysis.

Subcellular fractionation. For the subcellular fractionation (cytoplasm and nucleus), a protocol described by Dimauro and coworkers (2012) was used, specifically modified for hepatic and renal cells. Briefly, tissues were homogenized with a tight-fitting Teflon pestle attached to a Potter S homogenizer (Sartorius Stedim, Gottingen, Germany) set to 1500 rpm, in ice-cold STM lysis buffer (250mM sucrose, 50mM Tris–HCl pH 7.4, 5mM MgCl2) and protease inhibitors. Four strokes of 1 sec. each were applied, on ice. The resulting homogenate was centrifuged at 800 g for 15 minutes, thus obtaining a pellet containing

nuclei and cellular debris, and a supernatant with cytosol and mitochondria. The pellet was resuspended in 8mL of STM buffer, vortexed at maximum speed for 15 sec. and centrifuged at 500g for 15 min. This step was repeated on the obtained pellet three times to increase the purity of isolated nuclei, validated by microscopic inspection diluting an aliquot of the fraction in a trypan blue solution. The final nuclear pellet was resuspended in NET buffer (20mM HEPES pH 7.9, 1.5mM MgCl2, 0.5 M NaCl, 0.2mM EDTA, 20% glycerol, 1% Triton-X-100, protease inhibitors) and the nuclei lysed with 20 passages through an 18-gauge needle. The lysate was centrifuged at 9,000 g for 30 min at 4°C; the resulting supernatant, contained the nuclear proteins, was used for western blot analysis. Cytosolic proteins and mitochondria were separated centrifuging the starting supernatant at 11,000g for 15 min. After centrifugation, the resulting pellet contained mitochondria and was discarded; the supernatant, containing the cytosolic proteins, was used for western blotting.

Electrophoresis and Western Blot Analysis. The protein concentration in the homogenate samples was determined using the Coomassie Protein Assay Kit (Pierce Biotechnology, Rockford, IL, USA). For the electrophoresis, 30 µg of total, cytosolic or nuclear proteins were loaded onto a 15% SDS-polyacrilamide gel and electrophoresed under denaturing conditions, as described by Laemmli[78]. As molecular mass marker, a prestained proteins mix (ColorBurst Electrophoresis Marker, 8,000-220,000 Da, Sigma Aldrich) was also loaded in a lane. After the run, the proteins were transferred on nitrocellulose membranes (Immobilon-P, Millipore, Schwerzenbach, Switzerland) at 350mA for 60 minutes. The membranes were blocked in blocking buffer (1×TBS/ 1% Tween-20, 5% milk) for 60 minutes at room temperature and incubated overnight at 4°C with the metallothionein mouse monoclonal antibody (ThermoFisher Scientific, diluited 1:500). Membranes were washed 4 times for 15 min. each with TBST buffer and then incubated in the same buffer for 1h at room temperature with a secondary antibody labelled with horseradish peroxidase (peroxidase-conjugated anti-mouse IgG, diluited 1:2000). Membranes were washed in TBST; the relative densities of the immunoreactive bands were determined using the C-DiGit Chemiluminescent Western Blot Scanner (LI-COR). Normalization of signals was performed using histone H3 goat polyclonal antibody for nuclear proteins (Santa Cruz, diluited 1:200) and ß-actin mouse monoclonal antibody (Santa Cruz, diluited 1:200) for total and cytosolic proteins.

RNA purification and cDNA synthesis. Total RNA was extracted according to the TRI-Reagent (Sigma Aldrich) protocol. The quality of each total RNA was checked by electrophoresis on 2% agarose gel stained with ethidium bromide and measuring the optical density at 260/280 nm. A ratio of 1.8-2.0 was accepted for further reverse transcription. QuantiTect Reverse Transcription Kit (Qiagen) was used for the removal of genomic DNA contamination and for the subsequent cDNA synthesis. Approximately 1 µg of total RNA was used, according to the kit's protocol.

Quantitative Real-Time PCR analysis. The Real Time PCR reactions were carried out in triplicate for each sample in an Applied Biosystems 7500 Real Time System by using the Power SYBR Green Master Mix PCR (Applied Biosystems) following procedures recommended by the manufacturer. Each SYBR Green reaction (20µl total volume)

contained 12 μL of real-time PCR Master Mix, 1 μL of each of the forward and reverse primer (10 μM), 2 μL of cDNA diluted 1:1 and 4 μL of nuclease free water. Nuclease-free water for the replacement of cDNA template was used as a negative control. For internal standard control, the expression of β-actin gene was quantified (Scudiero et al., 2017). Primer sequences were designed using Primer Express software (Applied Biosystems). A single pair of specific primers for both *Rattus Norvegicus* MT1 and MT2 isoforms were designed, as previously described (Scudiero et al., 2017). The PCR was performed under the following conditions: holding stage of 95◦C per10 min; cycling stage (45 cycles): 95◦C × 10 s – 60◦C × 10 s – 72◦C × 10 s; melting stage: 95◦C × 5 s – 65◦C × 1 min – 95◦C × 30 s – 40◦C × 30 s. The melting curve analysis of PCR products was performed in order to ensure gene-specific amplification. Changes in the gene expression relative to the different samples were calculated according to the standard $2^{-\Delta\Delta Ct}$ method described by Livak and Schmittgen[79].

Statistical Analysis: Data are presented as mean ± standard error of the mean (SEM). Statistical analyses were carried out by StatView software (Altura Software, Inc.). One way ANOVA followed by Tukey's post hoc test was used to evaluate differences between the groups. P values smaller than 0.05 were considered statistically significant.

Results

Effects of high fat diet and DDE administration on MT expression in rat tissues. Firstly, we compared the relative abundance of MT transcripts in liver and kidney of rats fed with the standard diet. As expected, MT mRNAs were present in both organs, but more abundantly in liver (Image 1). Once established the constitutive level of MT gene expression in liver and kidney, we carried on a real-time PCR analysis to evaluate MT mRNA levels in liver and kidney of rats belonging to the different groups. Noteworthy, analysis revealed a different response to the HF diet and DDE exposure in the two tissues examined (Image 2). In liver, a strong decrease of MT expression, both in HF and DDE-treated rats, was observed (Image 2A); in particular, rats from HF, N+DDE and HF+DDE rats showed a level of MT transcript of about 1/3 compared to rats fed with a standard diet (group N). In kidney, we found a comparable amount of MT mRNA between rats of N and HF groups (Image 2B); on the contrary, DDE-treatments significantly increase of 5- and 3-folds the MT transcripts amount in N and HF rats, respectively (Image 2B).

Effects of high fat diet and DDE administration on MT localization in rat tissues. IHC analysis demonstrates that in the liver of control rats MTs are present in hepatocytes and localize in both cytosol and nucleus (Image 3A). In particular, as confirmed by western blotting, in the control animals there is the greatest amount of protein respect to treated animals. In fact, in the livers of the others groups analyzed, we found a decrease in the MT protein synthesis (Image 3B, total proteins). However, IHC and western blotting analyses on cytosolic and nuclear fractions indicate in treated livers an increase in positivity to MT-antibody in the nuclei and in the nuclear homogenate fraction, respectively (Fig. 3B, Cytosolic and nuclear proteins). These results indicate that both MT-mRNA and protein are constitutively present in the liver to control intracellular metals homeostasis, acting as scavenger of ROS under basal conditions. Under stress conditions, i.e. following HF diet

and/or DDE exposure, MT expression and synthesis decrease, concomitantly to an up-regulation in the same cells of proteins specifically involved to cope the severe stress conditions determined by HF and pesticide. However, the evident nuclear translocation of MT protein under stress conditions, strongly supports the hypothesis of a pivotal role of MTs in the protection to DNA from hydroxyl radical attack (Chubatsu and Meneghini, 1993; Vukovic et al., 2000)[80,81]. In addition, a high levels of MT in the nucleus of cells under certain conditions has been also related to the increased requirement for zinc for several metallo-enzymes and transcription factors during rapid cellular growth and following high rate of cell metabolism (Cherian, 1994; Cherian e Apostolova, 2000)[82,83]. The same IHC and western blotting analyses, performed on kidneys, retrieve different responses. In normal diet condition, MT-positivity is present in cytosol and nuclei of cells forming the convolute distal and proximal tubules (Image 4A). In presence of HF diet alone, the cytoplasmic positivity decreases, similarly to the liver, whereas, in presence of the pesticide (N+DDE and D+DDE groups) the MT-positivity appears also in the distal and some proximal tubules, together with an increase of positivity in nuclei (Image 4A, D+DDE, N+DDE). Western blotting on total cellular extracts confirms the results obtained with the Real-Time PCR analysis, indicating a down regulation of both MT expression and synthesis in presence of high fat diet alone and an up-regulation in presence of p,p-DDE (without differences between N+DDE and D+DDE groups) (Image 4B, total proteins). Western blotting analysis performed on cytoplasmic and nuclear fractions demonstrates that in renal cells, as well in hepatocytes, nuclear MT levels in treated groups increase significantly with respect to control animals. In particular, the higher increase is observed in nuclei of p,p-DDE-treated animals, both in presence or absence of HF diet (Image 4B, Cytosolic and Nuclear proteins).

Discussions.

MT expression and protein synthesis in the cells were associated to different biological functions, such as metals metabolism, control of damages due to by heavy metals and also as ROS scavengers in presence of stress[84]. In our study, we evaluated the effects on the MTs expression and synthesis in HF-diet condition and also in presence of the hydrophobic pesticide p,p-DDE in the Liver and Kidney rats. These organ was chosen because are two important organs involved in the excretion of xenobiotics and their metabolite. In fact, to eliminate many toxins from the organism, the hepatocytes activate the detoxification processes in which the chemicals that arrive from the intestine are modified to determinate reduction of their toxic power. In these reactions, a part of lipophilic species are conjugated with fatty acids or other hydrophilic compounds and eliminate through gallbladder vial, where other researchers have been shown the greatest levels of PCBs[85]. A parts will be also modified to become more soluble and excretable with urine formation. p,p-DDE undergoes to these mechanism above described[86]. In our study, we found in both organs Liver and Kidney analyzed a significative reduction of MT expression and synthesis in HF-diet condition alone. This data, could indicate a role of saturated fatty acids in the MT down regulation[87]. Other researcher associate reduced levels of both MT1,2 is associated with glucose intolerance and liver steatosis in mice[88], indicating that fatty acids accumulation may inhibits MT expression in the organs examined in our experimental conditions. In presence of p,p-DDE, both experimental groups (D+DDE and N+DDE) respond similarly in the organ

examined, but in different way in both liver and kidney. In the liver, in fact, a similar trend of MT down regulation was observed in presence of p,p-DDE. This data was surprising because normally, in presence of stress where pro-oxidant species accumulate in the cells, MT expression and synthesis were described in dependent way to the antioxidant (or electrophile) response element (ARE) activated in response to redox status[89]. However, recent studies conducted on adult testis of rats, indicate that the accumulation of lipid peroxides determine inhibition of MTs levels[90]. Since in our previous studies conducted on liver we found in presence of p,p-DDE increment of lipid peroxide in the total homogenate, we hypnotized that also in the liver could be activate MTs down regulation due to by these pro-oxidant species. At renal level, in different way respect to Liver, appear that MT expression and synthesis is up-regulated in presence of p,p-DDE. The greatest MT expression was observed in N+DDE group but the protein levels are similar in both p,p-DDE-treated groups, as indicate by total western blotting analysis. We don't know if in the kidney the effect of p,p-DDE on the lipid peroxidation follows the hepatic trend or they are less accumulated to hypothesize a different mechanism respect to liver. In addition to that, increase of nuclear MT positivity was observed in the liver and kidney of treated rats (D, D+DDE and N+DDE). Our investigation have been demonstrate by western blotting data that MT nuclear increase is significant in presence of pesticide, without differences depending to the diet.

Conclusions.

In conclusion we have been shown that liver and kidney respond to different mechanism in presence of p,p-DDE regarding MT expression levels and protein synthesis. Nuclear positivity, normally observed in both tissue analyzed[91], appear increased in presence of pesticide in both tissue analyzed. This data could indicate that MTs into the cell nucleus, as described in literature[92],[93] may have a protective role during cellular stress. This protective role appear important to prevent the oxidative damages on DNA by the pro-oxidant species accumulate in the cells. Therefore, although in the liver the effect of p,p-DDE is to MTs down regulation, the amount synthesized remains more localized at the nuclear level. In this way, MTs absolve the ancillary role of ROS scavenger, functioning as DNA protector from oxidative damage.

Potential protective role of the mitochondrial channel UCP2 to regulate ROS accumulation and oxidative damages in male *Wistar* rat Liver.

Summary

Nutrition is an important aspect with which we must act daily in order to promote an optimal functioning of the organism. The choice of foods and the knowledge of the foods consumed every day is one of the first parameters of environmental variability to which the organisms are exposed in terms of nutrition[94]. Today, we are subjected to a continuous and rapid changing in the relationship with food driven in part by the food industries. In fact, agrochemicals compounds (such as the pesticides) are used to meet the global demand for the agricultural products, which have adverse effects on the environmental species (Christos A. Damalas and Ilias G. Eleftherohorinos, 2011)[95]. In this work we focused our attention on the liver mitochondria ability to maintaining the function of this organ. We evaluated the effects of a chronic oral administration of p,p-DDE (dichlorodiphenylethylene), the first metabolite of p,p-DDT (dichlorodiphenilethane). This is an ancestral insecticide used in the past in several countries for the control of the principal disease vectors. Given its hydrophobic nature, we also evaluated the effects of this pesticide in presence of a dietary rich in saturated fatty acid. We have conducted experiments to evaluate the expression of the mitochondrial protein UCP2 (uncoupling protein isoform 2) that, as a member of this family, determines decoupling of the mitochondrial respiration from the oxidative phosphorylation (Amalia Ledesma et al. 2002)[96]. The results obtained in our study indicate ROS accumulation in the liver of treated rats respect to controls. In addition, we demonstrate up-regulation of UCP2 and mitochondrial decoupling in particular in presence of DDE. Therefore, we hypothesized that in stressful conditions, the liver can implements the adaptive mechanisms to buffer the excessive amount of ROS produced especially during mitochondrial respiration[97]. However, this functional regulation may have only a partial role after short period because the imbalance between oxidant species and defense mechanisms appear in favor to peroxides accumulation and probably damages caused by them (Pablo Muriel, 2009)[98].

Introduction

UCPs are a family of mitochondrial proteins. All members of this family are formed by six trans-membrane segments inserts into the lipidic matrix of the inner mitochondrial membrane. (Marcelo J. Berardi et al, 2011) [99]. Today five isoforms are known, UCP1-5 (Amalia Ledesma et al. 2002)[100], but in this paper we focused our attention on the isoform two (UCP2) that appear to be important as mitochondrial scavenger of ROS produced by mitochondria (Negre-Salvayre et al., 1999) [101]; (Horimoto et al, 2004) [102]. These proteins in fact, dissipate the electrochemical proton gradient performed during mitochondrial respiration, releasing the energy accumulated in the electrochemical proton gradient in form of heat. Different mechanisms appear leads to UCPs expression. For example, the UCPs may regulate a lot of biological mechanisms such as the adaptive thermogenesis, mechanism in which is directly implicate the UCP1 in the brown adipose tissue (Andriy Fedorenko et al, 2012)[103]; the ATP synthesis and all mechanisms directly or indirectly linked to ATP utilization, for example the insulin secretion from the beta pancreatic cells that is inhibited

by UCP2 activity (C.-Y. Zhang et al, 2001)[104]. In physiological conditions, the UCP2 expression and the protein synthesis is very low in the tissues and for the Liver it is essentially localized in the Immunocompetent cells (Dominique Larrouya et al, 1997)[105]. Moreover in some conditions, for example during mitochondrial ROS production, the up-regulation of UCP2 was observed in the hepatocytes suggesting a role as a regulator of ROS in the liver. (A Nègre-Salvayre et al, August 1997)[106]. In our study we demonstrate that our experimental conditions used induce hepatic stress. In consequence to this stress we found UCP2 modulation in terms of gene expression and protein synthesis. For this reason we hypnotized that this mitochondrial channel plays a role in the liver as adaptive mechanism to control mitochondrial ROS production and in consequence the cellular oxidative stress. In fact, if the stress conditions are exacerbates, cell damage and liver injury occurs.

Materials and methods

Experimental model. As experimental model, were used 32 male Wistar rats. Since the exposure to p,p-DDE is in general the result of the introduction of low doses through the food, in this study it was decided to administer DDE at low doses (10 mg / kg b.w.) orally. We have chosen this dose, because it has been reported that its oral administration for 6 weeks not influence physical development, sexual maturation, and serum metabolic parameters in male rats during the pubertal period and when is administered for 4 weeks to older rats (Yuji Makita et al, 2005)[107].Were preformed four groups constituted by 8 animals for each group. N group (standard control diet, 15,47 KJ/g); N+DDE group (standard control diet, 15,47 KJ/g +10mg/kg b.w. of DDE); D group (high fat diet, 19,23 KJ/g) and D+DDE group (high fat diet, 19,23 KJ/g +10mg/kg b.w. of DDE). All rats were housed individually, acclimatized in a temperature-controlled room (24° C) and subjected to a circadian light-dark cycle (12 hours light / 12 hours dark). At the end of the experimental period, the rats were anesthetized by an intraperitoneal injection of chloral hydrate (40mg/100g of body weight) and were sacrificed by decapitation. Treatment, housing and sacrifice of animals were performed in accordance with the guidelines of the Italian Ministry of Health.

Morphological analysis: Hematoxylin & Eosin stain. After slides preparation, the sections were deparaffinized in xylene 100% for 4 minutes and hydrated in decreasing ethanol concentration arriving to water. (100°, 95°, 75°, 50°, H_2O). Nuclear stain was obtained with hematoxylin (3-5 minutes for each slide) and differentiated by washing in running tap water until the sections were marked in dark blue. The other parts of cell were marked with Eosin 0,5% (1 minute for each slide). Sections was washed in distillated water for 1 minute and the Eosin intensity was observed at microscope. In case of excessive coloration with Eosin (dark pink), it is possible decolorize the sections in ethanol 75°. In the end, the sections were dehydrated in increase ethanol concentration, clarified in xylene and mounted with coverslip.

Preparation of mitochondrial M3 fraction. Liver fragments used for mitochondrial extraction, were washed and homogenized in 220mM Mannitol, 70mM sucrose, 20mM HEPES, 2mM EDTA and 0,1% fatty acid-free BSA, pH 7,4 (1:10, w/v) with a Potter Elvehjem homogenizer (Heidolph, Kelheim, Germany) set to 500 rpm (4 strokes/min). Homogenate was filtrated and centrifuged at 900g for 10 minutes. The pellet was discarded

and the supernatant, that contain mitochondria, was rapidly centrifuged at 11,000g for 15 min. The pellet contains total sub cellular mitochondrial fraction. Mitochondrial suspension was washed for three times and resuspended in 80mM LiCl, 50mM HEPES, 5mM Tris P, 1mM EGTA, and 0,1% fatty acid-free BSA, pH 7.4. To permit longer protein conservation, protease inhibitors were added (Sigma Aldrich chemicals).

Real-Time PCR. MT mRNA was quantified with qReal-Time PCR. The analyses make using the Applied Biosystem 7500 Real-Time PCR System and the Power SYBR® Green PCR Master Mix (Life Technologies) following the procedure recommended by the manufacturer. Samples amplification was conducted at 20 μL (final Volume) for each reaction. Each reaction containing 12 μL of real-time PCR Master Mix, 1 μL of forward and reverse primers (10 μM), 2 μL of cDNA diluted 1:1 and 4 μL of nuclease free water. Reactions were conducted firstly with an initial step at at 95 °C for 1 minute, followed by 40 cycles of 95 °C for 15 s at and 60 °C for 40 s. A melting curve analysis of PCR products was performed from 60 to 95 °C in order to ensure gene-specific amplification. All data were conducted also to beta-Actin that was used as a normalize gene expression levels in each sample (N. De Marco et al, 2010)[108]. Changes in the gene expression in the samples were obtained in according to standard $2^{-\Delta\Delta Ct}$ method described by Livak and Schmittgen, 2001[109]. The primers used are follow described:

Ucp2 primers

forward, 5'- AGCAGTTCTACACCAAGGGC -3';
reverse, 5'- AGAGGTCCCTTTCCAGAGGC -3'

RNA isolation. Total RNA was extracted from the liver fragments in presence of Tri-Reagent (1 ml Tri-Reagent per 50mg of tissue) using a Polytron. In the obtained homogenate was added 2-propanol (500μL per 1mL of tissue homogenate) and centrifuged at 12.000 x g for 10 minutes. In this way, three different cellular phases were obtained: **Top layer:** clear, aqueous, contains total RNA; **Middle layer/interphase:** white, contains DNA; **Bottom layer:** pink, organic phase, contains proteins. Aqueous phase was collect in another eppendorf. Therefore, total RNA was precipited adding 2-propanol (1:1 v/v respect to aqueous phase) at maximal speed for 30 minutes. The pellet obtained was resuspended in DEPC-water.

Ucp2 cDNA sequencing and probe preparation for *In Situ Hybridization*. Using a canonical PCR with a retrotranscription protocol with DNAse activity, total mRNA was retro transcribed in cDNA and quantified with a Nanodrop. The primers Forward and Reverse for Ucp2, described above, were tested in a canonical PCR. After *Ucp2* amplification by PCR, the correspondent cDNA was purified, inserted into a plasmid vector pSC-A and cloned in competent cells. Blue-white screening was done to evaluate the cells with insert. Therefore, a mini prep of insert was conducted. Then, plasmid DNA purification (containing the insert) permits the Ucp2 fragment elution. The elute purity was verified by another canonical PCR using primers M13 Forward and Reverse (complementary to plasmid DNA bordering the amplified). The Ucp2 fragment (230pb) observed in the agar's gel at

1,2% of agarose, indicate that all steps had been execute correctly. The sequencing of Ucp2 amplified was carried out using the Sanger method and the sequence homology observed was 100% respect to Ucp2 gene of *Rattus Norvegicus*. Then, using primers M13 F&R and nucleotides marked with digossigenin, was obtained the probe used for an *In Situ Hybridization* experiment. This technique was used to hybridize the Ucp2 mRNA sequence present in the hepatic cells. DNA probe was detected by using a primary antibody anti-digossigenin for the mRNA localization.

In Situ Hybridization **protocol.** After slide preparation, the sections were deparaffinized, hydrated and treated with Proteinase K 10µg/ml at 37°C (5 minutes) in 1M Tris/Hcl pH 7,0; 0,5 M EDTA pH 7,2 to eliminate the endogenous DNAse and RNAse activity. Therefore, they were pre-treated with a Pre-hybridation mix solution containing 50% formamide, 1X Denard's, 100 µg/ml Salmon sperm and 100µg/ml t-RNA in DEPC water at the probe hybridization temperature, calculated as 56,2°C. However, it was choosen to hybridize the probe at 42°C to favor the bond between probe and mRNA. Hybridization overnight with digoxigenin-labeled probe in the humid chamber was done. Each section was covered with parafilm. The second day, all slides were washed in three time with decreasing sodium chloride/sodium citrate solutions (SSC) containing 50% formamide (2X SSC + 50% formamide, 1X SSC + 50% formamide, 0.5% SSC + 50% formamide) and blocked in -2% Blocking solution in Maleicacid (30 minutes at roomtemperature). Then, the sections were incubate O.N. at 4°C with antibody Anti-dig 1:2500 in Blocking solution 2%. After O.N., the sections were washed in six times with 100 mM TBS containing 1X-Tween-20 and the and the reaction was revelated using BM-purple (Roche Cat. No. 11 442 074 001) + 1X-Tween-20 (for N and N+DDE groups) and BCIP-NBT (Roche Cat. No. 11 383 221 001) + 1X-Tween-20 (for D and D+DDE groups). In the end, the reaction was blocked in 1X-PBS-1mM EDTA and the slide were mounted with watery mountant and coverslips.

UCP2 Immunolocalization. After the sacrifice, Liver tissue fragments were washed in cold ice NaCL 0,9% for a few seconds and fixed in bouin for 12 hours, dehydrated and included in paraffin. After slides preparation, the sections were deparaffinized with xylene 100% for 4 minutes and hydrated by passing through decreasing ethanol concentration and, finally, in distilled water. For the reaction was used Novolink Polymer Detection Systems (RE7280-CE, Leica Biosystems) that is based on a novel Compact Polymer technology. Primary antibody (UCP-2 goat-polyclonal Antibody(C-20): sc-6525), 1:200, was incubated overnight at 4°C. For nuclear contrast, all slides were immersed in hematoxylin for 5 minutes and the color rendering was done under source water for 15 minutes. The sections were dehydrated in increasing ethanol concentration, clarified in xylene and the slides were mounted.

Western blotting. For UCP2 detection, were loaded 30µg of mitochondrial extract. Proteins were denatured in 2X Laemmly buffer (final concentration: 120mM Tris HCl, pH 6.8, 20% glycerol, 4% SDS, 0.05mM DTT) at 95°C and loaded onto a 13% SDS–polyacrylamide gel together with a pre-stained protein marker (Color Burst Electrophoresis Marker m.w. 8,000-220,000 Da, Sigma Aldrich). After the run, the proteins were transferred on nitrocellulose membranes (Immobilon-P, Millipore, Switzerland) at 350mA for 60 minutes. The

membranes were blocked in blocking buffer (1×TBS/ 1% Tween-20, 5% milk) for 60 minutes at room temperature and incubated with the antibodies of interest diluted in milk/TBS-Tween buffer (1×TBS/1% Tween-20, 2% milk) and incubate O.N. at 4°C:

Primary antibodies
UCP-2: goat-polyclonal Antibody (C-20): sc-6525, 1:200;
GPX-1: rabbit polyclonal antibody: Thermo Fisher scientific PA5-26323, 1:1000;
SOD-1: rabbit polyclonal antibody, Thermo Scientific PA5-27240,1:500;
COX-IV: mouse-monoclonal Antibody: sc-376731, 1:200 (mitochondrial loading control guide);
beta-Actin: mouse monoclonal antibody: sc-70319, 1:200 (total loading control guide).

Secondary antibodies
Anti-mouse: Santa Cruz Biotechnology, goat-anti mouse, IgG-HRP: SC-2005, 1:5000;
Anti-rabbit: Santa Cruz Biotechnology, donkey-anti rabbit, IgG-HRP: SC-2313, 1:5000;
Anti-goat: Santa Cruz Biotechnology, donkey-anti goat, IgG-HRP: SC-2020, 1:5000;

After O.N. with primary antibody, membranes were washed 4×15 minutes with TBST solution, incubate in blocking buffer and then incubated for 1h at room temperature with a secondary antibody labeled with horseradish peroxidase, diluted in milk/TBS-Tween buffer (1×TBS/1% Tween-20, 5% milk). Membranes were washed 4×15 minutes with TBST solution and relevated with a chemiluminescent method, using luminal solution (final concentration 2,5 mM) in presence of cumaric acids (final concentration 0,4 mM) and H_2O_2 (final concentration 100mM). The bans obtained were quantified using C-DiGit Chemiluminescent Western Blot Scanner (LI-COR). Fold change was calculated and expressed in a column graphic on software graph pad.

Statistical analysis. All data were shown as mean ± standard error of the mean (SEM). Statistical analyses were carried out with Graph pad software. Differences between mean values obtained to control and treated group were analyzed by one-way analysis of variance (ANOVA) followed by Bonferroni post-test for the RT-PCR and t-test for Western blotting analysis. The differences were considered significant when P value was "$p < 0,05$".

Results:

Morphological hepatic alteration. Morphological analysis demonstrates, in D group vs N, lipids accumulation in the cells that present characteristic ballooning form (black arrow), as described by Elizabeth M Brunt and Dina G Tiniakos, (2010)[110]. The lipid drops in the cytoplasm appear very big and occupy the entire cellular volume (Image 1, D group). In the D+DDE group, principally in the cells around of vessels, it was observed a difference respect to D group. In fact, the cytosol of the hepatocytes is not very rich in lipids. In addition in the cells around of principal vessels are present lipid drops that appear sometime really small and sometime really big (red arrow, image 1, D+DDE group). Their presence confer vacuolated appearance for the cells. This condition is described in literature as a progression to microvesicular steatohepatitis (Pouneh S et al, 2003)[111]. These data could

indicate, in combination of DDE, lower accumulation of fats in the cells that probably are used in part from the mitochondria in the beta-oxidation reactions, as observed previously in our laboratory (Sica R. PhD thesis, 2014) [112]. In this way, these organelles provide to the energy surplus required during the detoxification pathway activated in the liver in presence of chemical substances introduced with foods. Cellular vacuolization was observed also in the cells around of vessels in the N+DDE group (Image 1), suggesting a potential effect of DDE in the progression to steatohepatitis, condition that generates cellular stress and liver damages[113].

p,p-DDE induces oxidative stress in the liver. Our previous studies conducted on hepatic mitochondria isolated from tissue after treatment with p,p-DDE indicate Lipid peroxidation and mitochondrial decoupling (Sica R. PhD thesis, 2014). Measures conducted on hepatic homogenate indicate significant increase of the mitochondrial H_2O_2 in all group vs N. Moreover, in presence of DDE, a greater significant increase of lipid peroxides respect to N and D groups were observed indicating a role of DDE to oxidative stress generation in the Liver. This data was confirm by SOD-1 western blotting analysis, where we observe significant increase of this antioxidant enzyme in D group vs N and in greater ways in both p,p-DDE treated groups, indicating that liver cells put in place a serious of mechanism during ROS accumulation in the tissue[114]. Mitochondrial respiratory measures conducted in presence of succinate, oligomycin, and also FCCP as synthetic decoupling (Sigma Aldrich chemicals), were done to calculate q and ŋ parameters that represents the grade of coupling and the thermodynamic efficiency respectively[115]. In regard to them, we found in DDE-treated groups significative reduction of these parameters respect to N and D groups. We didn't check differences between D and N groups. These data indicate mitochondrial decoupling in presence of pesticide. Therefore, we hypothesized the probable implication of the uncoupling protein 2 for explain this data. Since in the literature are described the effects of ROS on the up-regulation of the UCP2 and the effects of this protein in the control of ROS production, as indicate by Mailloux RJ and Harper ME (2011)[116], we evaluated the UCP2 gene expression and the amount of the protein in our experimental conditions.

UCP2-primers validation and fragment sequencing. To be sure about the quality of the primers designed in "Blast", we validate with a conventional PCR the mRNA amplification quality. We have checked this analysis on the N+DDE c-DNA, because in this group, treated only in presence of DDE, we have found lipid peroxides accumulation and mitochondrial decoupling. As expected, the fragment length measured with PCR was 230 pairs of bases, and the band obtained during this analysis was only one (Image 2). This result indicates specificity for the primers used in our investigation. After this analysis, the fragment obtained with PCR was purified, amplified in a plasmid vector and in the end sequenced. The result obtained has given 100% of identity at the fragment of UCP2 mRNA of *Rattus Norvegicus* (Image 2).

UCP2 gene expression and mRNA localization. We demonstrate with real time PCR a basal UCP2 expression in the control animals (Image 3a). This data, indicates that in the liver there is a cellular population in which this mitochondrial carrier is normally expressed and have an important function. In literature is described that the basal UCP2 expression in the liver is associated to Kupffer cells as indicate by Dominique Larrouy et al., 1997[117]. Our

data confirm this previous literature results because using in situ hybridization we have checked Ucp2 mRNA localization in the Kupffer cells in the control group and not in the hepatocytes (Image 4A, N group). In presence of saturated fatty acids alone, there is a significant fold increase of UCP2 mRNA respect to control (Image 4A, D group). This data suggest that saturated fatty acids have a role in the transcriptional regulation of this gene. In presence of DDE we found a significant increase of UCP2 mRNA level, in particular when the pesticide is not associated with high fat diet (Image 3a). These data confirm that in presence of ROS (D+DDE and N+DDE groups) there is an important up-regulation of the UCP2 gene. Associate with the increasing of UCP2 mRNA measured with the Real Time PCR, we shown also a changing of mRNA localization in the liver through in situ hybridization (Image 4A, DDE-treated groups). Data obtained with this experiment indicate that in N group the mRNA localization is associated only to the Kupffer cells (as described above). In the D group we observed mRNA localization also in the hepatocytes. This localization in the hepatocytes was verify also for the both DDE-treated groups. Then, we concluded that the up-regulation of UCP2 is extended in the hepatocytes in stress conditions. Is not known what is the possible pathway in which is directly or indirectly activate the UCP2 gene expression and protein synthesis in presence of DDE. A lot of mechanism were indicate in literature as probably transcriptional mediators, for example PPARα, PGC1α and SREBP[118,119,120].

UCP2 protein detection. Different analyses were conducted for the UCP2 detection. Firstly, Immunohistochemical stain conducted on liver sections demonstrate low positivity in normal conditions. In particular, as described above, we identify UCP2 positivity in the Kupffer cells (Image 4B, N group). In presence of hyperlipidic diet occurs an increase of UCP2 positivity in the hepatocytes to indicate a possible direct or indirect role of the saturated fatty acids in the UCP2 up-regulation (Image 4B, D group). The images obtained with optical microscopy (magnification of 100X) indicate that the mitochondria are marked with the antibody as confirmed by western blotting data on the mitochondrial proteins. Moreover, IHC and western blotting analysis indicate even in the groups in presence of DDE increase of UCP2 (Image 3B/4B, DDE-treated groups). This significant increase compared to hyperlipidic diet could be dictated by ROS accumulation in presence of the pesticide that have a positive effect on transcription, protein synthesis and probably on post-translational regulation of UCP2. Significative differences observed by WB in the N+DDE vs D+DDE group may be due to that, in combination with fats, DDE could remain in part stored into the lipids in inert form without direct effects on the mitochondria[121,122].

Discussions

In this study, our results indicate that the UCP2 play a possible protective role during the oxidative stress in the liver. Gene expression and protein synthesis indicate in presence of saturated fatty acids alone (D group) a slight but significant up-regulation of UCP2 gene in the hepatocytes. Despite this result was confirmed by Real Time and Western blotting analysis, when we measured the grade of coupling in this group of rats we did not observed significative differences with control animals. In fact, for this parameter, we found only a tendency to its diminution. This result was surprising because in presence of UCP2 we

would have expected a decrease of q parameter in these animals. Our hypothesis is directly associated to the post-translational modifications on the UCP2 channel. In fact in the literature it was described for the UCP2 a post-translational modification knows as glutathyonilation[123]. In presence of stress conditions, a lot of mitochondrial proteins are glutrathionylated on thiols groups undergo to the reversible mechanism indicate as deglutathionylation phenomena. Therefore, thiols groups of mitochondrial proteins that were bound to GSH, release GSH used by enzymes GSH-dependent and change their conformational structures. This mechanism appear to be also associated to UCP2 channel that when is present in glutrathionylated form is inactive (Ryan J, 2011).[124] In conditions of stress, that appear clear in our study in particular for the both groups in presence of DDE, the grade of coupling q is decreased respect to control group in significant way. This data could suggest that in these two groups the UCP2 is present in form active and dissipate the electrochemical proton gradient. Protein deglutathionylation was not confirmed in our study with experimental data, but we suggest that this mechanism may be possible because in the stress conditions we demonstrate by western blotting an increase of GPX1 enzyme in all groups vs control animals (Image 5). This enzyme uses GSH to eliminate the excess of hydrogen peroxide produced by SOD activity, up-regulated in predominant way in presence of DDE (Image 5). We demonstrate in addition that GPX-1 is particularly up-regulated in presence of fatty acids (Image 5b, D and D+DDE groups) respect to N+DDE group, remaining in any case up-regulated respect to N. In presence of a slight ROS accumulated in form of lipid peroxides (D group, Table 2), there is UCP2 protein increase and strong up-regulation of GPX1. Only a trend to diminution of q parameter it was observed respect to control animals. For this reason, in high fat diet alone treated-animals we hypnotized that the GPX1 activity might be enough to tampon the mitochondrial hydrogen peroxide generation and in a big part the lipid peroxides accumulation. In this way, the up-regulation of UCP2 could have only a preventive role in case of the ROS accumulation during time. In presence of high ROS levels accumulated in form of lipid peroxides (D+DDE and N+DDE groups, Table 2), in regard to UCP2 and GPX1 we observed opposite results: in D+DDE group we shown that the UCP2 was increased vs N and D groups respectively and GPX1 up-regulated in the same way to D group. On the contrary, in N+DDE group, we observed in regard to UCP2 channel the greater up-regulation. Also the GPX1 enzyme is up regulated respect to control, but not in the same way to the groups in presence of saturated fatty acids. Our hypothesis to explain these data is that in presence of saturated fatty acids there is a particular pathway activated in the liver for the control of the lipid peroxidation by the antioxidant system activity, in particular by GPX-1. DDE could be activates a different pathway in the hepatocytes, using in particular mitochondrial decoupling. In this system, DDE could play indirect roles in the transcription, synthesis and function of UCP2, for example by transcriptional factors such as PPARα/γ (Nakatani T. et al, 2002.)[125]; (Villarrova F. et al, 2007)[126]. Since in presence of this pesticide are accumulate mitochondrial ROS, (Echtay KS et al, 2002)[127], they regulate UCP2 post-translational regulation by glutathyonilation / de-glutathyonilation processes (Ryan J. Mailloux and Mary-Ellen Harper, 2012)[128], activating mitochondrial decoupling. This process generates decrease of the electrochemical proton gradient and less superoxide anion, preserving mitochondrial function.

Conclusions

We concluded that, in a system where the mitochondria suffer more of the damage caused by ROS produced in presence of DDE, the protonic gradient dissipation could be preferred as a preventative purposes in order to adjust the slowed flow of electrons. In a system where the DDE probably has a minor effects, for example in association of saturated fatty acids, another pathway could be more activate for the control of oxidative stress and the UCP2 is less regulate respect to the conditions in presence only of DDE. Obviously, as shown by lipid peroxidation data resumed in the table 2, oxidative damage were confirmed in all groups but in particular in presence of DDE. Thus, we can assume that despite the liver mechanisms are activated for the cellular preservation, a chronic exposure to low doses of DDE for 4 weeks generates hepatic oxidative stress. To confirm our hypothesis in which UCP2 channel play a protective role during hepatocellular stress, future studies could be conducted in UCP2-/- animals to clarify the negative effect generate by ROS accumulated in presence of DDE.

p,p-DDE causes oxidative stress in *Wistar* rats Liver: preliminary studies in *Huh7* cells *in vitro*.

Summary

The liver is a central organ of metabolism[129]. It plays important digestive and excretory functions, accumulates and processes the nutrients, synthesizes new molecules, detoxifies the blood from harmful chemicals, and much more[130]. The detoxification pathway, infact, alters chemically the structure of the toxins to make them less toxic[131]. Our research, conducted in presence of p,p-DDE (1,1-Dichloro-2,2-bis(4-chlorophenyl)ethylene), a chemical synthetic pesticide derivate from p,p-DDT degradation, was done to highlight the systems implemented by the liver to control pesticide-induced damage and its toxic effects in rats. Four experimental groups were performed to control the effects of this pesticide in association or not with a diet rich in saturated fatty acids: N (normal diet); D (High fat diet); N+DDE (Normal diet + DDE); D+DDE (High fat diet + DDE). The toxic power of p,p-DDE was also studied *in vitro* on hepatocarcinoma cellular model (Huh7). *In vivo* we demonstrate that in the liver there is the association between toxic effects and antioxidant responses to control cellular function. SOD2 up-regulation in all experimental groups could be used to eliminate a part of superoxide anion produced by mitochondria in presence of pesticide. In the N+DDE group the greatest increment of SOD2 was measured. This data suggest that DDE has more effects in absence of a lot of lipids in the diet. Another response element, Grp78, was increased in response to our experimental conditions. This chaperon play a role during ER-stress in the protein folding, controlling the physiological reticular function[132]. Apoptotic pathway appear associated to p,p-DDE, in fact, we observed increase of mt-BAX and immunoreactivity to cleaved casp3. *In vitro*, Huh7 cells respond to pesticide similarly to what has been observed *in vivo*. Increase of superoxide anion, H_2O_2 accumulation and mitochondrial dysfunctions were found. Apoptosis induced by mitochondria appears confirmed by the incremented of BAX, cl-casp9 and cl-PARP levels associated to the decrease of inactive casp3 levels. In addition, mitochondrial dynamics change was observed after treatment. The mitochondria appear more fragmented and assume donut morphology. In conclusion, we can say that p,p-DDE has pro-oxidant role in both models *in vivo* and *in vitro*. The liver activate more match mechanisms to contrast the negative effects associated to the pesticide; In the Huh7 culture cells, mitochondrial damage, reduction of ATP produced and apoptotic signals bring the cells to programmed death.

Introduction

Dichlorodiphenyltrichloroethane (DDT) is an ancestral hydrophobic pesticide belongs to the PCBs family, particularly used during the last century[133]. It was synthesized in the 1874 by Othmar Zeidler at the University of Strasburg but its use was only employed in the 1939, when Paul Herman Müller discovered the toxic power of DDT against several arthropods. In particular, in that period, several studies were conducted to find some synthetic molecules to control malaria vector[134]. For this reason, in the 1948, Müller won the Nobel Prize for discovering the effects of DDT as a contact poison against arthropods, in particular for the insects[135]. Chemically, DDT looks like a white powder. Its utilization was extent in agriculture without limitation[136,137]. When DDT arrives in the environmental matrix,

undergoes to abiotic and biotic degradation generating different metabolites[138]. One of this, p,p-DDE, is the first and the most persistent metabolite of DDT[139]. Different studies were carried out to validate the harmful effects associated to DDT utilization. In fact, already in 1962, some toxic effects on the environment were highlighted[140]. For this reason the utilization of DDT was banned in Europe, North America and in more parts of Asia where the malaria cases were eradicated[141]. Today, the World health organization (WHO) permits DDT utilization in the equatorial countries where the malaria cases are endemics[142],[143]. However, even if it is only used in these hot zones, different studies demonstrate that dangerous concentrations of DDT and metabolites, in particular p,p-DDE, were found far from the site of use[144,145]. These molecules in fact, can be subject to grasshopper effect and arrive at long distance by rein[146]. Moreover, p,p-DDE is a fat-soluble pesticide and accumulates in the lipids. In this way it go against to bioaccumulation and biomagnification processes in the food chain[147]. For these reason, our studies, conducted in presence of p,p-DDE, were done to clarify what are the pathways activate *in vivo* and in culture cells in presence of this pesticide.

Materials and methods.

In vivo studies conducted on liver of Wistar rats.

Experimental model. Our study in vivo was conducted on Kidney of male Wistar rats to identify the effects of DDE, used at the concentration of 10mg/Kg b.w., on different pathways activated by response induced in presence of this pesticide. Since DDE is a liposoluble chemical, we used also a diet rich in saturated fatty acids to verify if in their presence there was synergic effects of fats and DDE. For these reasons, we performed four experimental groups: N (Normal diet, 15,47 KJ/g), N+DDE (Normal diet 15,47 KJ/g + DDE), D (High fat diet, 19,23 KJ/g), D+DDE (High fat diet, 19,23 KJ/g + DDE). Diet composition was resumed in table 1. All rats were housed individually, acclimatized in a temperature-controlled room (24° C) and subjected to a circadian light-dark cycle (12 hours light / 12 hours dark). This dose was chosen on the basis of previous data showing that the oral administration of such dose for 4 or 6 weeks did not affect physical development, sexual maturation, and serum metabolic parameters in male adult or pubertal rats (Yuji Makita et al, 2003). After treatment, the rats were sacrificed with decapitation subsequently anesthetization by an intraperitoneal injection of chloral hydrate (40mg/100g of body weight).

Western blotting. Total homogenate and mitochondrial protein extracts were obtained ad describe by I. Dimauro et al. 2012, validate by western blotting analysis of specific proteins of each cellular part. A part of homogenate was used for total protein analysis and a part was used to isolate mitochondria[148]. Proteins obtained from total homogenate and from mitochondrial lysis were quantified with Bradford method. 30µg of proteins were charged in polyacrylamide gels at 13% (SOD2, BAX, COXIV), and 10% (CD68 and Grp78). The proteins run was made together a pre-stained protein marker (Color Burst Electrophoresis Marker m.w. 8,000-220,000 Da, Sigma Aldrich) in presence of SDS. After running, the proteins were transferred on nitrocellulose membranes (Immobilon-P, Millipore, Switzerland) at 350mA for 60 minutes. Membrane blocking was made in blocking buffer

(1×TBS/ 1% Tween-20, 5% milk) for 60 minutes at room temperature and incubated O.N at 4°C with the antibodies of interest, in 1×TBS/ 1% Tween-20, 2% milk.

Primary Antibodies:
SOD2: Thermo Scientific PA5-30604, rabbit polyclonal antibody, 1:500;
COXIV: Santa Cruz Biotechnology (H-84): SC-292052, rabbit polyclonal antibody,1:200;
Grp78: Santa Cruz Biotechnology (N-20): SC-1050, goat polyclonal antibody, 1:200;
CD68: Santa Cruz Biotechnology (ED1): SC-59103, mouse monoclonal antibody, 1:100;
BAX: Santa Cruz Biotechnology (G-23): SC-832, rabbit polyclonal antibody,1:200;
Actin: Santa Cruz Biotechnology (C4): SC-47778, mouse monoclonal antibody, 1:200;

The second day, membranes were washed 4×15 minutes with TBST solution, incubate in blocking buffer and then incubated for 1h at room temperature with a secondary antibody labeled with horseradish peroxidase, diluted in milk/TBS-Tween buffer (1×TBS/1% Tween-20, 5% milk).

Secondary Antibodies
Anti-mouse: Santa Cruz Biotechnology, goat-anti mouse, IgG-HRP: SC-2005, 1:5000;
Anti-rabbit: Santa Cruz Biotechnology, donkey-anti rabbit, IgG-HRP: SC-2313, 1:5000;
Anti-goat: Santa Cruz Biotechnology, donkey-anti goat, IgG-HRP: SC-2020, 1:5000;

Then, membranes were washed 4×15 minutes with TBST solution and relevated with a chemiluminescent method, using luminal solution (final concentration 2,5 mM) in presence of cumaric acids (final concentration 0,4 mM) and H_2O_2 (final concentration 100mM). The bans obtained were quantified using C-DiGit Chemiluminescent Western Blot Scanner (LI-COR). Fold change was calculated and expressed in a column graphic on software graph pad.

Immunolocalization. Immunolocalization of SOD2, CD68 and cl-casp3 was done on liver section prepared for optical microscopy. After sacrifice, liver fragment were directly washed in fresh cold ice NaCL 0,9% and fixed in bouin for 12 hours, dehydrated and included in paraffin. After slides preparation, the sections were deparaffinized with xylene 100% for 4 minutes and hydrated in ethanol solutions arriving to distilled water . Novolink Polymer Detection Systems (RE7280-CE, Leica Biosystems) was used for the analysis. This kit is based on a novel Compact Polymer technology and the reactions were conducted as indicate by the manufactory. Primary antibodies were incubated overnight at 4°C. (cl-Casp3 (D175) (5A1E) Cell Signaling rabbit monoclonal antibody, 1:300); SOD2: Thermo Scientific PA5-30604, rabbit polyclonal antibody, 1:300; (CD68**:** Santa Cruz Biotechnology (ED1): SC-59103, mouse monoclonal antibody, 1:200). Nuclear contrast was obtained in Hematoxylin. Finally, the sections on the slides were dehydrated, clarified in xylene and mounted with coverslip.

Electronic microscopy. After sacrifice, liver rats were sectioned and a part was used to prepare samples subsequently analyzed with electronic microscopy. Each sample was fixed in fresh cold fixing solution prepared with Gluteraldehyde 2,5% dissolved in Milloning

buffer (Sodium Phosphate monobasic (NaH_2PO_4•$2H_2O$), Sodium Phosphate dibasic (Na_2HPO_4•$2H_2O$), 0.5% Sodium Chloride (NaCl)), approximately for 1h. After time, the samples were washed in cold Milloning buffer used to prepare the fixing solution to eliminate the Glutaraldehyde. Then, each sample was put into 2% Osmium tetroxide solution, at room temperature for 2h, washed in 0,5% sodium chloride buffer and dehydrated in increase alcohol solution (50°, 75°, 96°, 100°). After dehydration, the samples were puts in propylene oxide solution (5 minutes) and then, they were introduced in mixture composes at 50% of EPON and propylene oxide, O.N., at room temperature. This passage permits the propylene oxide evaporation and the EPON infiltration in each sample that will be fixed. Next day, the samples were included in EPON solution (specifically prepared to inclusion) containing 24,25 mL Epon 812, 9,25 mL DDSA (Dodecenylsuccinic anhydride) and 16,5 mL MNA (methyl nadic anhydride) arriving to final volume 50mL. Finally, BDMA (N,N-Dimethylbenzylamine), Catalyst for epoxy resins, was added. Each sample was included in specific molds, in the EPON solution above described and putted at 60°C for 72h. The liver fragment included were used to prepare the sections for SEM (Scanning Electronic microscopy) microscopy. Before the imaging analyses with microscope, the sections were colored in uranyl acetate (3% Uranyl acetate in 50% distillated water and 5% ethyl alcohol) and Pb-citrate (Pb-citrate solution: 2,66g Pb-nitrate $Pb(NO_3)_2$; 3,52g sodium citrate $Na_3(C_6H_5O_7)$•$2H_2O$) to increase the contrast between the organelles in the cell citosol. The solution was clarified using NaOH 1N, pH=12, final volume=100mL.

In vitro studies conducted on Huh7 cells in the laboratory of molecular medicine directed by Antonio Zorzano (IRB Barcelona): [November 07, 2016 – May 07, 2017]

p,p-DDE: doses experiment. Huh7 cells were tested with 5 different doses of p,p-DDE solved in DMSO, for 24h of exposition. (Control cells; p,p-DDE 5µM/0,002% DMSO; p,p-DDE 10µM/0,003% DMSO; p,p-DDE 30µM/0,01% DMSO; p,p-DDE 50µM/0,02% DMSO; p,p-DDE 100µM/0,03% DMSO). Control cells were not treated with DMSO in this experiment. After treatment, the samples were incubated with MitoSox probe (MitoSox Invitrogen detection technologies, Cat. No.M36008). MitoSox discriminates for the mitochondrial superoxide anion produced in life cells. The sample were incubated for 30 minutes with the probe above mentioned in the growth medium (DMEM 1X 4.5g/L glucose (+) L-glutamine (+) Pyruvate; 10% FBS, 0.5% HEPES pH 7.2-7.6 and 10000U/mL Pen; 10mg/mL Strep). Then, the medium was aspired and the cells were wash two times with sterile PBS 1X (1.4 mM KH_2PO_4, 8 mM Na_2HPO_4, 140 mM NaCl, 2.7 mM KCl, pH 7.4), trypsinized and recovered with fresh medium in eppendorf. (Trypsin/medium final concentration 1:10). Cytometric analysis was conducted at final concentration of MitoSox probe 5 µM and 510/580nm excitation/emission as indicate on data sheet. Fluorescence was detected with Gallios flow cytometer calibrated using, at the first, a cellular sample without the probe to eliminate the fluorescence background due to by chemicals used. This experiment was prepared to verify what was the dose tested that would determine significant increase of mitochondrial superoxide produced in consequence to treatment with pesticide.

Mitochondrial superoxide production. After the first experiment in presence of MitoSox, to evaluate the dose of p,p-DDE to be used subsequently during investigation, another experiment with MitoSox probe was conducted at 30µM of p,p-DDE/0.01% DMSO. 30µM represents the dose with which in the previous one experiment it was measured significant increase of superoxide anion produced by mitochondria in the cells treated with p,p-DDE. In this case, control cells were treated with the same dose of DMSO used to dissolve the pesticide.

Cellular Oxidative stress: Total ROS accumulation. Control and treated cells were incubated with CellRox probe (CellROX® Deep Red C10422) in the growth medium (DMEM DMEM 4.5g/L glucose (+) L-glutamine (+) Pyruvate; 10% FBS, 0.5% HEPES pH 7.2-7.6 and 10000U/mL Pen; 10mg/mL Strep) for 30 minutes. After incubation, the medium was eliminated and the cells were washed in two times with sterile PBS 1X (1.4 mM KH_2PO_4, 8 mM Na_2HPO_4, 140 mM NaCl, 2.7 mM KCl, pH 7.4), trypsinized and recovered with fresh medium in eppendorf. (Trypsin/medium final concentration 1:10). Cytometric analysis was conducted at final concentration of CellRox 5 µM and analyzed at 640/665nm excitation/emission, as indicate on data sheet. Fluorescence of samples was detected with Gallios Flow cytometer calibrated using the first sample read without the probe, to eliminate the fluorescence background due to by chemicals used.

TMRE experiment. To verify if in presence of p,p-DDE there was a changing of the mitochondrial membrane potential in the cells treated with pesticide respect to controls, was used TMRE probe (Cat. No. T669, Life technology) that enters in the mitochondria in dependent manner to $\Delta\psi$, as indicate on data sheet. Before the experimental analysis in

presence of p,p-DDE, Huh7 were tested in presence of three different doses of TMRE (500nM, 1µM and 10µM incubated for 15 minutes in cellular growth conditions) in +/- CCCP (30µM) 1h of pre-incubation. After incubation with CCCP, cellular medium was eliminated and TMRE, diluted in fresh medium, was added in the wells (15 minutes of incubation). After 15 minutes the medium was eliminated, the cells were washed in three time with sterile PBS 1X (1.4 mM KH_2PO_4, 8 mM Na_2HPO_4, 140 mM NaCl, 2.7 mM KCl, pH 7.4), trypsinized and recovered with fresh medium in eppendorf. (Trypsin/medium final concentration 1:10). Cellular suspensions were analyzed by flow cytometer and the TMRE emission was registered. Also in this case, a sample without probe was used to eliminate the background of the chemicals used. Therefore, we have been chosen TMRE 10 µM as the experimental dose because in this condition it was observed significant fluorescence registered but also significative decrease of Fluorescence in presence of CCCP respect to the cells in absence of it. Then, TMRE experiment in treated cells at 24h of exposition with the pesticide was done, as described above, +/- CCCP for each experimental condition.

Cell homogenate. After the treatment period, control cells and p,p-DDE-treated cells were washed with PBS 1X (1.4 mM KH_2PO_4, 8 mM Na_2HPO_4, 140 mM NaCl, 2.7 mM KCl, pH 7.4) and detached from the capsule surface using a scraper and lysed in cold ice lysis Buffer solution (50mM Tris pH 7.4, 150 mM NaCl, 1mM EDTA, 1% NP40. Lysis was prepared in presence of: phosphatase Inhibitors (2mM NaOVa, 100mM NaF, 20mM NaPPi); deacetylase Inhibitors (5mM Nicotinamide, 1mM Na-Butirrate); protease inhibitors (1 tablet cOmplete Protease Inhibitors (Roche) /10mL lysis buffer. The homogenate was centrifuged at 750g for 10 min. Pellet, that contains cellular debris (membrane, some organelles, cells not broken and nuclei) was discarded. Supernatant was stored at -20°C. It contains proteins and all molecules that were present in the cells. It was used to quantify the fold change of H_2O_2 accumulated in the treated cells vs control cells by Amplex Red-Hydrogen Peroxide Kit and to quantify the proteins modulation by Western Blotting.

Sub cellular fractionation. Subcellular fractionation was used principally to isolate mitochondria. It was used a protocol described by I. Dimauro et al. 2012, validate by western blotting analysis of specific proteins of each subcellular part[149]. After isolation, mitochondrial fraction was precipited at 11,000g for 20 minutes and lysed in cold ice lysis Buffer solution (above described to obtain total proteins extract).

Proteins quantification. Proteins concentration in the samples were quantified with Pierce™ BCA Protein Assay Kit, Thermo Scientific, Cat. No. 23225. This method is accurate and quick to know the protein concentration of biological samples. As indicate in the User guide, it was prepared a standard curve using a white sample and four standard curve points of Bovine Serum Albumin (BSA stock solution 2mg/mL) next to samples in examination. All samples were tested in Pierce 96-Well Plates (Cat. No. 15041) and read at 560 nm in a plat reader. The medium obtained from both values was used to calculate protein concentration.

H_2O_2 quantification in the total homogenate. To evaluate H_2O_2 accumulation in the cells, was used Amplex® Red Hydrogen Peroxide/Peroxidase Assay Kit, Cat. No. A22188**.** The analysis was conducted on total protein extract and the experiment was conducted as

described on data sheet. H_2O_2 was quantified with a spectrophotometer and it was represented graphically as fold change of H_2O_2 expressed in pmol/mg of proteins.

Western blotting. Western blotting analyses were conducted on total proteins homogenate and on mitochondrial extract. Were loaded 50µg (total proteins extract) and 80µg(mitochondrial proteins extract). Proteins were denatured in 2×Loading buffer (final concentration: 120mM Tris HCl, pH 6.8, 20% glycerol, 4% SDS and 0,05mM DTT) at 95°C and loaded onto to SDS–polyacrylamide gels together with a prestained protein marker (Spectra Multicolor Broad Range Protein Ladder, Cat. No. 26623 - 10,000-240,000 Da). After the run, the proteins were transferred on PVDF membranes (Immobilon-P, Millipore, 0,45µm, Schwerzenbach, Switzerland) at 350mA for 60 minutes. The membranes were blocked in blocking buffer (1×PBS/ 1% Tween-20, 5% milk) for 60 minutes at room temperature and incubated overnight at 4°C with the antibody of interest. The second day, membrane were washed in 1×PBS/ 1% Tween-20 and incubated 1h at room temperature with the secondary antibodies labeled with horseradish peroxidase enzyme in 1×PBS/ 1% Tween-20, 5% milk. Finally, membranes were washed in 1X PBS/1% Tween-20 and the protein bands were revelated with ECL system (Amersham ECL Western Blotting Detection Reagent) using X-ray Film for Western Blot Detection (Thermo Scientific CL-XPosure Film) in automatic revelator. To quantify the bands optical density, was used BIO RAD Quantity One® 1-D Analysis Software.

Primary Antibodies used:
SOD2: NB100-1992 (Abcam) SOD2/Mn-SOD Antibody, Rabbit Polyclonal, 1:2,000.
Casp3: 9662 (Cell Signaling), Rabbit Polyclonal 1:2,000.
BAX: Bax Antibody 2772 (Cell Signaling), Rabbit Polyclonal 1:4,000.
Casp9: 9508 (Cell Signaling), Mouse monoclonal, 1:2,000.
PARP: PARP Antibody #9542 Rabbit Polyclonal, 1:2,000.
Grp78: 3177 (Cell Signaling) Rabbit Monoclonal, 1:4,000.
Mfn2: Anti-Mitofusin 2 antibody (ab56889), Mouse monoclonal, 1:2,000.
Drp1: 611112 (BD Transduction Laboratories), mouse monoclonal, 1:2,000.
pDRP1: Phospho-DRP1 Antibody (Ser616) #3455, Rabbit Polyclonal, 1:2,000.
PGC1a: ab18058(Abcam) Anti-Vinculin antibody [SPM227], Rabbit Polyclonal, 1:2,000.
OPA1: NB110-55290 (Novus Biologicals), Rabbit Polyclonal, 1:2,000.
TIM44: Anti-TIMM44 antibody [EPR16821] (ab194829), Rabbit monoclonal, 1:4,000.
ATF6: Sc-22799 (Santa Cruz Biotechnology), Rabbit Polyclonal, 1:2,000.
pIRE: Anti-IRE1 (phospho S724) antibody (ab48187) Rabbit Polyclonal, 1:2,000.
Actin: A1978 (Sigma Aldrich) Anti-β-Actin antibody, mouse polyclonal, 1:4000.
Vinculin: ab18058 (Abcam) Anti-Vinculin antibody [SPM227], Mouse Monoclonal, 1:4,000.

Secondary antibodies used:
Anti-Rabbit: 711-035-152 Peroxidase-AffiniPure Donkey Anti-Rabbit IgG, 1:10,000.
Anti-Mouse: 715-035-150 Peroxidase-AffiniPure Donkey Anti-Mouse IgG, 1:10,000.

ATP measure. To quantify total ATP in the cellular homogenate it was used ATP Determination Kit (Invitrogen detection technologies, Cat. No. A22066). Cells were rapidly homogenate in homogenization buffer (6 M guanidine HCL, 100 mM Tris (pH 7.8), 4 mM EDTA) on ice. 10 µL of homogenized sample were used to measure protein content with Pierce kit above described. The remaining samples were boiled for 5 minutes and centrifuged for 3 min at maximum speed in a refrigerated tabletop centrifuge that has been prechilled to 4ºC. Supernatant was transferred in a tube and pellets were discarded. Therefore,10 µL of the supernatant were transferred to individual tubes. Now, reagents preparation, standard curve and Samples analyses were done as indicate by manufactory on data sheet. The ATP concentration was obtained by comparing the luminescence measured for each sample to the ATP standard curve.

Confocal microscopy. Huh7 cells were growth on microscope support glass slide (22mm Round Microscope Glass Slide Cover Slips Blank Slides Coverslip Thickness 0.13 - 0.17mm) and treated with p,p-DDE 30µM when were arrive to 70-80% of confluence. To observe the mitochondria optimally, it is important that the cells do not have a total confluence on the slide. In this way, each cell can be observed in an optimal manner without there being any cellular overlap. The cells were incubate 20 minutes before the analysis with Mitotracker DeepRed, final concentration 5µM. After time, growth medium was eliminated, the cells were washed two time with sterile PBS 1X (1.4 mM KH_2PO_4, 8 mM Na_2HPO_4, 140 mM NaCl, 2.7 mM KCl, pH 7.4), and fresh medium was added for each sample. The images were obtained with animated Z stack and magnification of 63X to observe mitochondria optimally.

Statistical analysis

The graphics were obtained with Graph Pad Software. The experiments conducted in vivo, were analyzed in duplicate for each sample and compared using t test analysis. All experiments conducted in vitro were analyzed in triplicate or in quadruplicate and compared using the analysis of variance (ANOVA). In both cases, the results were represented graphically as medium ± SD (Standard deviation). Significant variations between the groups analyzed were considerate for $p<0,05$.

Results

***In vivo* analyses**

Hepatic stress. Our previous studies conducted on liver, have been demonstrated that the experimental conditions used *in vivo* produce increase of hydrogen peroxide released from isolated liver mitochondria. This result indicates that mitochondria of treated rats produce superoxide anion in significant way respect to control rats. In addition to that, to clarify if in presence of superoxide anion there was ROS accumulation in the liver in our different experimental conditions, we have also evaluated the accumulation of lipid peroxides in the total tissue homogenate. The results indicate that in D group there was significant accumulation of lipid peroxides vs N (table 2). Lipid peroxidation appear amplified in greater ways in p,p-DDE-treated rats (D+DDE N+DDE, table 2) without differences

between both groups. For this reason we have concluded that saturated fatty acids and p,p-DDE play different roles in the hepatic oxidative stress, in which the pesticide seems to play a predominant role. ROS accumulation in the liver may be depending by different factors[150], but in our studies and in literature appear clear that p,p-DDE causes mitochondrial damage, particularly for the electron transport chain[151]. This effect could be the first cause of superoxide production in correlation to hydrogen peroxide released from mitochondria. Another parameter measured on mitochondrial proteins was the amount of SOD2 by western blotting analysis (Image 1B). The results indicate that this enzyme is slight up-regulated in presence of HF-diet (D and D+DDE group) and in greater ways in N+DDE group. SOD2 immunohistochemical analysis confirms western blotting data (Image 1A). In all treated groups, SOD2 immunolocalization was observed on the mitochondria in the cells around of vessels (Image 1A , picture 1/2). In consequence to this stress in presence of DDE, our investigation have focused the attention on the apoptotic pathway in which the mitochondria have an important role during pro-oxidant species accumulation in the liver. In particular our experiments, have been demonstrated that in presence of DDE there was significant cyt-C release from mitochondria and several morphological alterations of the organelles (table 2)[152]. This mechanism is probably implicates in the apoptotic pathways activation, that it was monitored by cleaved caspase-3 immunolocalization (Image 2A). In addition, it was evaluated the recruitment of monocytes/macrophages in the tissue by using immunohistochemistry and western blot analysis of CD68, as a cellular marker for these cells (Image 3A).

Pro-apoptotic signals activated in the liver. The first analysis was conducted on mitochondrial BAX, a pro-apoptotic protein directly associated to mitochondrial permeabilization, cyt-c release and activation of apoptosis[153]. We demonstrate by western blotting data that in D group there were no differences regarding the amount of mitochondrial BAX respect to control animals (Image 2B). In presence of saturated fatty acids in association with DDE (D+DDE group) we shown that there is a significative increase of this pro-apoptotic proteins vs N and D groups (Image 2B). This condition was also observed in p-p-DDE-treated groups where we found mitochondrial BAX increase respect to controls (Image 2B). These results are in according with mitochondrial release of cyt-C monitored in our previous studies[154], indicating that this pesticide plays a role in the mitochondrial apoptotic pathway activation. To confirm apoptotic pathways activation, also the caspase-3 cleaved form was monitored in the liver of rats. For this analysis we used a preliminary experiment of IHC stain. In the D animals we found also some positive cells around of principal vessels (Image 2A, D group). In D+DDE group we found positivity to cl-Casp-3 principally localized in the cytosol of the vacuolated cells around of vessels (Image 2A, D+DDE group). In the end, also for the N+DDE group we observed positivity to cl-Casp-3 in the cytosol of perivasal cells (Image 2, N+DDE). In addition to these results, during the apoptotic processes, death cells will be eliminated through the phagocytic cells recruited in the organ by chemotactic signals. To monitor the effect of p,p-DDE on the monocytes/macrophages recruitment, we measured the amount of CD68 (glycoprotein expressed in monocytes/macrophages) in the total protein extract[155] (Image 3A/3B, western blotting data). In this way, the apoptotic cells will be eliminated to maintain the tissue integrity. In our experimental conditions, we found that in presence of saturated fatty acids

(D and D+DDE groups) there is a significant increase of CD68 respect to controls. This result could indicate that saturated fats have a possible pro-inflammatory role put in place to regulate cellular turn-over in condition of lipotoxicity[156]. In D+DDE group we did not found differences in comparison to D group. In the end, in the N+DDE group we found the greater increment of CD68 in the liver, indicating macrophages recruitment (Image 3B).

ER-morphology variation in condition of stress. The electronic microscopy was used to monitor ER-morphology in the liver (Image 4). In association to that, the amount of Grp78 in the total protein extract was quantified by western blotting as a monitor of ER-stress[157]. The sections analyzed shown a normal morphology in the control group, in fact, we didn't observed reticular bulges and the cisterns have tubular form and are parallels to each others. In D group we observed that the ER cisterns seems swollen in some points in the cells. Also in presence of p,p-DDE this condition was observed, but in extensive way respect to D group. This ER-morphologic change, in association to Grp78 up-regulation could indicate hepatic ER-stress. Regarding to Grp78, we observed significant up-regulation of this chaperon in all treated groups, in according to ER-morphology change.

***In vitro* analysis**

Mitosox and Cell-Rox experiments indicate a possible role of p,p-DDE in the oxidative stress generation. To assess whether the Huh7 was a good model for toxicological analyzes, and in particular if in this cellular line the DDE activates the same pathways observed *in vivo*, my first experiment was done using MitoSox probe to evaluate what dose of this pesticide would determine a significant increase of superoxide anion produced by mitochondria, that was a condition also observed *in vivo*. The results obtained indicate that there is a correlation between p,p-DDE dose used and the superoxide anion produced by cells (Image 5). In particular, it was observed significant increase of superoxide at 30µM of p,p-DDE after 24h of exposition. Since control cells were not treated in presence of DMSO, it was conducted another experiment at 24h and 30µM of p,p-DDE, using 0.01% DMSO also in control cells. The results obtained indicate that superoxide anion increases in significant way respect to control after 24h of exposition. In addition, ROS accumulation measured in live cells using CellRox probe in cytofuorimetric analyses, confirms a role of DDE in the oxidative stress generation *in vitro* (Image 6).

Cellular hydrogen peroxide accumulation. This analysis was conducted on the total protein extract. The same samples were used to monitor the amount of SOD2 by western blotting. Results indicate increase of hydrogen peroxide in the samples treated with DDE respect to controls. This experiment confirm the results obtained on the liver rat *in vivo* in which the hydrogen peroxide released from mitochondria were increased in presence of p,p-DDE. Western blotting experiment to MnSOD/SOD2 was conducted to validate if the hydrogen peroxide accumulated in the cells treated with pesticide would be associated with the up-regulation of this enzyme. The result obtained confirm SOD2 up-regulation (Image 7A). We concluded that there is a correlation between hydrogen peroxide accumulation in the cells and SOD2 suggesting that SOD2 may be used to control the excessive accumulation of superoxide anion in the cells. In this way, a part of H_2O_2 formed by SOD could be eliminate by the cellular antioxidant activity. In comparison to *in vivo* studies,

where SOD2 was up-regulated in particular in presence of p,p-DDE, this antioxidant enzyme seems a good parameter to monitor mitochondrial stress induced in presence of p,p-DDE *in vivo* and *in vitro*.

Variation of mitochondrial membrane potential. TMRE is another probe used in my investigation *in vitro*. When the mitochondrial membrane potential is compromised, and decreases respect to the normal growth conditions, TMRE- fluorescence registered with Cytofluorimetric analysis is lower. Our results indicate that after 24h in presence of the pesticide there is a significative reduction of TMRE-probe emission registered with machinery and for this reason we can conclude that the mitochondrial membrane potential is decreases in presence of the pesticide (Image 7B). This result is reinforced by western blotting data obtained on TIM4 (a constitutive protein normally used as mitochondrial control guide). In fact, we did not notice significative variations of TIM44 indicating that mitochondrial mass is approximately not varied in presence of p,p-DDE after 24h of exposition.

Mitochondrial stress and ATP reduction in presence of DDE. In presence of p,p-DDE we observed a change of different parameters: increase of superoxide anion produced by mitochondria, increase of hydrogen peroxide accumulated in the cells, decrease of mitochondrial membrane potential and increase of SOD2. These parameters indicate mitochondrial stress. In this stress condition we demonstrate also a reduction of total ATP produced in the cells in significant way respect to controls (Image 7B).

Mitochondrial Dynamic change. Another important goal of this research was the analysis of mitochondrial dynamic proteins. In our experimental conditions *in vitro* I evaluated if the mitochondrial dynamic proteins were regulated respect to control cells. The amount of total fixion and fusion proteins analyzed (DRP1, MFN2 and OPA-1) demonstrate significant increase of these proteins in presence of p,p-DDE (Image 8A/8B). In association to this data, the increase of PGC1α measured by western blotting on total protein extract indicate mitochondrial biogenesis in presence of pesticide[158],[159] (Image 8A). This mechanism may be implemented by cells to replace damaged mitochondria and not to increase their number in the cells[160]. The results obtained on Huh7 cells model are very similar to the results obtained in our experimental model *in vivo*. In fact, our previous investigation on liver rat indicate in presence of p,p-DDE increase of MFN2 and DRP1 at mitochondrial level[161]. In regard to OPA1, Huh7 cells shown protein cleavage in treated cells (Image 9). For this reason, in regard to the mitochondrial dynamics variation, it was supposed that the pesticide determines a sequence of events in which it is verify mitochondrial alteration probably due to by ROS accumulation, disoligomerization of OPA-1 complexes, both mitochondrial potential and ATP reduction and changing of their morphology. Confocal microscopy confirms mitochondrial morphology variation (Image 10). Mitotracker Deep red was used to localize the mitochondria in the cells. Firstly, mitochondrial fragmentation in presence of pesticide was observed. This result is in according to others studies in presence of ROS that have been demonstrate correlation between ROS accumulation and mitochondrial fragmentation in different cell lines[162],[163]. In addition, associated to this fragmentation it was observed in more cells a lot of donut mitochondria that were described in condition of stress[164].

ER-stress. The first protein analyzed by western blotting, Grp78, is up-regulated in p,p-DDE treated cells respect to control cells (Image 11) . We have been able to demonstrate that this hepatic cell line responds in the same way of the liver rats in regard to this chaperon up-regulation. Truncated ATF6 was monitored as another responsive element activates in presence of ER-stress. It appears increase in presence of pesticide (Image 11). We didn't observe differences between control and treated cells for pIRE1a, indicating that UPR signaling after 24h of exposition is only partially activated in Huh7 cells[165] (Image 11).

Apoptotic pathway activation in presence of DDE. (Image 12) In condition of mitochondrial dysfunction in which I measured decreasing of mitochondrial membrane potential and ATP synthesis, ER-stress and ROS accumulation in the cells treated with DDE, it was analyzed some proteins modulated during the apoptosis. We focused our attention to understanding what was the mitochondrial role in this pathway *in vitro*. The analyses were conducted by western blotting on total proteins extract. Results obtained indicate in presence of DDE caspase-9 cleavage, decreasing of caspase-3 full length and PARP cleavage compared to control cells. In addition, I also demonstrate accumulation of BAX in according to literature data that indicate a role of BAX in the mitochondria permeabilization during apoptosis[166]. In fact, the accumulation of BAX in association to increase of cleaved caspase-9 may indicate that the cytochrome c was released from mitochondria, resulting in apoptosome activation and cleavage of caspase-9. Consequently, the decreasing of full caspase-3 could be due to its activation in presence of DDE, as suggest by cleaved PARP measured.

Discussions.

The results obtained on liver rats and in hepatic Huh-7 cell line, indicate toxicity in presence of p,p-DDE. *In vivo*, increased of SOD1 and SOD2 were observed, indicating pro-oxidant role of the pesticide after 4 weeks of oral administration. The increment of SOD2 at mitochondrial level was particularly observed in N+DDE group where the pesticide is not associated to saturated fatty acids. In addition, in the both two groups treated with DDE, increased levels of BAX in the mitochondrial protein extract (associated to cl-caspase 3 IHC stain in treated rats), confirm that this pesticide is probably implicates in the apoptotic pathway activation by mitochondria, as indicate with previous studies obtained on liver that demonstrate increment of cytosolic cyt-c[167]. Furthermore, we have not satisfactory experimental results to establish what is the treatment by which the apoptotic pathway is more or less active in presence of the pesticide but we hypnotized that p,p-DDE explicate its toxic power in greater manner when is not associated to HF-diet, in according to our results. In condition of apoptosis, a lot of phagocytic cells implicated in the elimination of cells death, are recalled in the tissue. Our experiments in fact, have been shown that in presence of pesticide, where the apoptotic pathway appear stimulated, there is an important increment of CD68 as marker of macrophages infiltration[168]. Probably these cells were recalled in the tissue by chemotactic signals and absolve in their specific functions to control the maintenance of tissue functionality[169]. Are not very clear *in vivo* what are the sequences of events that activate apoptosis, but in our studies it seems that is a part of the redox imbalance due to mitochondrial damage caused by pesticide. p,p-DDE toxicity was demonstrated also *in vitro*, where at 30 μM of pesticide were increased both superoxide anion and hydrogen peroxide accumulation in the cells. As observed *in vivo*, in Huh7 cells there is increase of SOD2 levels that could be the cause of the hydrogen peroxide accumulation. The hypothesis of mitochondrial damage *in vitro* could be consolidated by a reduction of mitochondrial membrane potential (TMRE assay) and of the amount of total ATP after 24h of exposition, indicating that mitochondrial function is compromised. In addition, mitochondrial stress seems to associate with different pathways activated in the cells to control their functions:

- UPR responsive elements activation (ATF6 and Grp78 incremented), that are used in the cells as compensatory mechanisms to respond, initially, to the stress conditions;
- Mitochondrial dynamics variations and mitochondrial biogenesis, in order to eliminate a part of damaged mitochondria[170] that they were replaced thanks to biogenesis;
- Cellular apoptosis as shown using BAX, cleaved caspase-9 and cleaved PARP.

Conclusions

In conclusion, our research group demonstrate *in vivo* a progression to oxidative damage in presence of p,p-DDE that explicates its toxicant power in greatest measure in condition of normal diet. In presence of fats, with probably, a part of pesticide remains sequestrated in inert form in the lipids indicating in part a possible antagonist role of fatty acids against the pesticide. Moreover, if p,p-DDE undergoes to bioaccumulation phenomena in the tissue rich in fats, future studies could be focused to the effects during a period of caloric restriction to simulate yo-yo effects, typical eating disorder behavior of the 20th century. In according to

in vivo analyses, and other studies conducted in presence of p,p-DDE[171], preliminary studies conducted on Huh7 cells indicate that organochlorinated insecticide determine alteration of mitochondrial function and apoptotic pathway activation probably started by mitochondria as confirmed by increased level of BAX, cleaved caspase 9 and PARP activation. Other experiments will be carried out in future using antioxidant molecules, such as N-acetylcysteine amide (NAC)[172], to confirm this data in regard to mitochondrial toxicity induced by ROS accumulation in presence of p,p-DDE and to validate if Huh7 cells are a good cellular model for preliminary studies of hepatic toxicology.

Final conclusions.

Our results demonstrate that p,p-DDE explicates its pro-oxidant role in the organs examined *in vivo* and in culture *Huh7* cell line. The results obtained *in vivo* indicate that in presence of saturated fatty acids alone, lipotoxic effects are generate in the testis, kidney and liver. In presence of p,p-DDE the organs respond with different and common mechanisms to mitigate the oxidative stress and the mitochondrial impairment induced by pesticide (clearly observed in the testis and liver). In both p,p-DDE-treated groups analyzed we found similar responses in regard to the up-regulation of antioxidant enzymes, chaperones and pro-oxidant species particularly measured in the liver. However, in D+DDE group where two stress-induce conditions are used together, we never found synergic effect of p,p-DDE and saturated fats. This data indicate that, probably, p,p-DDE predominantly explicates its toxic power in condition of normal diet alone. This data could be due to by the lipophilic characteristic of the DDE that, in presence of a rich lipid matrix, remains associated to the fatty acids. Other researchers have been demonstrate that the p,p-DDE accumulation in liver of rats is directly dependent to the fatty acid used in the diet[173]. Then, it is probably that in the organs of D+DDE animals, a part of pesticide remains associated to the fats in inert form. In this way, p,p-DDE does not generate its maximum toxic power. *In vitro*, in the human hepatocarcinoma cells, we found that 30μM of p,p-DDE determine mitochondrial damage. Reduction of mitochondrial membrane potential, permeabilization trough the pro-apoptotic protein BAX and reduction of the ATP produced, are the consequences of the ROS accumulation in the cells. Finally, apoptotic pathway is activated, as shown by cl-PARP increase. This protein, that is involved in the repair of DNA during the environmental stress[174], is cleaved during apoptosis functioning as a marker of apoptotic cells[175] for investigators. In addition, donut mitochondria and their fragmentation were observed respect to control cells. For this reason we concluded that p,p-DDE generates mitochondrial and cellular oxidative stress, reduction of ATP and activation of the apoptosis.

Tables and Images

Common Images used in the manuscripts.

Table 1: Diets composition.

	Normal diet	High fat diet	Normal diet + DDE	High fat diet + DDE
Energy (Kj/g)	15,47	19,23	15,47	19,23
Proteins%	29	29	29	29
Lipisd%	10	45	10	45
Type of lipids	Saturated	Saturated	Saturated	Saturated
Carbohydrates%	61	26	61	26
p,p-DDE	NO	NO	10mg/Kg b.w orally	10mg/Kg b.w orally

Table 2: Previous data obtained on Liver used to conduce new experiments *in vivo* and *in vitro*.

Experiment	N	N+DDE	D	D+DDE
H_2O_2 release from mitochondria	Basal levels	*	*	*
Lipid Peroxides (total homogenate)	Basal levels	**/#	*	**/#

Previous studies, indicate oxidative stress in the Liver, particularly evalued in presence of p,p-DDE. Our research group, have been demonstrate the correlation between p,p-DDE and oxidative stress in the liver of *Wistar* rats. *$p<0,05$ vs N; #$p<0,05$ vs D.

Tables and Images Manuscript 1:

Toxicity induced by the organochlorine pesticide p,p-DDE in *Wistar* rat testis. Apoptotic stimuli and compensatory mechanisms activated in conditions of stress.

Table 2: Our previous results.

Previous results	N	D	D+DDE	N+DDE
Testosterone Levels	-	↓ *	↓ *	↓ *#
Ox consumption (State 4)	-	No change	↓ *#	No change
Ox consumption (State 3)	-	No change	↓ *#	↓ *#
RCR (State 3/State 4)	-	No change	↓ *	↓ *#

Table2: Previous studies conducted on Testis. Testosterone levels, mitochondrial oxygen consumption and Respiratory Control Rate. *p<0,05 vs N; #p<0,05 vs D.

Image 1: Morphological analysis

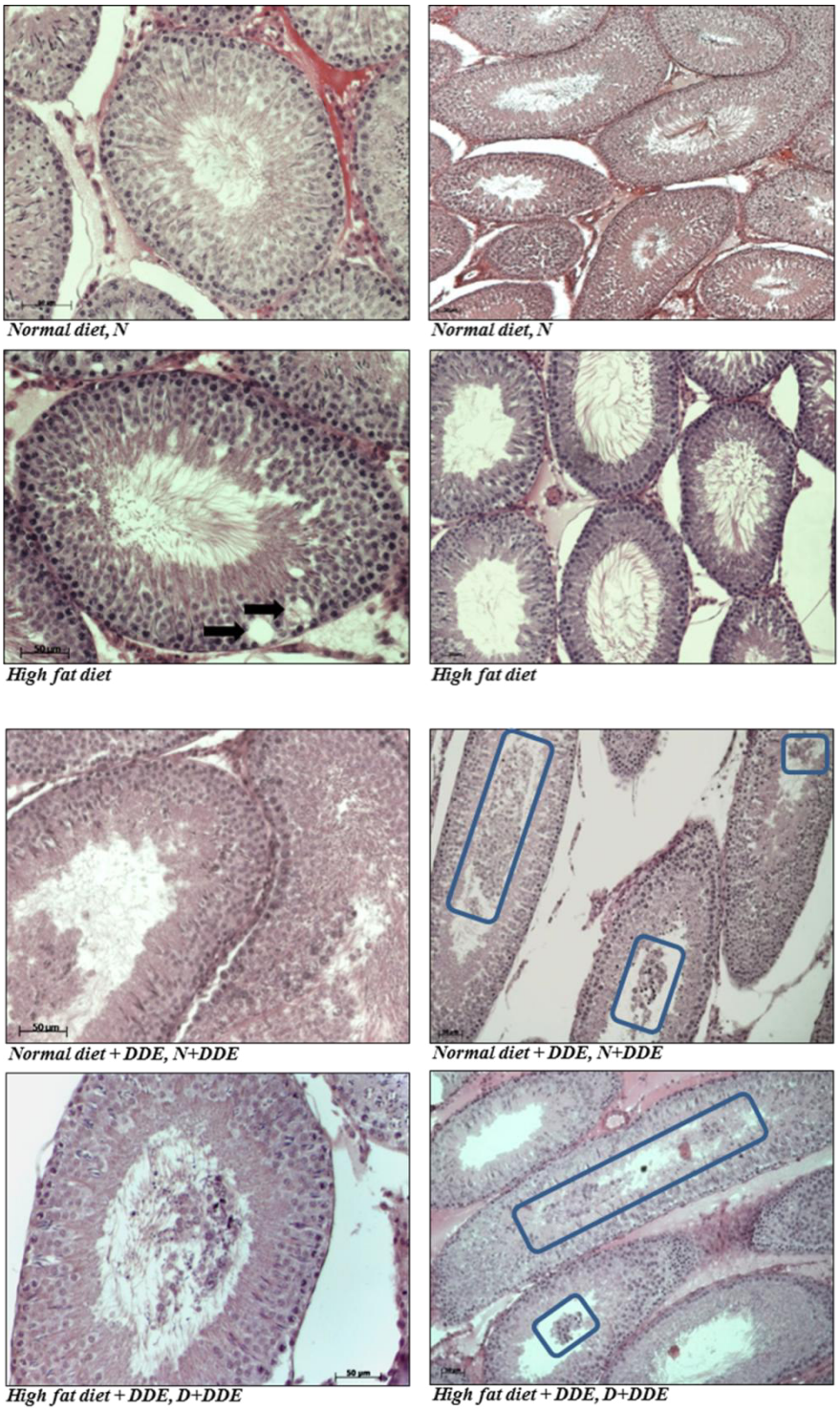

Vacuolization of the basal layer in some seminiferous tubule

Undifferentiated cells in the tubule lumen

Image 1: D group exhibits vacuolization of the basal layer in some seminiferous tubule (black arrows); In both groups in presence of the pesticide (D+DDE and N+DDE) it was observed release of undifferentiated cells in the tubular lumen (blue rectangles). Microscope magnifications used: 10X and 20X. Scale bar applied: 50µM

Image 2: Western blotting analysis

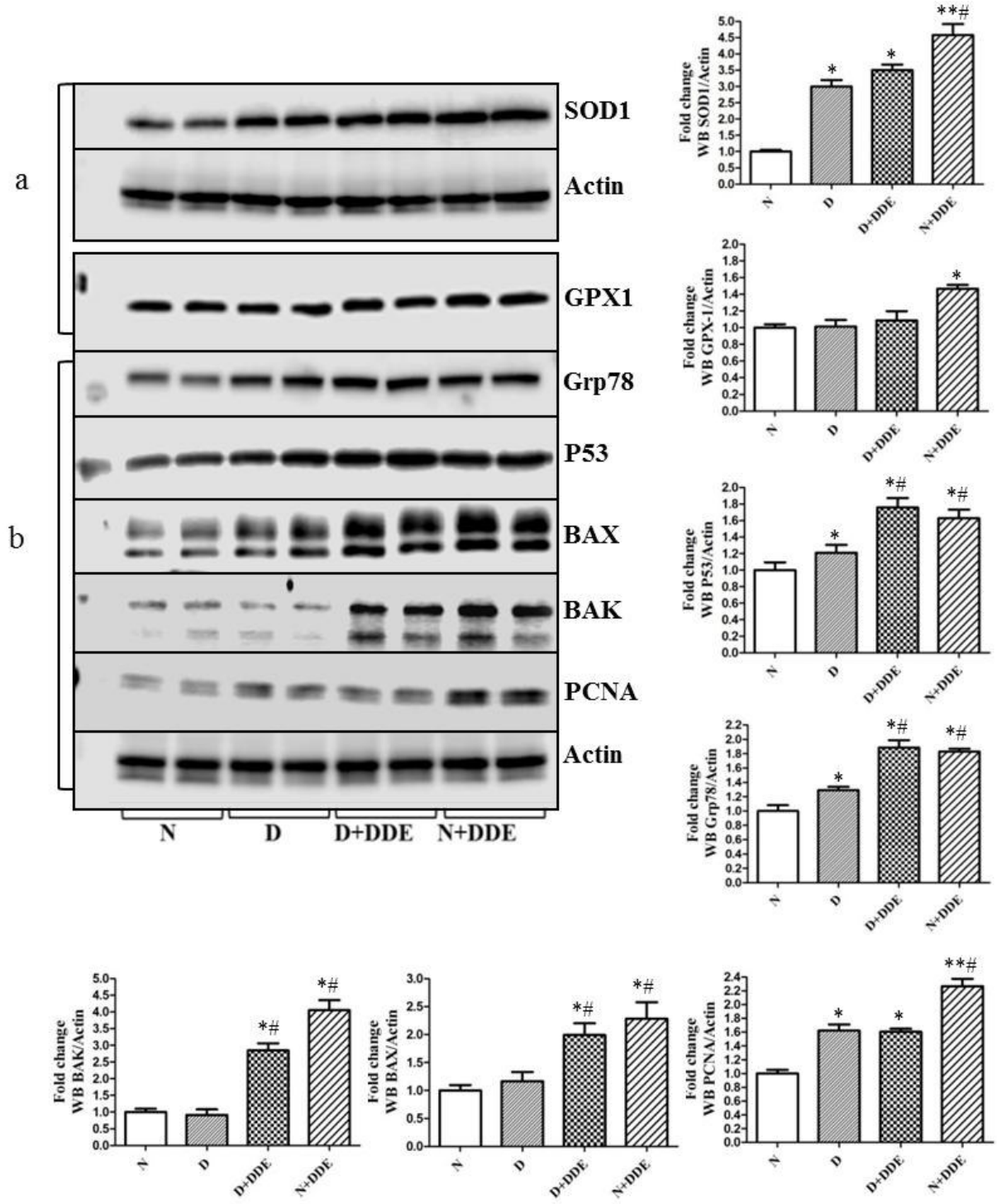

Image 2: Western blotting analysis

A) Western blotting Antioxidant enzymes: (SOD1 and GPX1)

B) Western blotting of proteins involved in the stress responses and apoptosis: (Grp78, P53, BAX, BAK, PCNA)

***p<0,05* vs N; # *p<0,05* vs D.**

Image 3: Apoptosis. Cleaved caspase 3 Immunolocalization in the seminal cells.

Normal and HFD conditions

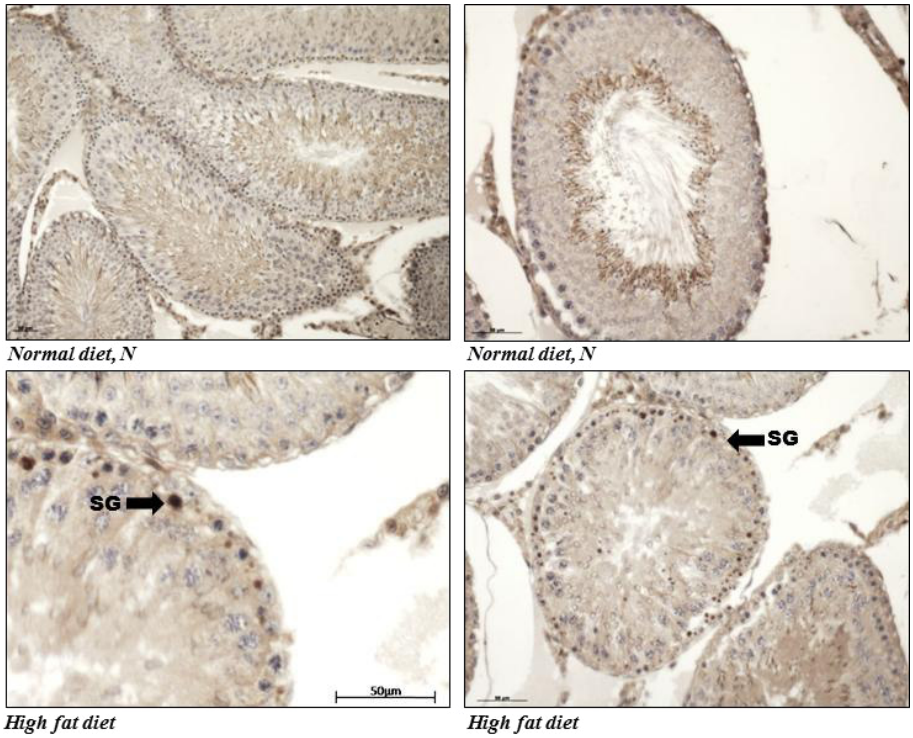

p,p-DDE-treated groups

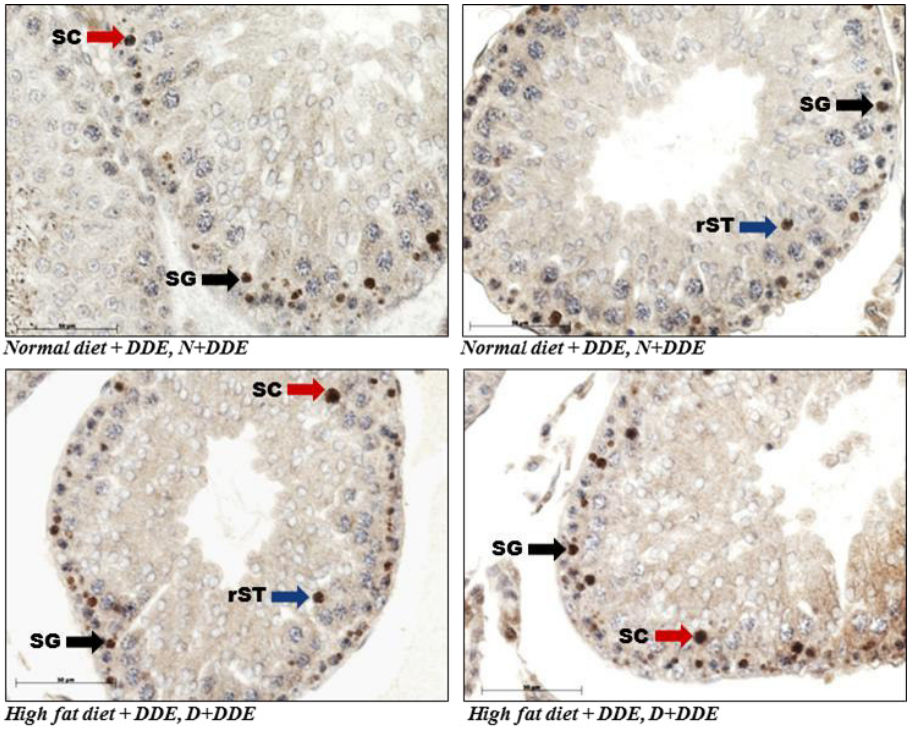

Image 3: cl-casp3 positive cells in the tubules. SG (Spermatogonia, black arrows); SC (Spermatocites, red arrows); rST (round Spermatidis, blue arrows); Magnification used: 10X, 20X, 40X. Scale bar applied: 50 µm.

Image 4: Apoptosis. Cleaved caspase 3 Immunolocalization in the Leydig cells.

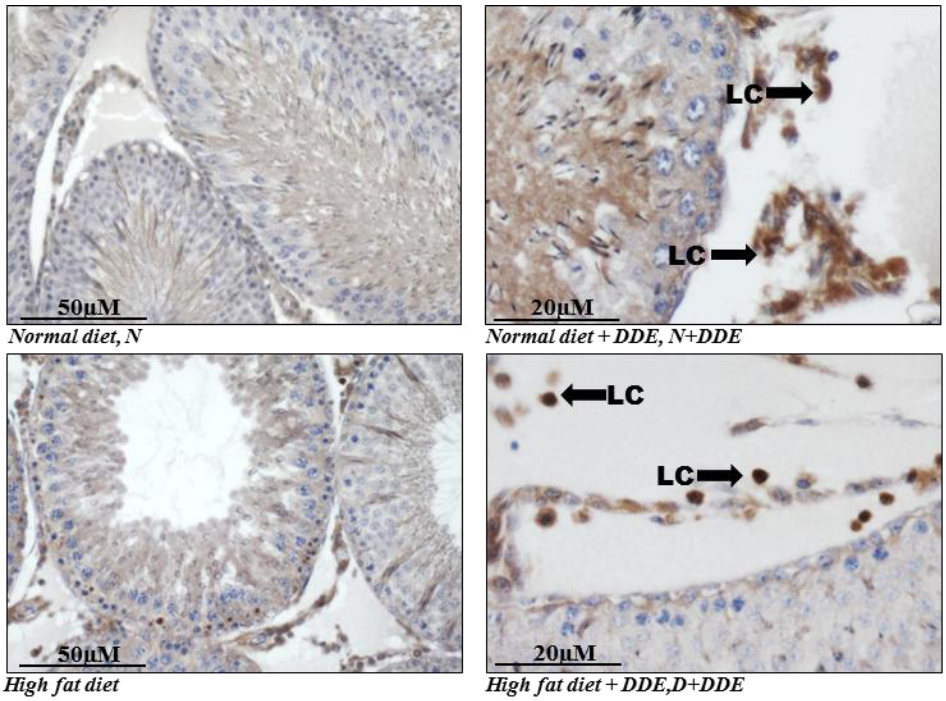

Image 4: cl-casp3 positive Leydig cells (LC). Magnification used: 20X, 40X. Scale bar applied: 20 µm, 50 µm.

Image 5: Metallothionein expression, protein synthesis and Immunolocalization.

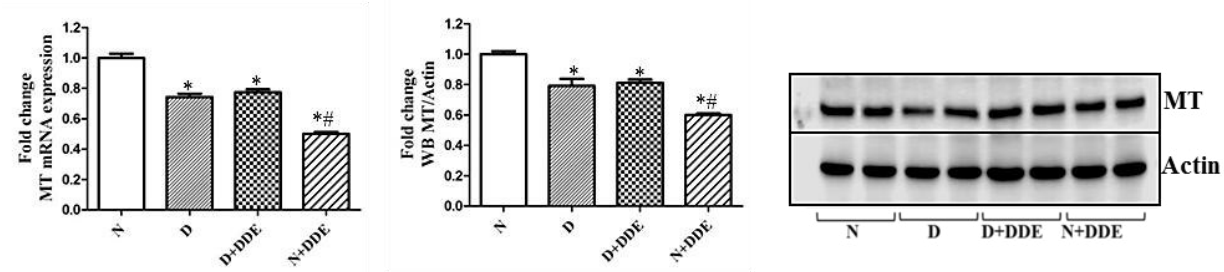

Image 5A. Down regulation of the gene expression and protein synthesis in HFD and p,p-DDE treated animals. **p<0,05* vs N; *#p<0,05* vs D.

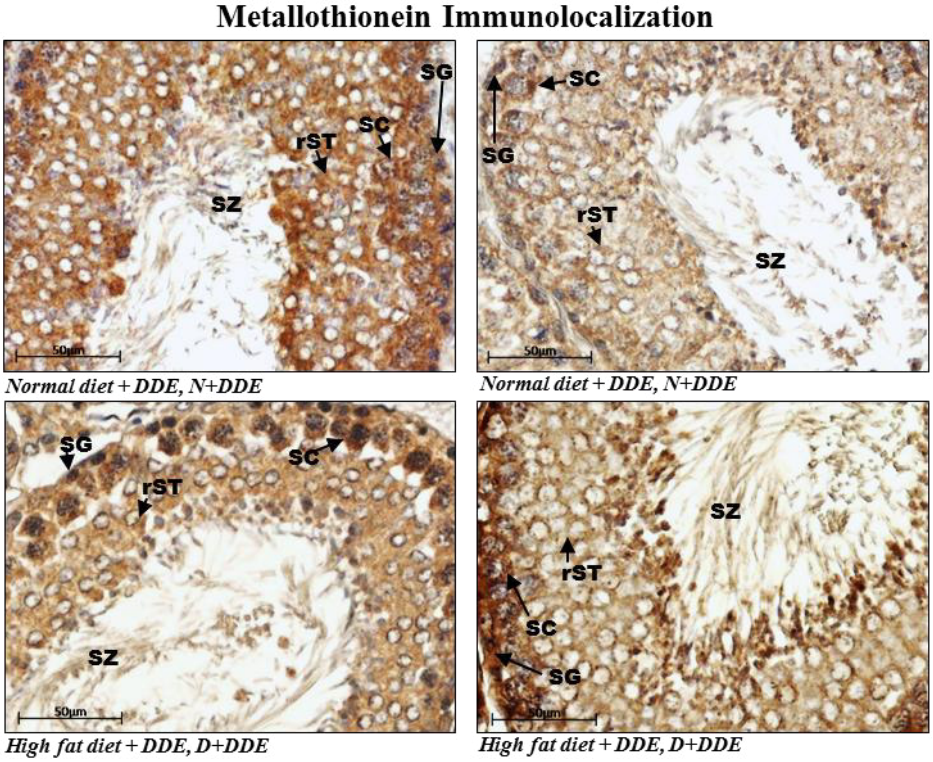

Image 5B. Immunolocalization change in presence of HFD and p,p-DDE. Maintaining of the positivity in basal cells compared to those in the differentiation phase. SG (Spermatogonia); SC (Spermatocites); rST (round Spermatidis); SZ (Spermatozoa). Magnification used: 40X. Scale bar applied: 50 µm.

Tables and Images Manuscript 2:

High fat diet and p,p-DDE: characterization of the endogenous sources used to contrast the kidney injury.

Image 1: Morphological analysis

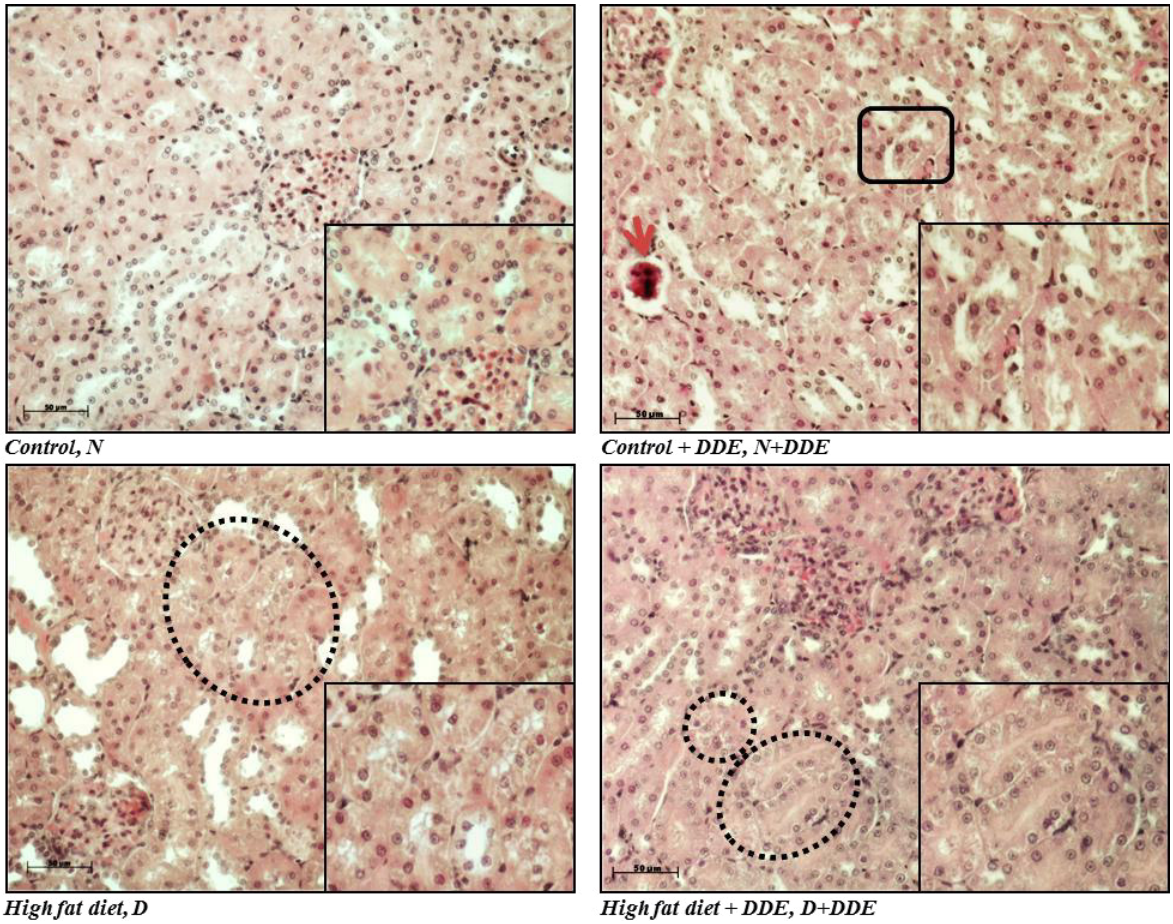

Image 1: Morphological changes. White patches in proximal tubule cells in HFD conditions (black circles). Alteration of some glomeruli (red arrow) and release of cells in the lumen of the tubules (black rectangle) has been observed. Magnification used: 10X; Scale bar applied 50 µm.

Image 2: Western blotting Antioxidant enzymes SOD1/2 and GPX1.

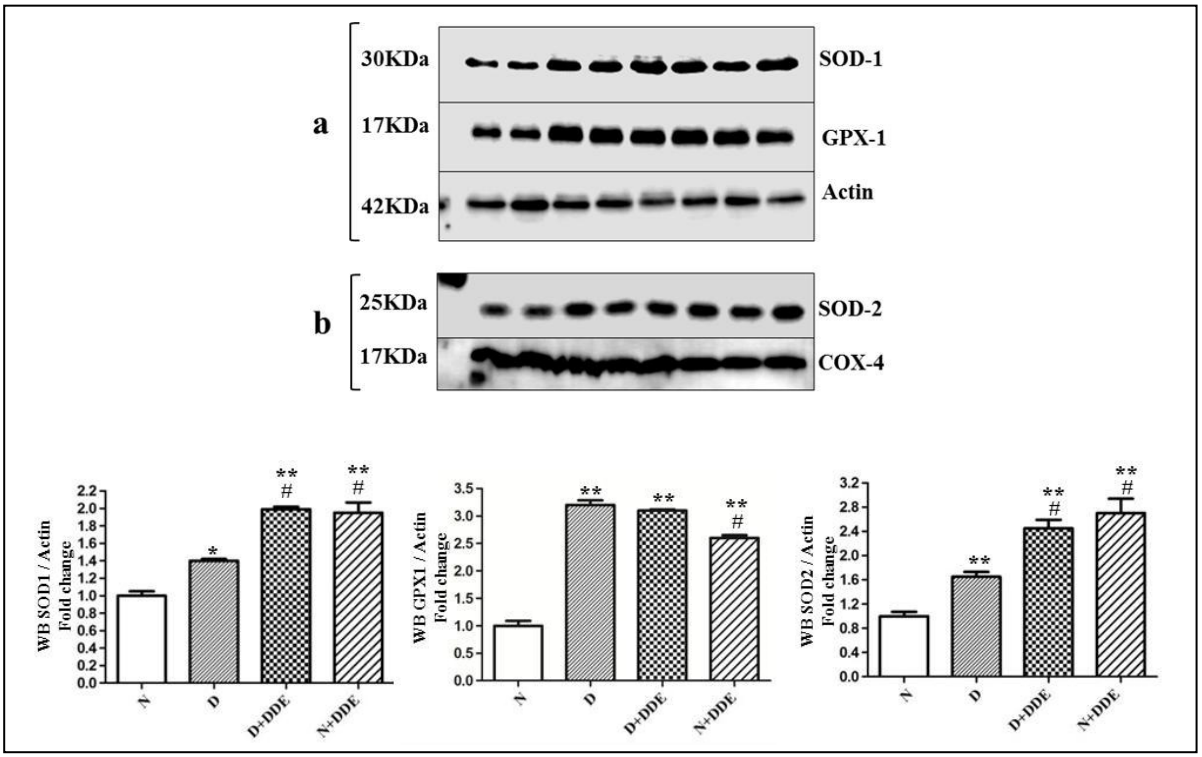

Image 2: Antioxidant enzymes up-regulation. SOD1/2 seem to be more up-regulated in presence of p,p-DDE (D+DDE and N+DDE groups); in the contrary, GPX1 seems to be up-regulated mostly in presence of saturated fatty acids (D and S+DDE groups). a) Cytosolic enzymes analyzed on total protein extract; b) Mitochondrial enzyme analyzed on mitochondrial protein extract. *$p<0,05$ vs N; **p<0,01 vs N; #$p<0,05$ vs D.

Image 3: ER-chaperones

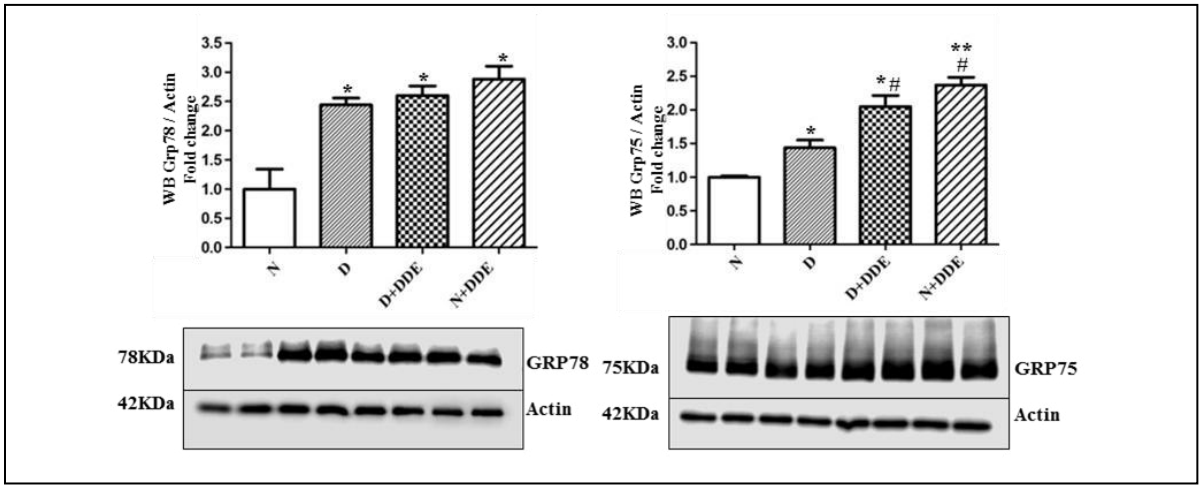

Image 3: chaperones up-regulation in condition of cellular stress. p,p-DDE-treated groups exhibit the greatest increment of the both Grp78 and Grp75 chaperones analyzed. *$p<0,05$ vs N; #$p<0,05$ vs D.

Image 4: Fibrotic effect of the p,p-DDE.

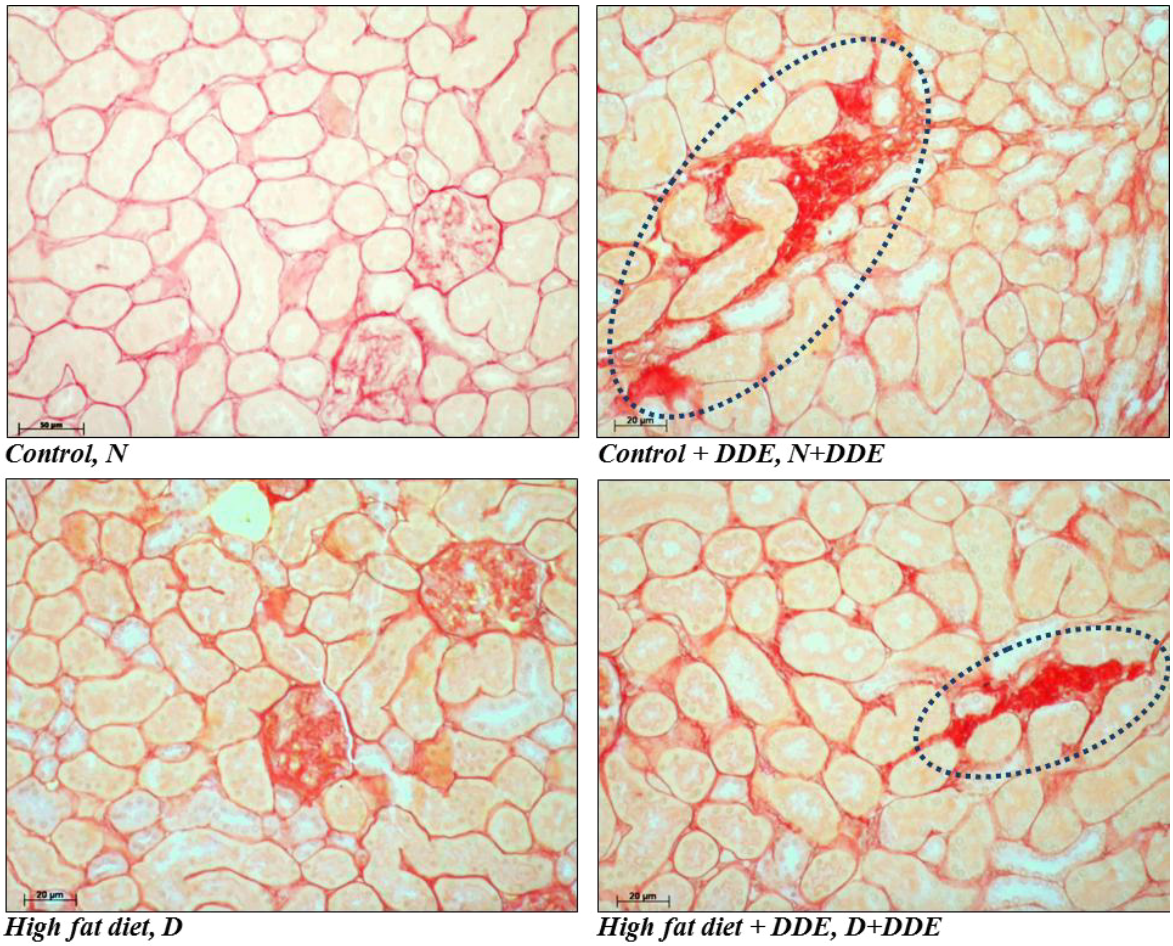

Image 4A: Picrosirius red used to monitor collagen deposition in the tissue. The analyses have been demonstrate differences in the collagen deposition (marked in red) only in presence of DDE. Collagen fibers are evidenced by blue circles. Magnification used: 20X; scale bar applied 20 µm.

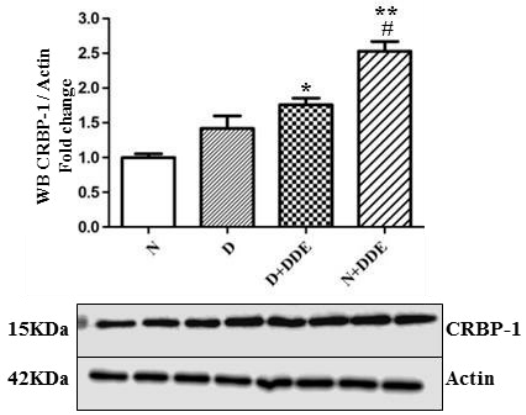

Image 4B: CRBP1: Cellular Retinol Binding Protein-1 have been described as a good parameter to identify renal fibrosis. In our experimental conditions, significant variations were observed only in presence of p,p-DDE, particularly without saturated fatty acids* **p<0,05* vs N; **p<0,01 vs N; *#p<0,05* vs D.

Image 5: Macrophages recruitment in the tissue.

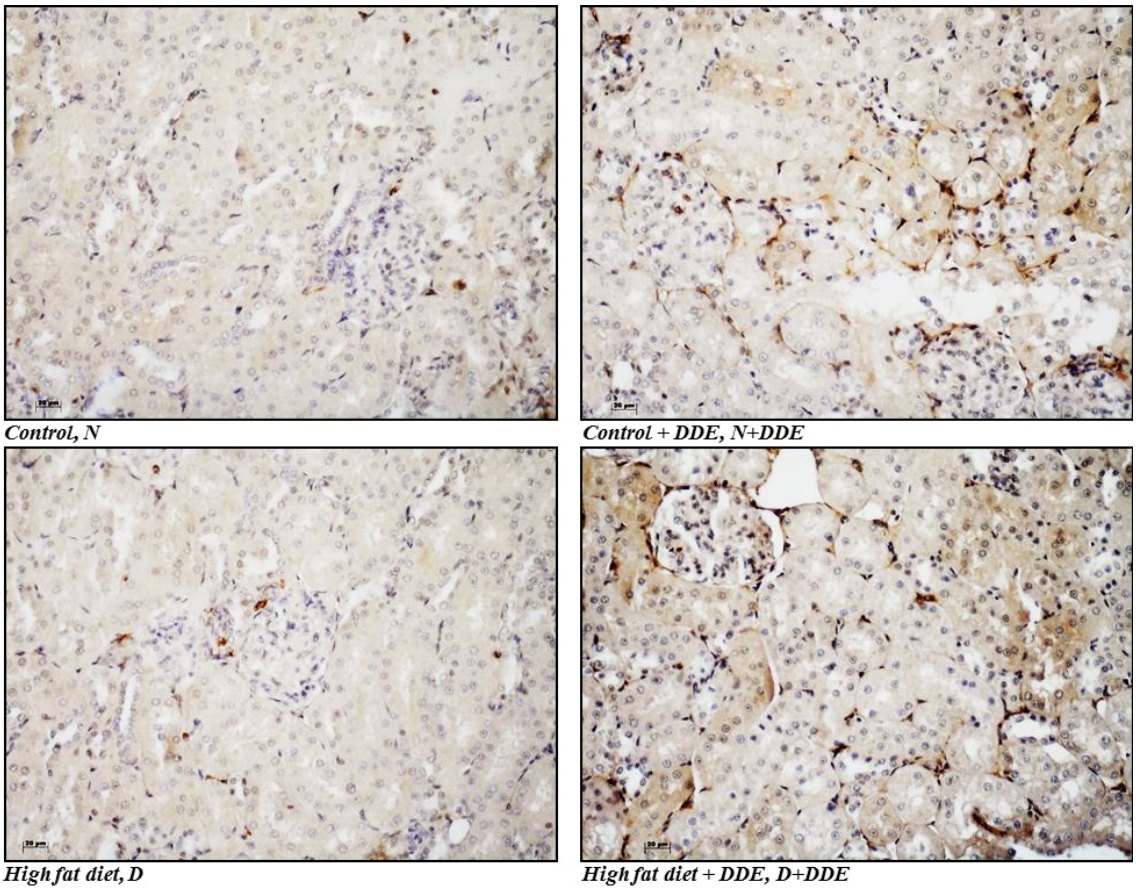

Image 5A: CD68+ was used as a marker to identify monocytes and macrophages in the Kidney. obvious increase in CD68 positive cells (D+DDE and N+DDE) was observed. Magnification used: 10X; scale bar 20µm. These data were confirmed by a western blotting analysis on total protein extract. *P<0,05 vs N; #P<0,05 vs D.

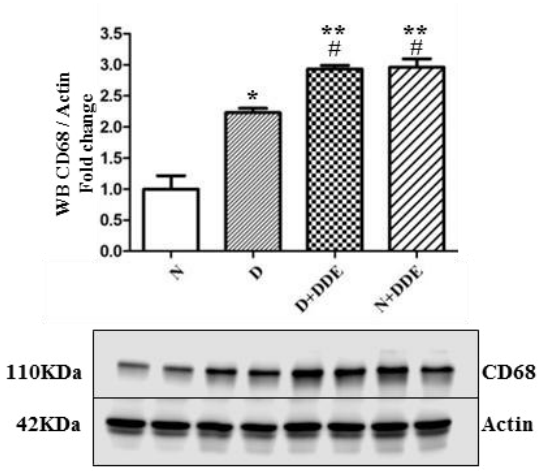

Image 5B: Western blotting data, indicate progressive increase of CD68 in treated groups vs N. Greatest increase seems associated to the groups treated with p,p-DDE. *$p<0,05$ vs N; **p<0,01 vs N; #$p<0,05$ vs D.

Tables and Images manuscript 3:

The involvement of Metallothionein in cellular response to p,p-DDE administration in rat tissues.

Image 1: MT mRNA levels compared in the Liver and Kidney of control animals.

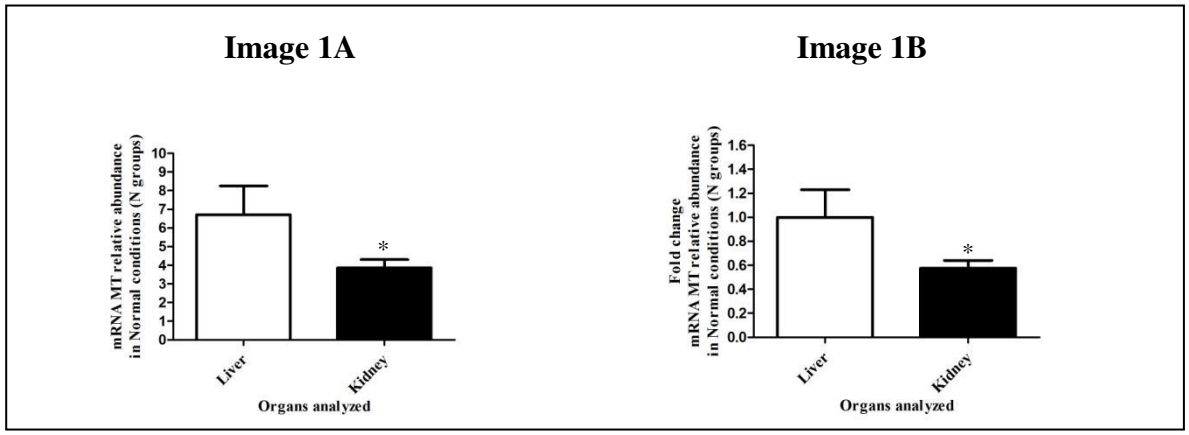

Image 1: Basal levels of the MT mRNA analyzed, indicate that Kidney MT gene expression is about half compared to the Liver. The result was expressed as relative abundance and Fold change to quickly appreciate the RT-PCR result. **p<0,05*

Image 2: MT expression under our experimental conditions in the Liver and Kidney.

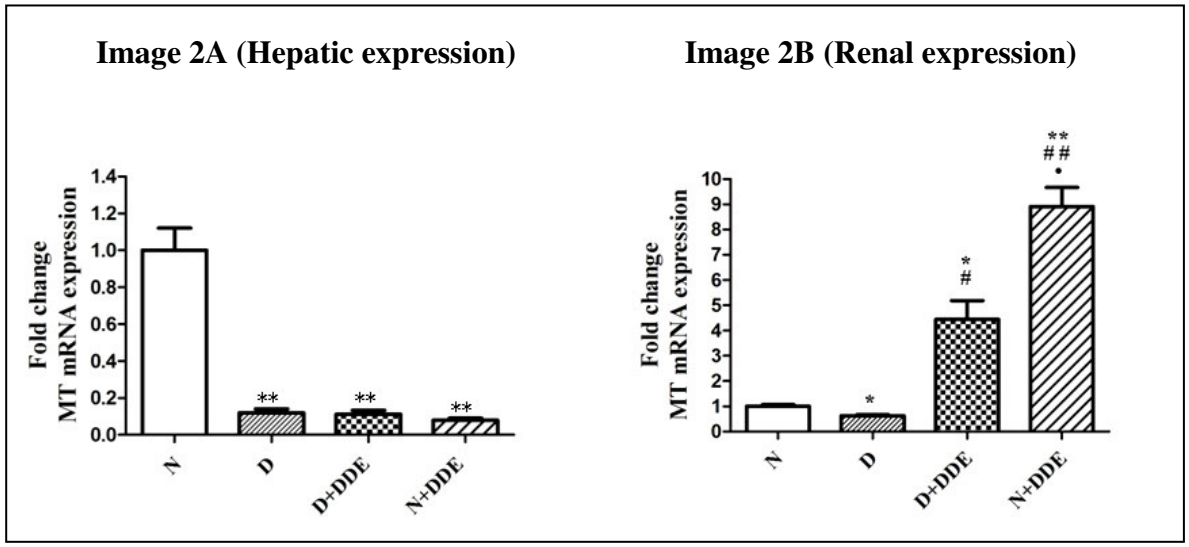

Image 2: Different treatment response for MT expression in Liver and Kidney. Down regulation is observed in D group vs N in both Liver and Kidney analyzed; p,p-DDE treated groups (D+DDE and N+DDE), shown down regulation in the Liver (Image 1A) and up-regulation in the Kidney (Image 1B). **p<0,05* vs N; **p<0,01 vs N; *#p<0,05* vs D; ##p<0,01 vs D; •*p<0,05* vs D+DDE.

Image 3: MT Immunolocalization and protein synthesis in the Liver

Image 3A: Immunolocalization

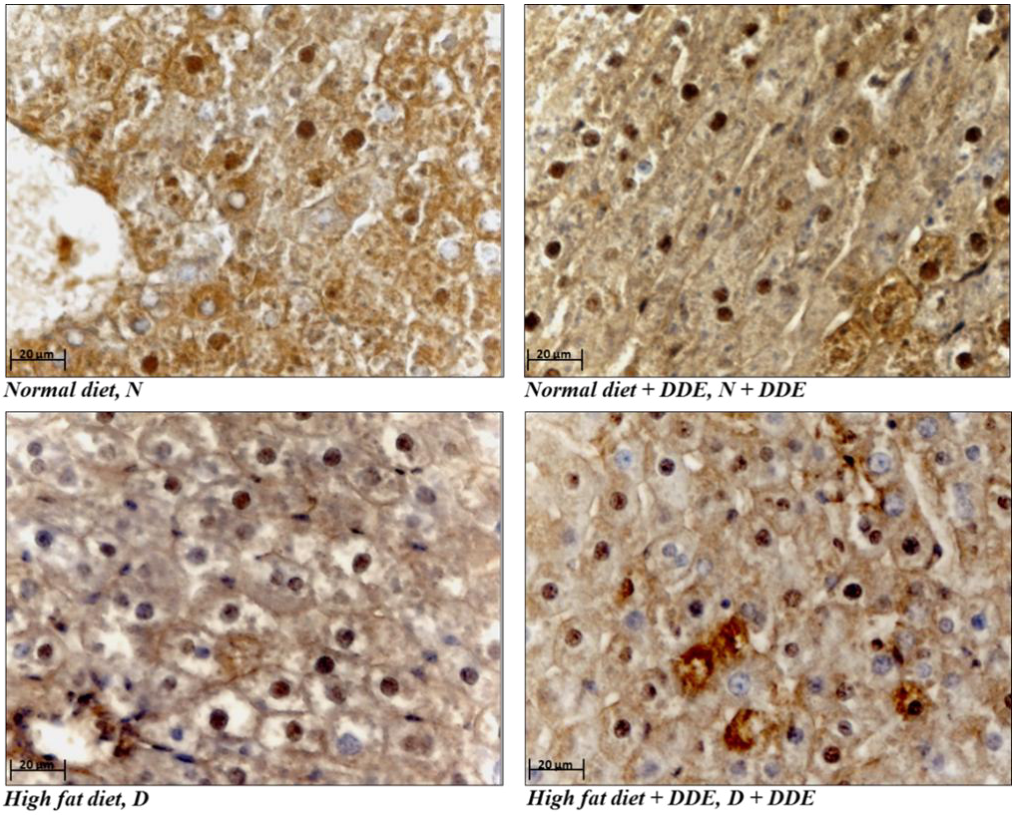

Image 3A: In normal conditions (N), MT localizes in the both cytosol and nuclei. Other experimental conditions exhibit reduction of the cytosolic positivity and increase of nuclear localization respectively. Magnification used: 40X; Scale bar applied: 20 µm.

Image 3B: Western blotting: Total protein and subcellular fractions (Cytosol and Nuclei)

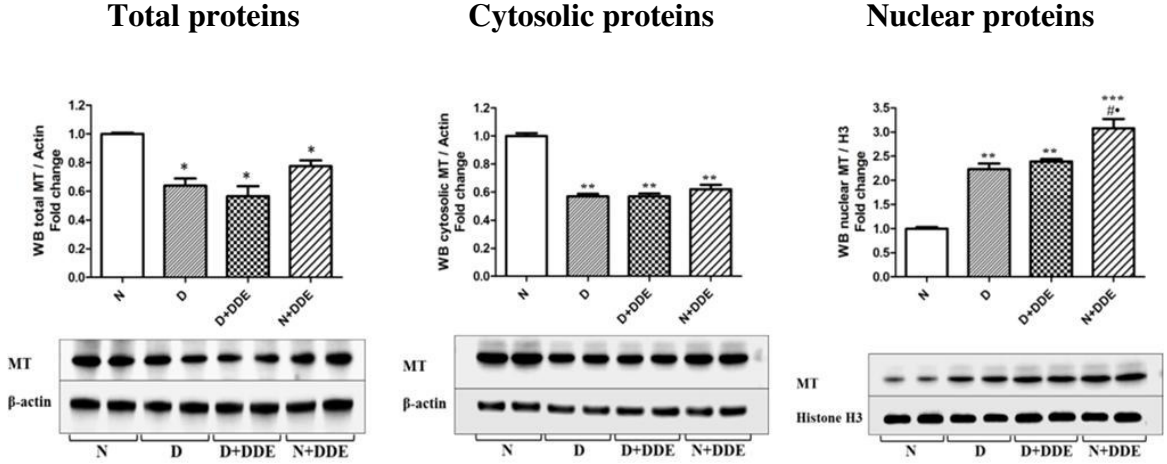

Image 3B: Total western blotting confirms the result obtained with RT-PCR. Cytosolic fraction seems decreased in all treated groups vs N. In the contrary, Nuclear fraction is increased significantly in all treatment vs N, but in particular way in N+DDE group. **p<0,05* vs N; **p<0,01 vs N; ***p<0,001 vs N; #*p<0,05* vs D; •*p<0,05* vs D+DDE.

Image 4: MT Immunolocalization and protein synthesis in the Kidney

Image 4A: Immunolocalization

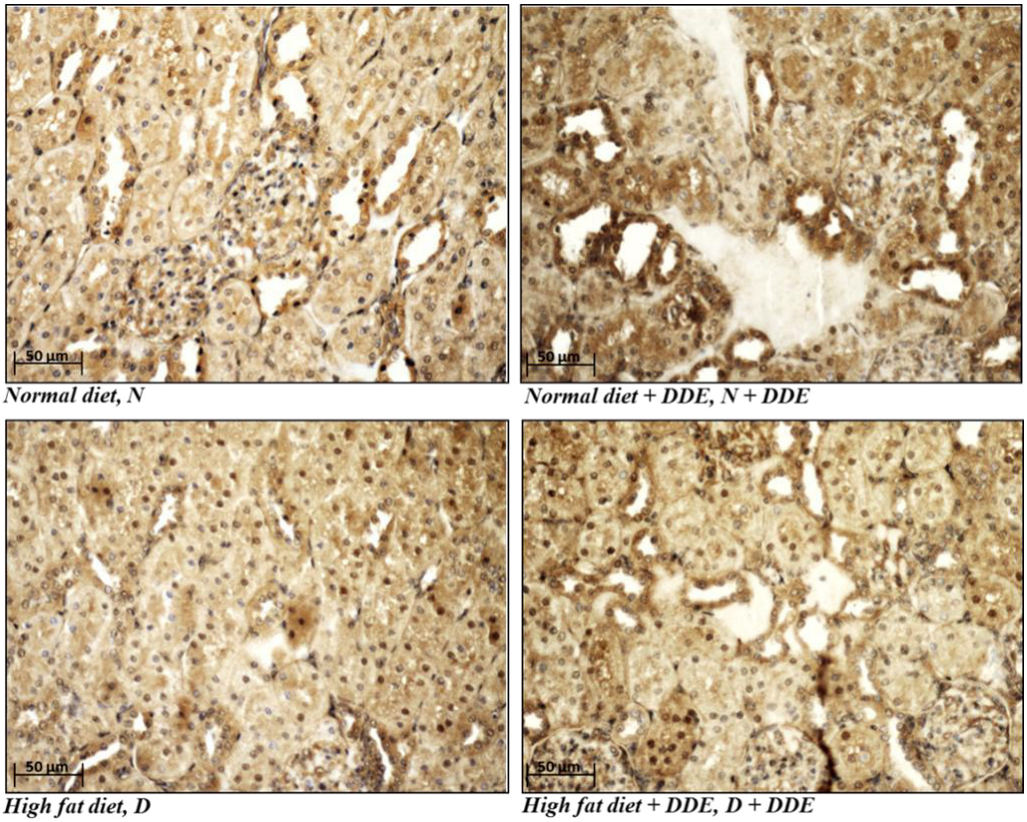

Image 4A: In normal conditions (N), MT localizes in the both cytosol and nuclei of the convolute tubules. In D group, MT positivity seems decreased in the cytosol and increased at nuclear level. In both p,p-DDE treated groups (D+DDE and N+DDE) it was observed increase of the positivity in the proximal and distal tubule cells at nuclear and cytoplasmic level. Magnification used: 10X; Scale bar applied: 20 µm.

Image 4B: Western blotting: Total protein and subcellular fractions (Cytosol and Nuclei)

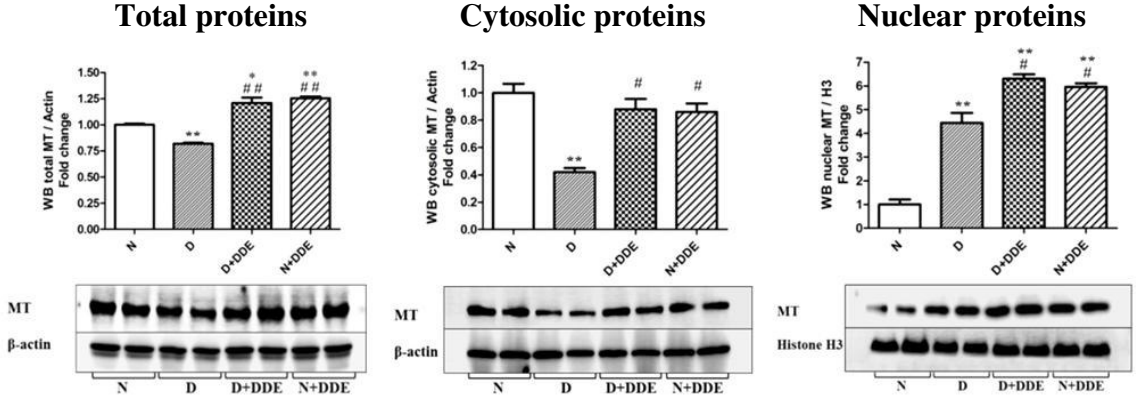

Image 4B: Total western blotting confirms the result obtained with RT-PCR. Nuclear fraction is increased significantly in all treatment vs N, but in particular in presence of p,p-DDE. *$p<0,05$ vs N; **p<0,01 vs N; #$p<0,05$ vs D; ##p<0,01 vs D.

Tables and Images manuscript 4:

Potential protective role of the mitochondrial channel UCP2 to regulate ROS accumulation and oxidative damages in male *Wistar* rat Liver.

Image 1: Morphological analysis

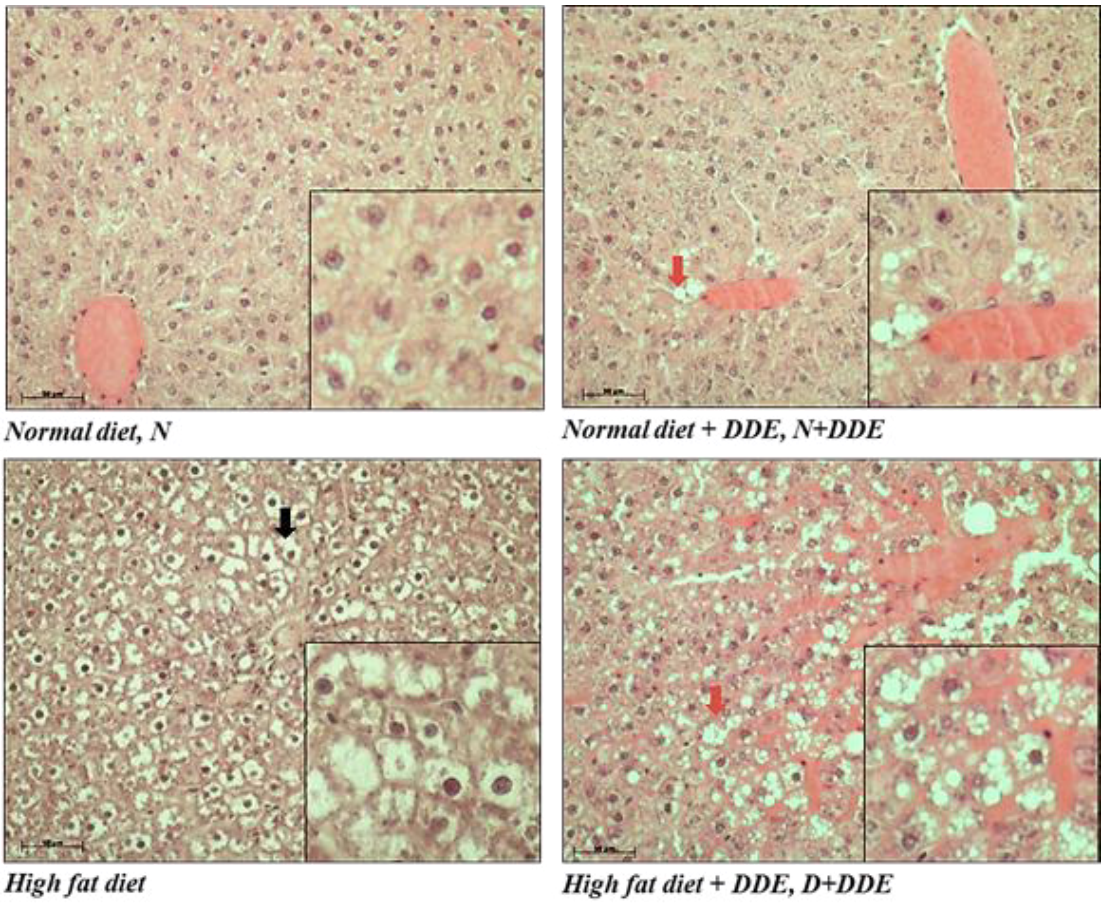

Image 1: Lipid accumulation in HFD condition (black arrow). Perivasal cellular vacuolization in presence of p,p-DDE (red arrows). Magnification used: 10X; scale bar applied 50 µm.

Image 2: Primer validation and sequencing

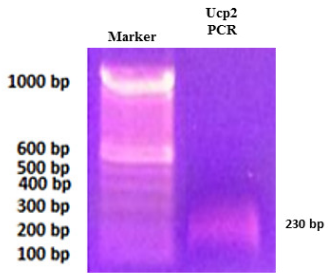


```
>EM_RO:AB005143; AB005143 Rattus norvegicus mRNA for uncoupling protein 2,
complete cds.
Length = 930

Score = 1150 (178.6 bits), Expect = 7.9e-44, P = 7.9e-44, Group = 1
Identities = 230/230 (100%)  Positives = 230/230 (100%), Strand = Plus / Plus

Query:     1 AGCAGTTCTACACCAAGGGCTCAGAGCATGCAGGCATCGGGAGCCGCCTCCTGGCAGGTA 60
             ||||||||||||||||||||||||||||||||||||||||||||||||||||||||||||
Sbjct:   311 AGCAGTTCTACACCAAGGGCTCAGAGCATGCAGGCATCGGGAGCCGCCTCCTGGCAGGTA 370

Query:    61 GCACCACAGGTGCCCTGGCTGTGGCTGTGGCCCAACCTACAGATGTGGTAAAGGTCCGCT 120
             ||||||||||||||||||||||||||||||||||||||||||||||||||||||||||||
Sbjct:   371 GCACCACAGGTGCCCTGGCTGTGGCTGTGGCCCAACCTACAGATGTGGTAAAGGTCCGCT 430

Query:   121 TCCAGGCCCAGGCCCGGGCTGGCGGTGGTCGGAGATACCAGAGCACTGTCGAAGCCTACA 180
             ||||||||||||||||||||||||||||||||||||||||||||||||||||||||||||
Sbjct:   431 TCCAGGCCCAGGCCCGGGCTGGCGGTGGTCGGAGATACCAGAGCACTGTCGAAGCCTACA 490

Query:   181 AGACCATTGCACGAGAGGAAGGGATCCGGGGCCTCTGGAAAGGGACCTCT 230
             ||||||||||||||||||||||||||||||||||||||||||||||||||
Sbjct:   491 AGACCATTGCACGAGAGGAAGGGATCCGGGGCCTCTGGAAAGGGACCTCT 540
```

Image 2: Canonic PCR demonstrates, as indicate during primers construction in «Blast program», cDNA fragment of 230bp. cDNA sequencing indicate identity with *Rat Norvegicus* at 100% with a fragment of the the Ucp2 cDNA in the database.

Image 3: Ucp2 gene expression and protein synthesis.

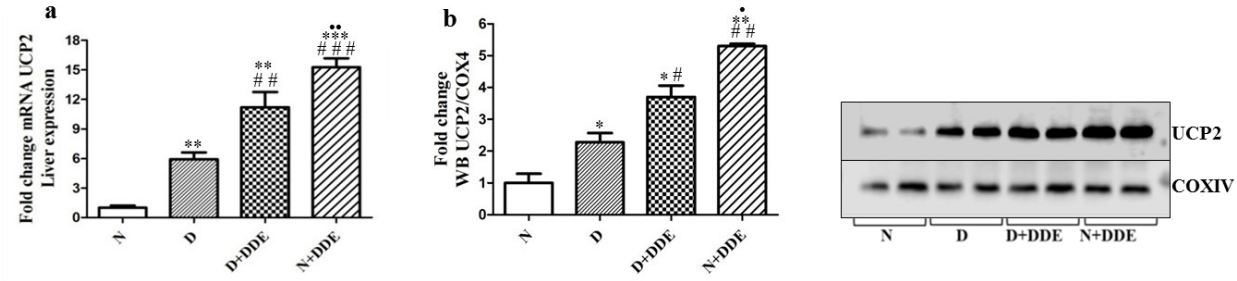

Image 3: RT-PCR and Western blotting were conducted to analyze the correlation between Ucp2 gene expression (graphic a) and the amount of protein (graphic b) in the mitochondrial protein extract. As observed, both mRNA and protein increase with the same trend. **p<0,05* vs N; **p<0,01 vs N; ***p<0,001 vs N; *#p<0,05* vs D; ##p<0,01 vs D; ###p<0,001 vs D; •*p<0,05* vs D+DDE; ••*p<0,01* vs D+DDE.

Image 4: Ucp2 mRNA localization (In situ hybridization).

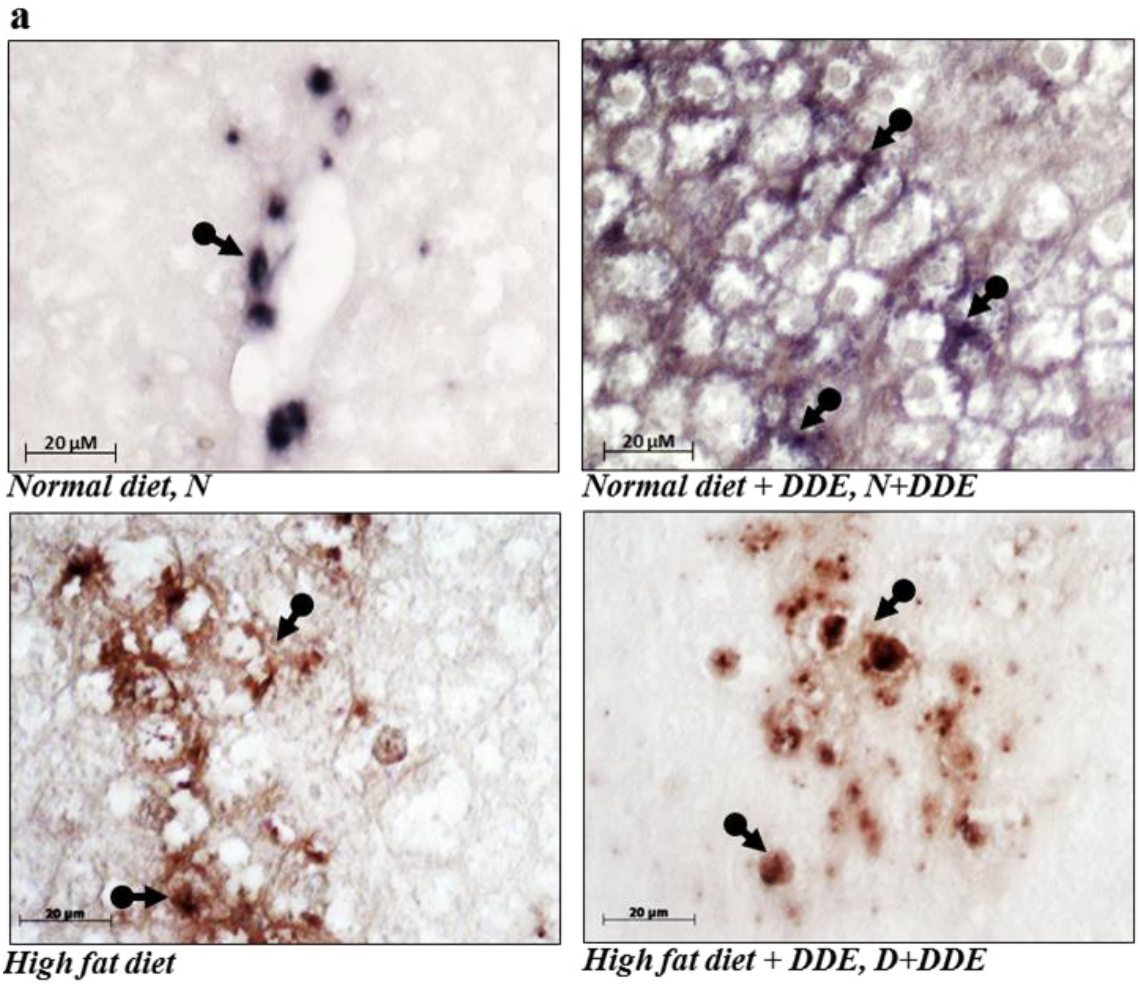

Picture a) mRNA localization in the macrophages was observed in the N group and not in the hepatocytes. In the other groups it was observed mRNA localization appears also extended in the hepatocytes. The protocol used for the sample was the same, but the detection system used in condition of normal diet was BN-purple; in condition of HF-diet was BCIP-NBT. Microscope magnification used: 40X. Scale bar applied 20 µm.

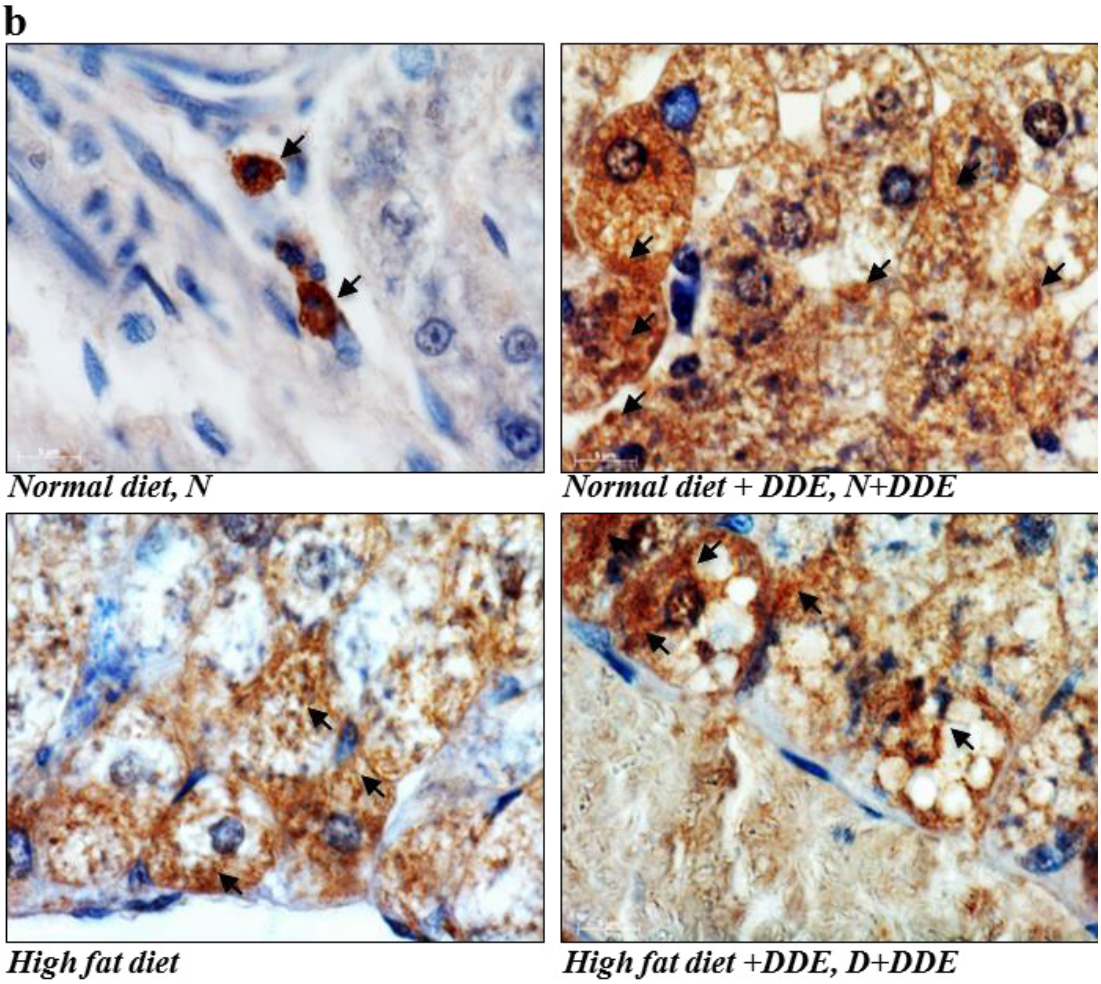

Picture b) Immunohistochemical localization confirms in situ hybridization. In normal condition only phagocytic cells were marked. In presence of HF-diet and p,p-DDE, Immunoreactivity was extended in the hepatocytes. In addition, we have been observed mitochondria marked with ati-UCP2 antibody used, confirming the reliability of the data (black arrows). Microscope magnification used: 100X. Scale bar applied 5µM.

Image 5: Antioxidant enzymes SOD1 and GPX1

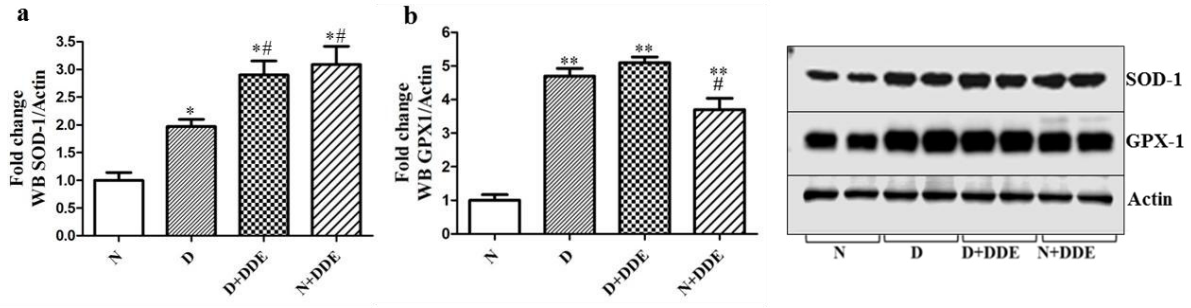

Image 5. SOD1 (graphic a) appears up regulated in according to previous study on lipid peroxidation, indicating cellular ROS accumulation. GPX-1 is up-regulated in all experimental conditions vs N. The greatest increment in presence of saturated fatty acids could indicate a role of fatty acids on the GPX1 stimulation. *$p<0,05$ vs N; **$p<0,15$ vs N; #$p<0,05$ vs D.

Tables and Images manuscript 5:

p,p-DDE causes oxidative stress in *Wistar* rat Liver: preliminary studies conducted in *Huh7* cells.

In vivo analysis: Liver.

Table 2: Previous data obtained on Liver used to conduce new experiments *in vivo* and *in vitro*.

Experiment	N	N+DDE	D	D+DDE
H_2O_2 release from mitochondria	Basal levels	*	*	*
Lipid Peroxides (total homogenate)	Basal levels	**/#	*	**/#
WB Cyt-c : cytosolic fraction	Basal levels	**#	No change	*#
WB Cyt-c : Mitochondrial fraction	Basal levels	**#	No change	*#

Previous studies, indicate oxidative stress in the Liver, particularly evalued in presence of p,p-DDE. Our research group, have been demonstrate the correlation between p,p-DDE and oxidative stress in the liver of *Wistar* rats. In our experimental conditions it was found a positive correlation with the apoptotic pathway induced by mitochondria and p,p-DDE treatments. *$p<0,05$ vs N; #$p<0,05$ vs D.

Since in the liver a series of responses to contrast the oxidative damage are activated from the same hepatocytes and by the accessory hepatic cells, it was put in place an *in vitro* study on human hepatocellular carcinoma cells Huh7 to clarify the effects of this pesticide on mitochondrial stress generation and cellular injury. This cellular model was chosen to conduct a preliminary studies in presence of p,p-DDE using a cellular type with a big area to conduce mitochondrial dynamic studies with confocal microscopy. *Huh7* cells do not present altered expression of proteins directly involved in the mitochondrial function, dynamics and metabolism.

Image 1A: SOD2 Immunolocalization

Picture 1

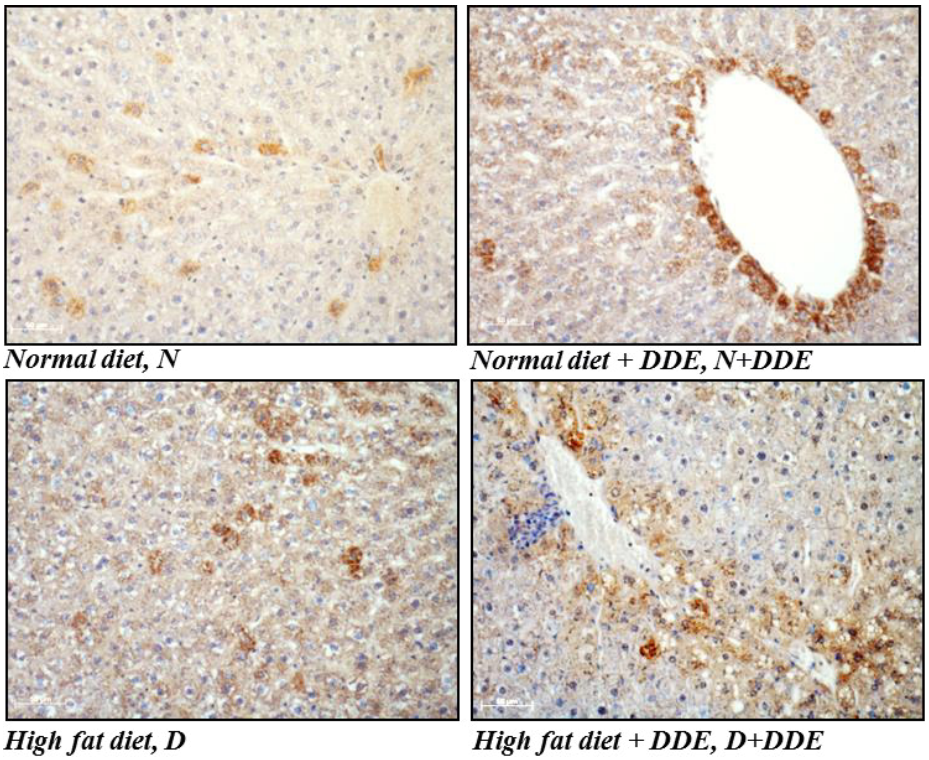

Normal diet, N | *Normal diet + DDE, N+DDE*

High fat diet, D | *High fat diet + DDE, D+DDE*

Picture 2

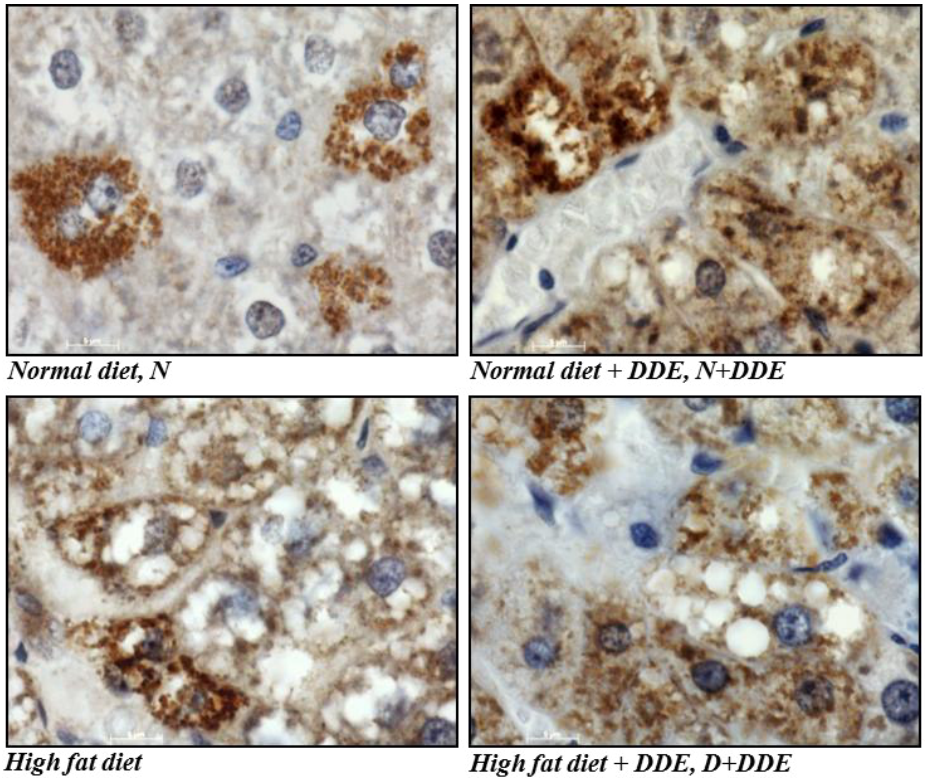

Normal diet, N | *Normal diet + DDE, N+DDE*

High fat diet | *High fat diet + DDE, D+DDE*

Image 1A: In control rats (N group) we have been observed a basal SOD2 levels, localized on mitochondria. In all treated groups (D, D+DDE, N+DDE) SOD2 Immunolocalization

seems extended in a lot of cells in the liver, in particular around of vessels. Magnifications used and scale bars applied: Picture A: 10X, 50 µm; Picture B: 100X, 5 µm.

Image 1B: SOD2 Western blotting analysis.

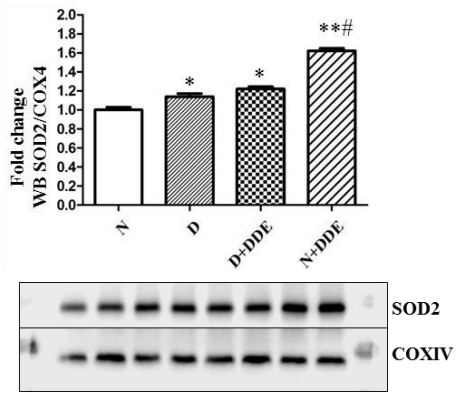

Image 1B: Western blotting data confirms SOD2 increment previously observed with IHC. The greatest up-regulation is associated to the p,p-DDE in normal diet condition (N+DDE). *$p<0,05$ vs N; **$p<0,01$ vs N; #$p<0,05$ vs D.

Image 2A: cl-casp3 Immunolocalization

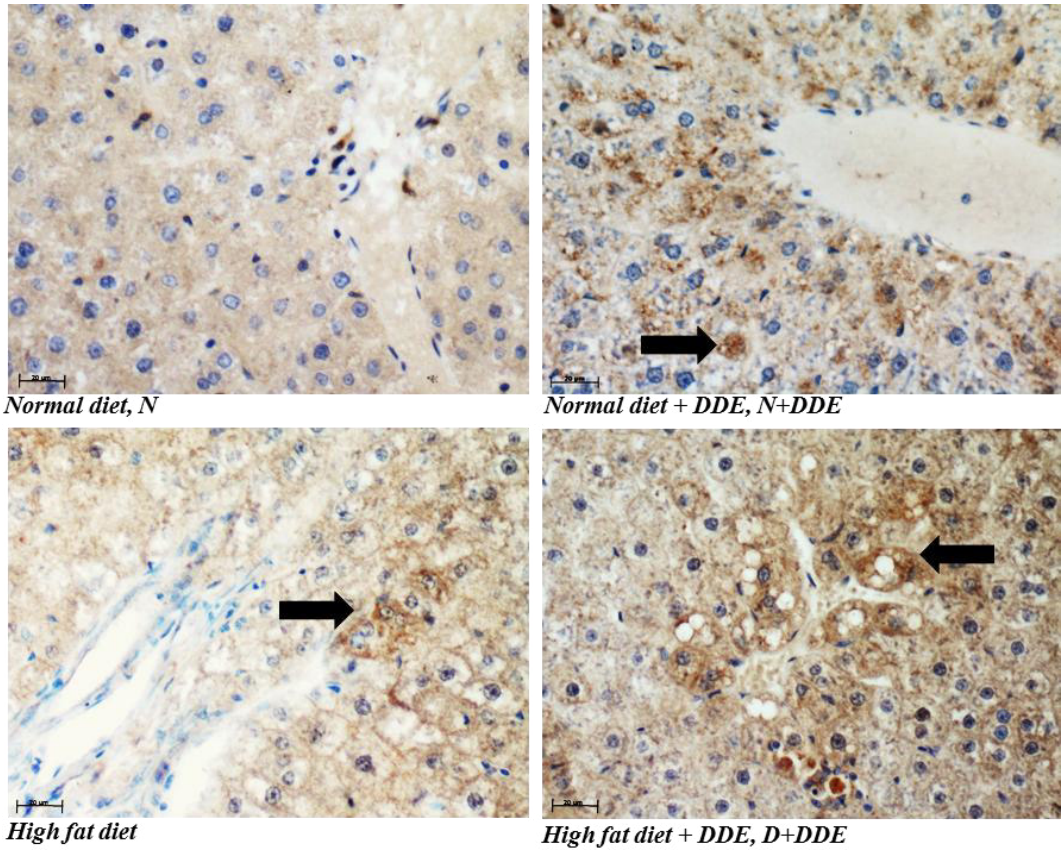

Image 2A: N group not presents cellular Immunoreactivity to cl-casp3. In treated animals (D, D+DDE, N+DDE) around of vessels there are positive cells (black arrow), that appear more in p,p-DDE-treated animals. Magnification used 40X; Scale bar applied 20 µm.

Image 2B: Mitochondrial BAX, Western blotting analysis.

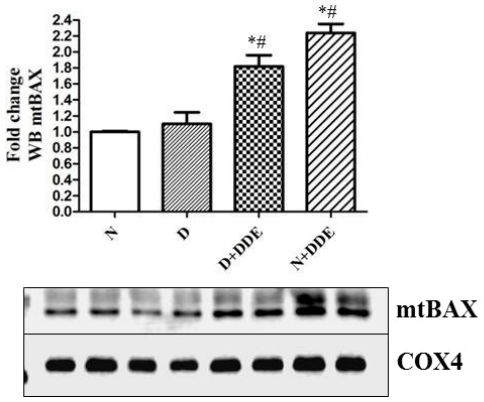

Image 2B: BAX, that induce mitochondrial outer membrane permeabilization, increase in presence of the pesticide. These data indicating pro-apoptotic role of the p,p-DDE that stimulates the apoptosis induced by mitochondria. *$p<0,05$ vs N; #$p<0,05$ vs D.

Image 3A: p,p-DDE effect on the macrophages recruitment in the Liver

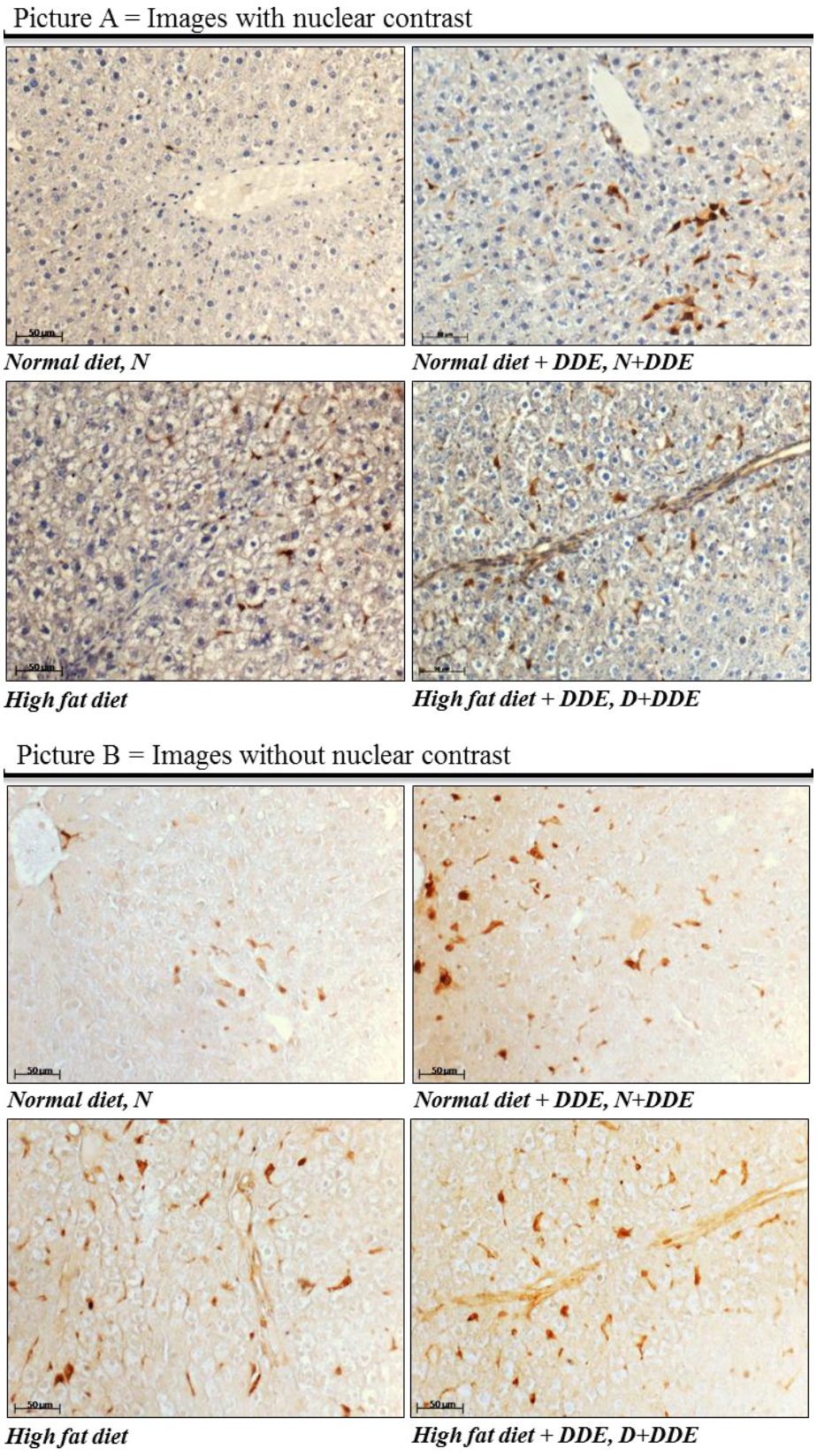

Image 3A: CD68+ cells. In normal diet conditions (N group) a basal Immunoreactivity was observed. In treated animals (D, D+DDE, N+DDE) CD68 increase as positives cells number, indicate recruitment of phagocytic cell in the Liver, probably to eliminate cells in death phase. Magnification used 20X; Scale bar applied: 50 µm.

Image 3B: CD68 Western blotting analysis.

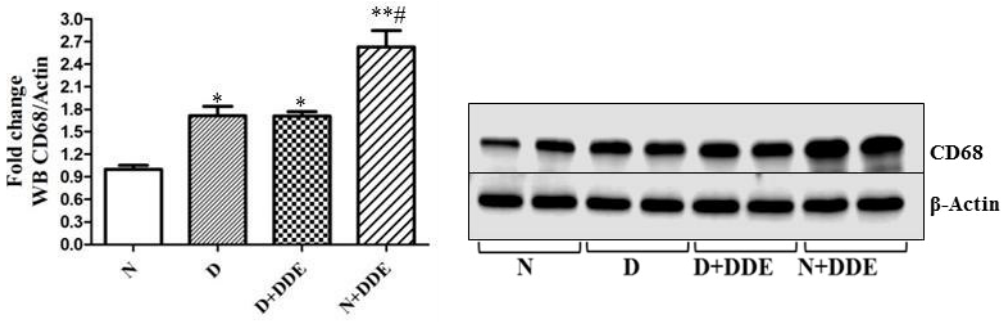

Image 3B: Western blotting data confirms IHC results, indicating greatest CD68 increment in N+DDE. *$p<0,05$ vs N; **$p<0,01$ vs N; #$p<0,05$ vs D.

Image 4: ER-morphology

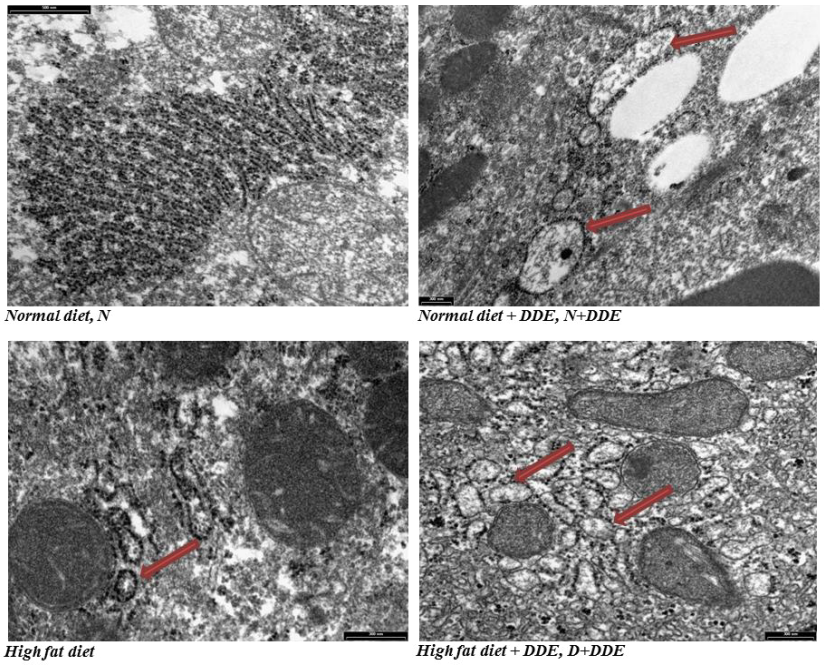

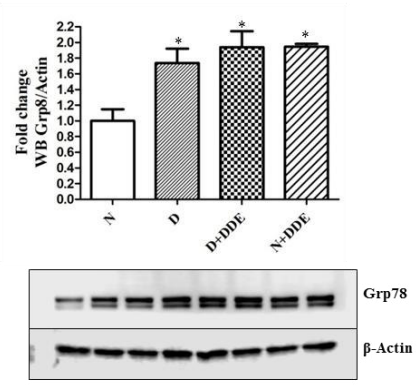

Image 4: Electronic microscopy have put in evidence dilated cisterns of endoplasmic reticulum, especially in presence of p,p-DDE (red arrows). The results in association to Grp78 increment, evaluated by WB in all treated groups, could indicate ER-stress in presence of HF-diet (D group) and also in DDE-treated conditions (D+DDE and N+DDE groups). Scale bar: N→ 500nm; other groups→ 300nm. *$p<0,05$ vs N.

In vitro analysis: Huh7 cells.

Image 5: p,p-DDE dose experiment to evaluate the mitochondrial superoxide anion produced in live cells.

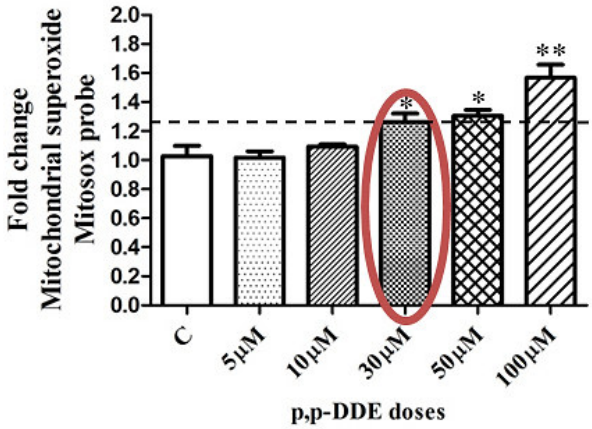

Image 5: Dose curve. Huh7 cells were treated at different doses of p,p-DDE (5µM, 10µM, 30µM, 50µM, 100µM) for 24h, indicating dose depending response to mitochondrial superoxide generation, measured by Flow cytometry Gallios, using MitoSox probe. As observed on graphically representation, 30µM is the first concentration point that causes significant superoxide production during mitochondria respiration. *P<0,05 vs Control; **P<0,01 vs Control.

Image 6: anion superoxide and total ROS accumulation in the cells

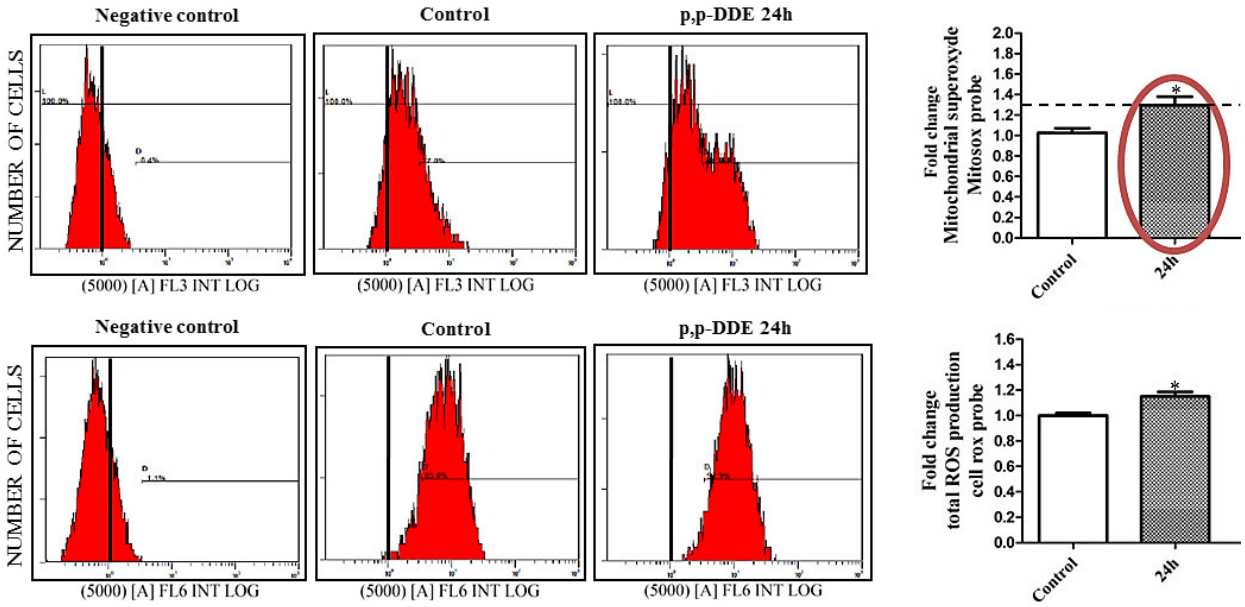

Image 8: Mitochondrial superoxide and Total cellular ROS. Huh7 control cells were treated using the same dose of DMSO required to dissolve the pesticide (0,01%). After p,p-DDE exposition (24h), the cells were incubated with MitoSox and CellRox probe in two different experiments, to detect the mitochondrial superoxide and the total cellular ROS, respectively. * *p<0.05* vs Control.

Image 7A: Correlation between mitochondrial SOD up-regulated in presence of p,p-DDE and hydrogen peroxide accumulated in the cells.

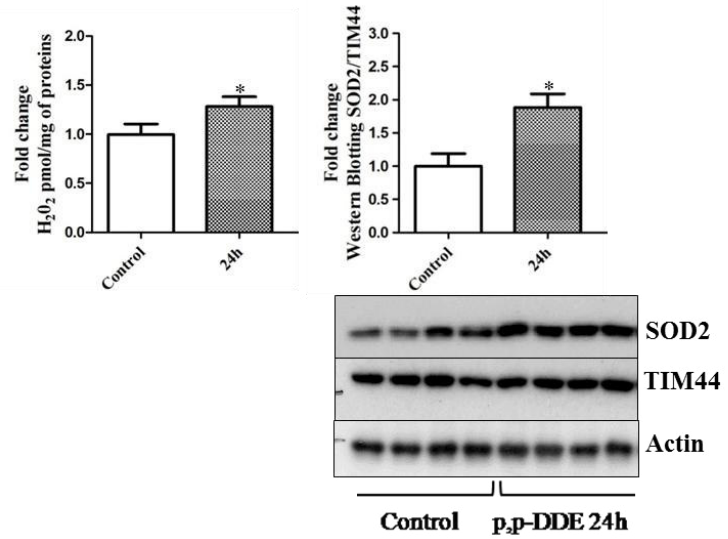

Image 7A: SOD2 is up-regulated in presence of p,p-DDE, probably to convert in part the excess of mitochondrial superoxide anion produced in presence of mitochondrial stress in H_2O_2. This molecule, not electrically charged, diffuses through the inner and outer mitochondrial membranes, generating its accumulation, measured on total homogenate using AmplexRed spectrophotometric method. * *p<0.05* vs Control.

Image 7B. Mitochondrial function compromised in presence of p,p-DDE.

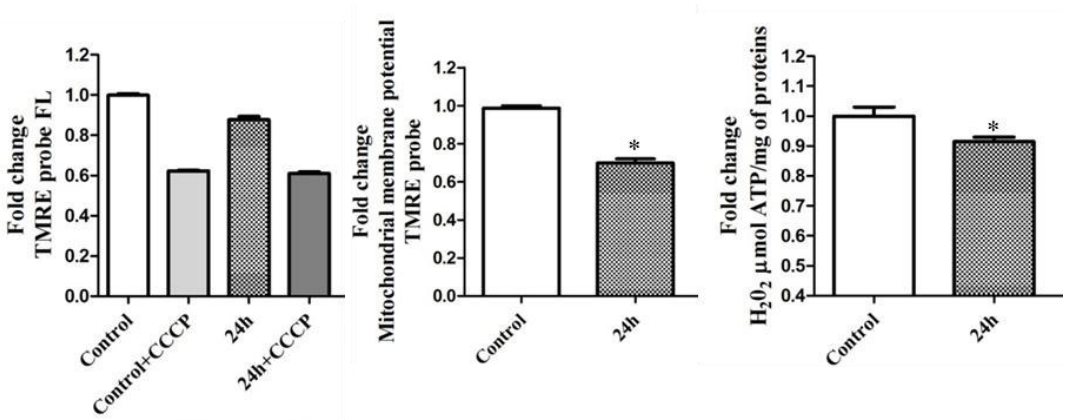

Image 7B: TMRE fluorescence emixion measured with Flow cytometry shows that in presence of p,p-DDE there is a decrement of the mitochondrial membrane potential. In according to this data, the ATP measure on total homogenate is decreases, indicating that p,p-DDE intact mitochondrial membrane potential with consequences on the ATP production. * *p<0.05* vs Control.

Image 8A: Mitochondrial dynamic proteins analyzed on total protein extract.

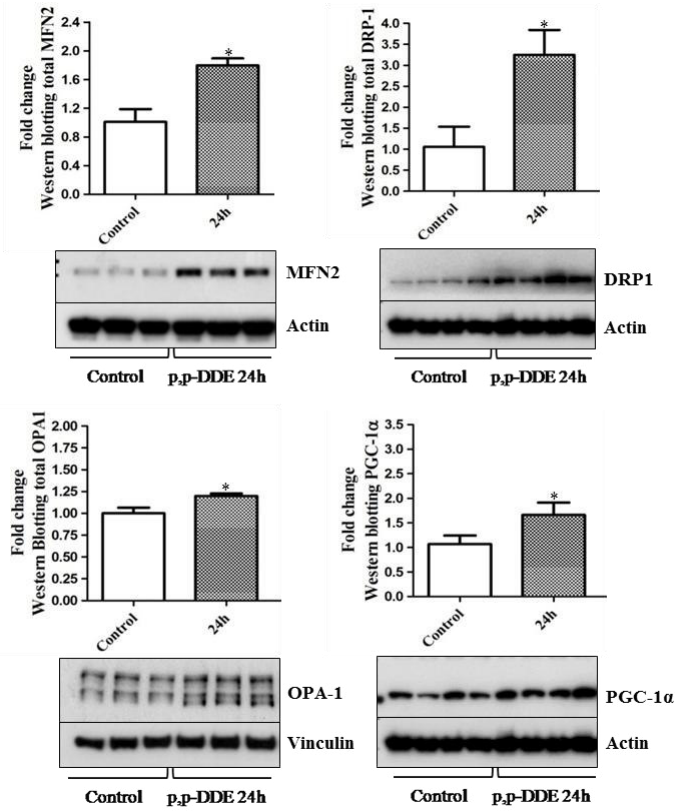

Image 8A: MFN2, DRP1 and OPA1 are increased in presence of p,p-DDE. In association to PGC-1α increment, this result indicates that the cells activate mitochondrial biogenesis probably to contrast mitochondrial damages. * *p<0.05* vs Control.

Image 8B: Mitochondrial dynamic proteins analyzed on mitochondrial protein extract.

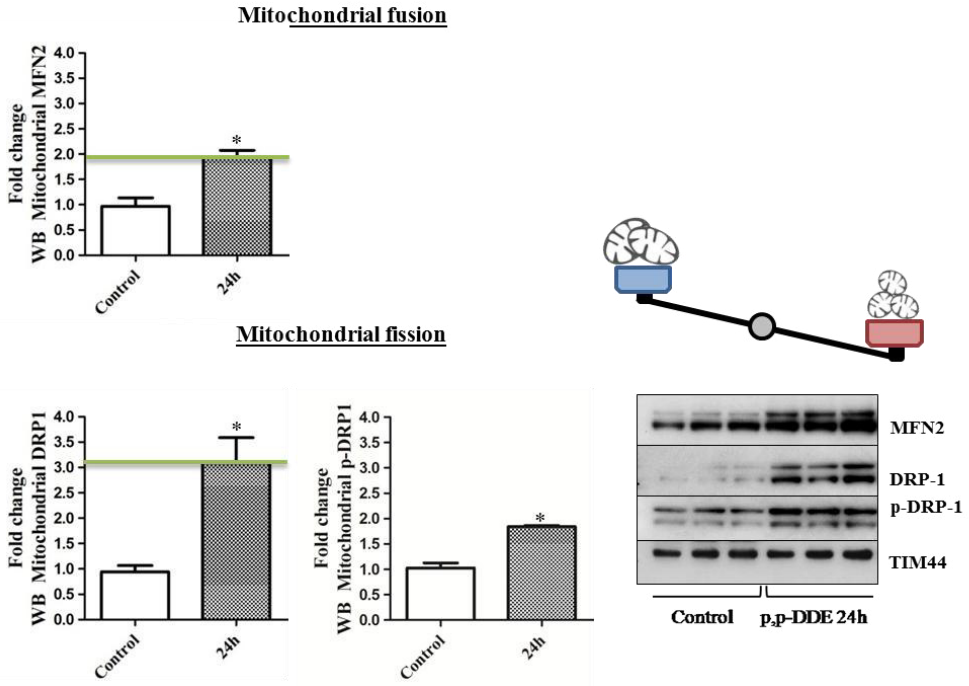

Image 8B: Also on mitochondrial extract, MFN2 and DRP1 increase. Fold change that mitochondria undergo mostly to fixion process in presence of stress. * *p<0.05* vs Control.

Image 9: OPA1 Isoforms.

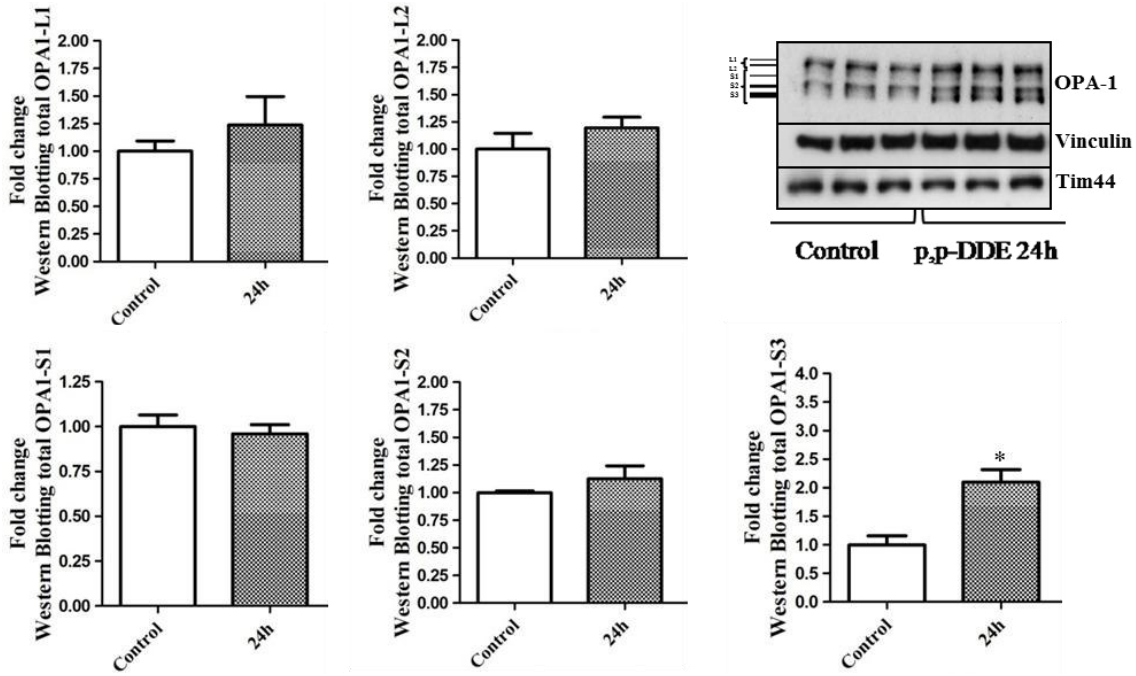

Image 9: p,p-DDE-treated cells activate increment of total OPA1. In addition, we found significant increase of OPA1 S3 isoform, probably indicating protolithic cleavage during mitochondrial ROS accumulation. This hypothesis may be reinforced by the result obtained in regard to the others isoform, that did not changed despite OPA1 up-regulation was observed. * $p<0.05$ vs Control.

Image 10: Confocal microscopy

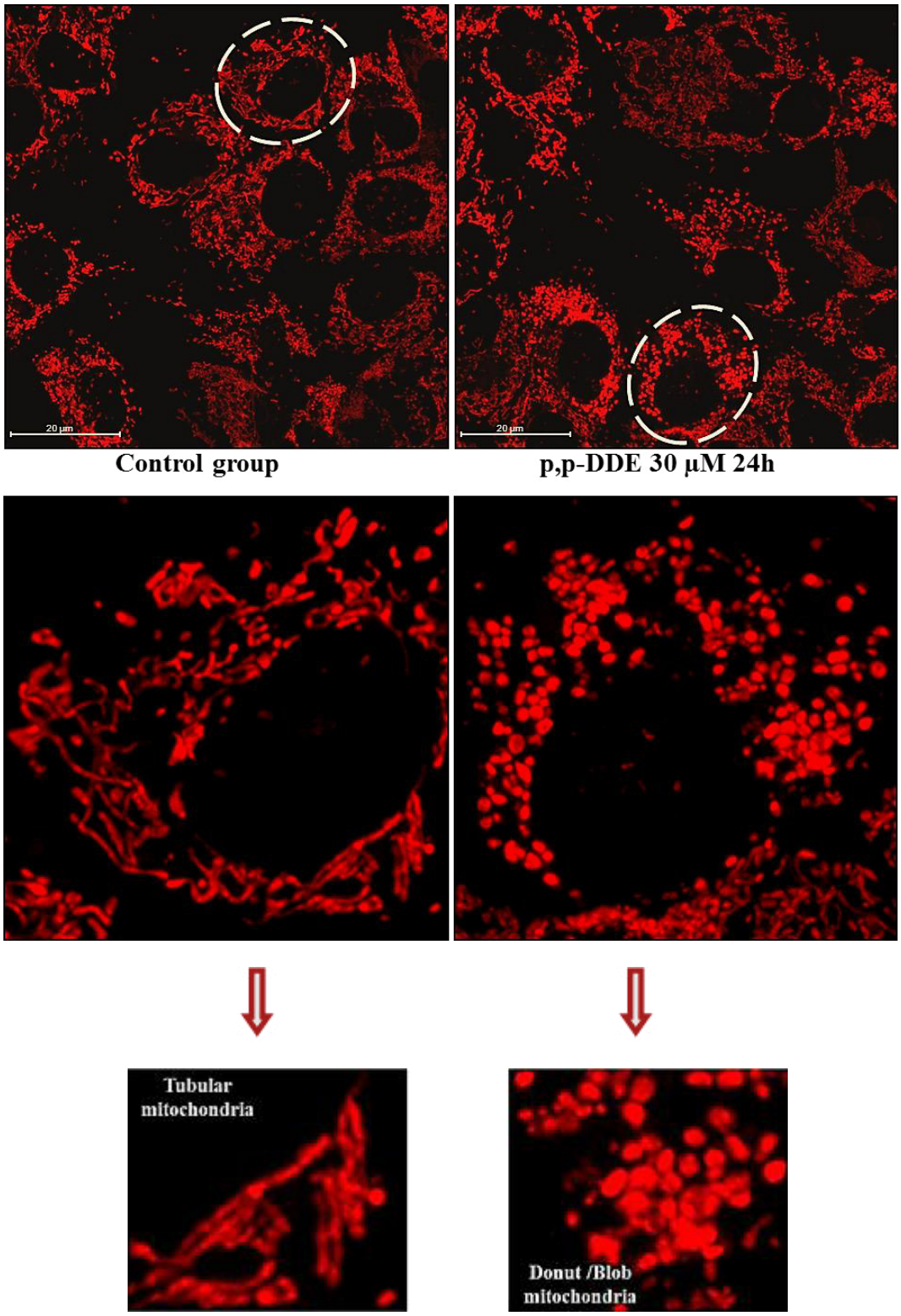

Image 10: Using Mitotracker DeepRed probe, mitochondria were localized and analyzed at microscope. In presence of p,p-DDE donut/Blob mitochondria (typically of stress conditions) were observed. Magnification: 63X, scale bar 20µm.

Image 11: ER-responsive elements

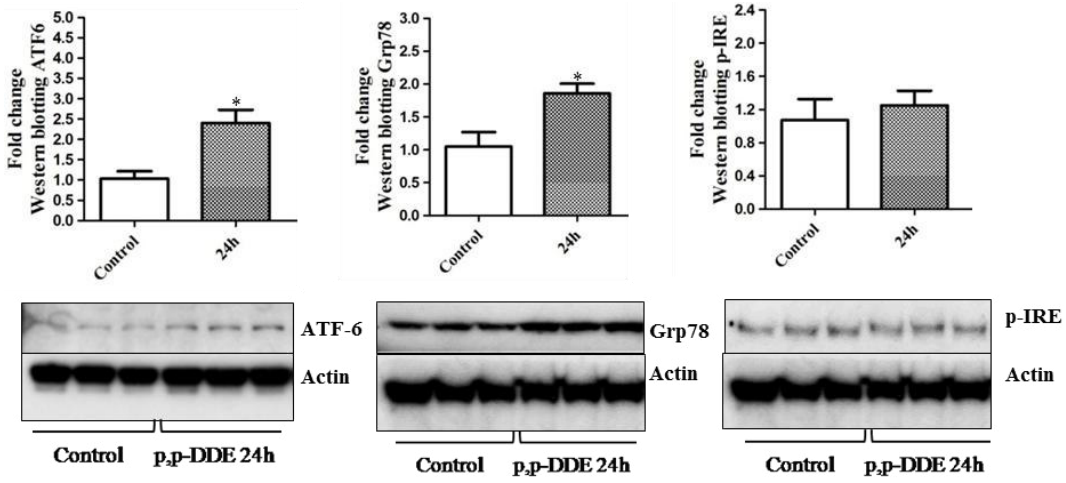

Image 11: ATF-6, Grp78 and p-IRE1a were analyzed on total proteins extract. As observed, only ATF-6 and Grp78 are increase after 24h of exposition. We didn't observed differences on p-IRE1a, indicating that UPR-pathway is only in part activated. *$p<0,05$ vs Control.

Image 12: Mitochondrial apoptotic pathway activated in presence of p,p-DDE.

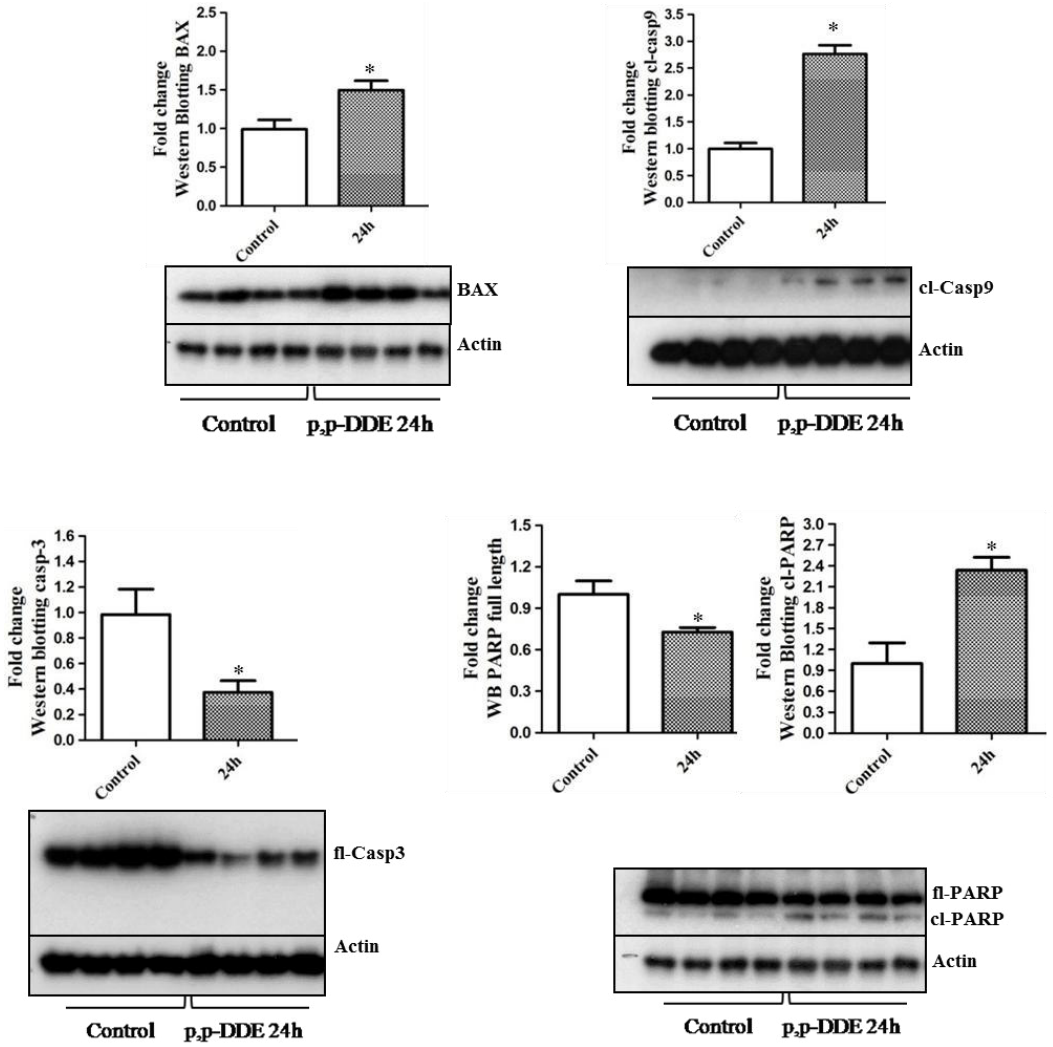

Image 12: Increase of BAX in total homogenate and increase of cl-casp9 could indicate that mitochondria undergo to outer membrane permeabilization, cyt-C release and activation of caspase 9. Caspase 3 full length decreases in presence of pesticide. This data suggest that also caspase 3 undergoes to its activation. In according to that, cl-PARP increase confirms that the apoptotic pathway is activated in presence of p,p-DDE after 24h of exposition. *$p<0,05$ vs Control.

References

[1] Obaid Faroon (Ph.D.), M. Olivia Harris (M.A.), ATSDR (Division of Toxicology, Atlanta, GA) Fernando Llados (Ph.D.), Steven Swarts (Ph.D.) Gloria Sage (Ph.D.) Mario Citra (Ph.D.), Daniel Gefell (M.S.), Syracuse Research Corporation (North Syracuse, NY). U.S. DEPARTMENT OF HEALTH AND HUMAN SERVICES Public Health Service Agency for Toxic Substances and Disease Registry. Toxicology profile for DDT, DDE and DDE. page 2, 33, September 2002.

[2] (http://www.malariasite.com/tag/ddt/).

[3] Mohamed Abou-Donia. Mammalian Toxicology. John Wiley & Sons, February 05, 2015.

[4] Henk van den Berg. Global Status of DDT and Its Alternatives for Use in Vector Control to Prevent Disease. May 29, 2009.

[5] William R. Kelce, Khristy R. Stone, Susan C. Laws, L. Earl Gray, Jon A. Kemppainen and Elizabeth M. Wilson. Persistent DDT Metabolite p,p-DDE is a potent androgen receptor antagonist.

[6] H. F. KRAYBILL, Ph.D.,* Washington, D.C., U.S.A. Significance of Pesticide Residues in Foods in Relation to Total Environmental Stress. Canad.Med. Ass. J., vol 100, Jan 25, 1969.

[7] IARC Monographs evaluate DDT, lindane, and 2,4-D. June 23, 2015.

[8] D Baris, S H Zahm, K P Cantor, A Blair. Agricultural use of DDT and risk of non-Hodgkin's lymphoma: pooled analysis of three case-control studies in the United States. Occup Environ Med 55, pages 522–527, 1998.

[9] Vladimir Turusov, Valery Rakitsky, and Lorenzo Tomatis. Dichlorodiphenyltrichloroethane (DDT): ubiquity, persistence, and risks. Environ Health Perspect110(2): 125–128; Feb 2002.

[10] Miroslav Machala, Luděk Bláha, Hans-Joachim Lehmler, Martina Plíšková, Zuzana Májková, Petra Kapplová, Iva Sovadinová, Jan Vondráček, Tina Malmberg, and Larry W. Robertson. Toxicity of Hydroxylated and Quinoid PCB Metabolites: Inhibition of Gap Junctional Intercellular Communication and Activation of Aryl Hydrocarbon and Estrogen Receptors in Hepatic and Mammary Cells. Chem. Res. Toxicol., 17 (3), pp 340–347, 2004.

[11] VeraDowling,Pascal C.Hoarau, Michèle Romeo JohnO'Halloran, Frankvan Pelt, NoraO'Brien, DavidSheehan. Protein carbonylation and heat shock response in Ruditapes decussatus following p,p′-dichlorodiphenyldichloroethylene (DDE) exposure: A proteomic approach reveals that DDE causes oxidative stress. Aquatic Toxicology, Volume 77, Issue 1, Pages 11-18, April 20, 2006.

[12] Yang Song, Xianmin Liang, Yafei Hu, Yinan Wang, Haige Yu, KediYang. p,p′-DDE induces mitochondria-mediated apoptosis of cultured rat Sertoli cells. Toxicology, Volume 253, Issues 1–3, Pages 53-61, November 20, 2008.

[13] Neila Marouani, Dorsaf Hallegue, Mohsen Sakly, Moncef Benkhalifa, Khémais Ben Rhouma, and Olfa Tebourbi. p,p'-DDT induces testicular oxidative stress-induced apoptosis in adult rats. Reprod Biol Endocrinol. 15: 40. May 26, 2017.

[14] F. C. Bishopp. Insect Problems in World War II with Special References to the Insecticide DDT. Am J Public Health Nations Health. 35(4): 373–378; Apr 1945.

[15] Beatrice Autino, Alice Noris, Rosario Russo, and Francesco Castelli. Epidemiology of Malaria in Endemic Areas. Mediterr J Hematol Infect Dis. 4(1), Oct 4, 2012.

[16] D. Michael Fry. Reproductive Effects in Birds Exposed to Pesticides and Industrial Chemicals. POLLUTANTS AND REPRODUCTION IN BIRDS. Environmental Health Perspectives. Vol. 103, Pages 165-171, October 7, 1995.

[17] Lundholm CD. DDE-induced eggshell thinning in birds: effects of p,p'-DDE on the calcium and prostaglandin metabolism of the eggshell gland. Comp Biochem Physiol C Pharmacol Toxicol Endocrinol; Vol 118(2): Pages 113-28, Oct 1997.

[18] Guillette LJ Jr and MP Gunderson. Alterations in development of reproductive and endocrine systems of wildlife populations exposed to endocrine-disrupting contaminants. Reproduction. Vol 122; Pages 857-864, Dec 1, 2001.

[19] M. Spanò, G. Toft, L. Hagmar, P. Eleuteri , M. Rescia, A. Rignell-Hydbom, E. Tyrkiel, V. Zvyezday, J.P. Bonde. Exposure to PCB and p, p′-DDE in European and Inuit populations: impact on human sperm chromatin integrity. Human Reproduction, Volume 20, Issue 12, Pages 3488–3499. December 1, 2005.

[20] Karl K. Rozman , John Doulland Wayland J. Hayes , Jr. Dose and Time Determining, and Other Factors Influencing, Toxicity. June 11, 2009.

[21] Brenda Eskenazi, Jonathan Chevrier, Lisa Goldman Rosas, Henry A. Anderson, Maria S. Bornman,Henk Bouwman, Aimin Chen, Barbara A. Cohn, Christiaan de Jager, Diane S. Henshel, Felicia Leipzig, John S. Leipzig, Edward C. Lorenz, Suzanne M. Snedeker, and Darwin Stapleton. The Pine River Statement: Human Health Consequences of DDT Use. Environ Health Perspect.; Vol 117(9): Pages 1359–1367. Sep. 2009.

[22] Ernie Hood. Endocrine Disruption and Flame-Retardant Chemicals: PBDE-99 Effects on Rat Sexual Development. Environ Health Perspect. 114(2): A112–A113. Feb 2006.

[23] Anne Platt Mc Ginn. Malaria, Mosquitoes, and DDT The toxic war against a global disease. World watch Institute. WORLD WATCH magazine. May/June, 2002.

[24] D A Abramowicz. Aerobic and anaerobic PCB biodegradation in the environment. Environ Health Perspect, 103(Suppl 5): pages 97–99, Jun 1995.

[25] L S Birnbaum. Endocrine effects of prenatal exposure to PCBs, dioxins, and other xenobiotics: implications for policy and future research. Environ Health Perspect. 102(8): 676–679; Aug 2009.

[26] L S Birnbaum. Endocrine effects of prenatal exposure to PCBs, dioxins, and other xenobiotics: implications for policy and future research. Environ Health Perspect; 102(8): pages 676–679; Aug 1994.

[27] AdrianCovaci, Jacobde Boer, John JakeRyan, StefanVoorspoels, PaulSchepens. Distribution of Organobrominated and Organochlorinated Contaminants in Belgian Human Adipose Tissue. Environmental Research. Volume 88, Issue 3, Pages 210-218, March 2002.

[28] Yuji Makita, Toshiaki Matsuura, Rika Ogata, Yesid Romero,Minoru Omura, Akiyo Tanaka, Miyuki Hirata and Naohide Inoue. Systemic effects of orally administered p, p'-dde on immature male wistar rats during pubertal period. J occup health 45: 223–227, 2003.

[29] N. DeMarco, L. Iannone, R. Carotenuto, S. Biffo, A. Vitale, C. Campanella p27(BBP)/eIF6 acts as an anti-apoptotic factor upstream of Bcl-2 during Xenopus laevis development. Cell Death Differ. 17, pp. 360-372, 2010.

[30] K.J. Livak, T.D. Schmittgen. Analysis of relative gene expression data using real-time quantitative PCR and the 2(-Delta Delta C(T)) Methods, pp. 402, May 2001.

[31] Sica R. Effects of pesticide 2,2-Bis(4-chlorophenyl)-1,1-dichloroethylene (DDE) on the liver and testicular mitochondrial bioenergetics, morphology and dynamics in the rat. PhD thesis, May 5 2015.

[32] Lee AS.The ER chaperone and signaling regulator GRP78/BiP as a monitor of endoplasmic reticulum stress. Methods;35(4):373-81, Apr 2005.

[33] Selvakumaran M[1], Lin HK, Miyashita T, Wang HG, Krajewski S, Reed JC, Hoffman B, Liebermann D. Immediate early up-regulation of bax expression by p53 but not TGF beta 1: a paradigm for distinct apoptotic pathways. Oncogene; 9(6):1791-8, Jun1994.

[34] Tim L. Beumer, Hermien L. Roepers-Gajadien, Iris S. Gademan, Tycho. M.T.W. Lock, Henk B. Kal, Dirk G. De Rooij. Apoptosis regulation in the testis: Involvement of Bcl-2 family members. Genetics, Gene Regulation, and Expression. 12 June 2000.

[35] Jong-Min Kim Shampa R. Ghosh Alexander C. P. Weil Barry R. Zirkin: Caspase-3 and Caspase-Activated Deoxyribonuclease Are Associated with Testicular Germ Cell Apoptosis Resulting from Reduced Intratesticular Testosterone. Endocrinology, Volume 142, Issue 9, 1 September 2001, Pages 3809–3816; 01 September 2001.

[36] Kim JM[1], Luo L, Zirkin BR. Caspase-3 activation is required for Leydig cell apoptosis induced by ethane dimethanesulfonate. Endocrinology;141(5):1846-53, May 2000.

[37] Chin JL, Banerjee D, Kadhim SA, Kontozoglou TE, Chauvin PJ, Cherian MG. Metallothionein in testicular germ cell tumors and drug resistance. Clinical correlation. Cancer. 72(10):3029-35, Nov 15, 1993.

[38] Neila Marouani,[1] Dorsaf Hallegue,[1] Mohsen Sakly,[1] Moncef Benkhalifa,[2] Khémais Ben Rhouma,[1] and Olfa Tebourbi[1] p,p'-DDT induces testicular oxidative stress-induced apoptosis in adult rats. Reprod Biol Endocrinol, May 26, 2017.

[39] Arnold J. Levine: p53, the Cellular Gatekeeper Review for Growth and Division. Cell, Vol. 88, 323–331, February 7, 1997.

[40] MÜLLER, P., DDT. The Insecticide Dichlorodiphenyltrichloroethane and its Significance. Vol. I., Lehrb. Monogr. Geb. exakt. Wiss., chem. Reihe. pp.299, 1955.

[41] Des W. Connell. Bioaccumulation Behavior of Persistent Organic Chemicals with Aquatic Organisms. Reviews of Environmental Contamination and Toxicology Vol 101, pp 117-154, 1988.

[42] James E. Peterson, Wm. H. Robison Metabolic products of p,p′-DDT in the rat. Toxicology and Applied Pharmacology, Volume 6, Issue 3, Pages 321-327, May 1964.

[43] Anne Platt Mc Ginn. Malaria, Mosquitoes, and DDT The toxic war against a global disease. World watch Institute. WORLD WATCH magazine. May/June, 2002.

[44] Council Directive of 21 December 1978 prohibiting the placing on the market and use of plant protection products containing certain active substances (79/117/EEC)

[45] http://www.worldatlas.com/articles/is-ddt-still-being-used.html.

[46] Barry C. Kelly, Frank A. P. C. Gobas, Michael S. McLachlan. Intestinal absorption and biomagnification of organic contaminants in fish, wildlife, and humans. Environmental Toxicology and Chemistry. Volume 23, Issue 10, Pages 2324–2336, October 2004.

[47] Pocock DE and Vost A.: DDT absorption and chylomicron transport in rat; Lipids. Vol.6 pp.374-81; Jun 9, 1974.)

[48] W.N.Charman, V.J.Stella. Transport of lipophilic molecules by the intestinal lymphatic system. Advanced Drug Delivery Reviews. Vol.7, Issue 1, Pages 1-14; Jul–Aug, 1991.

[49] Mohammed A, Eklund A, Ostlund-Lindqvist AM, Slanina P. Distribution of toxaphene, DDT, and PCB among lipoprotein fractions in rat and human plasma. Arch Toxicol. 64(7):567-71;1990.

[50] Genuis SJ, Lane K, Birkholz D. Human Elimination of Organochlorine Pesticides: Blood, Urine, and Sweat Study. Biomed Res Int. 2016;2016:1624643. Epub; Oct 5, 2016.

[51] Manushi Siddharth, Sudip K. Datta,Savita Bansal, Mohammad Mustafa, Basu D. Banerjee, Om P. Kalra, Ashok. Study on organochlorine pesticide levels in chronic kidney disease patients: Association with estimated glomerular filtration rate and oxidative stress. Jurnal of biochemical and molecular toxicology. May 29, 2012.

[52] A. Stacchiotti, L.F. Rodella, F. Ricci, R. Rezzani, A. Lavazza and R. Bianchi. Stress proteins expression in rat kidney and liver chronically exposed to aluminium sulphate. Histol Histopathol 21: 131-140, 2006.

[53] Amy SLee. The glucose-regulated proteins: stress induction and clinical applications. CellPress. Volume 26, Issue 8, Pages 504-510, August 1, 2001.

[54] Szabadkai G, et al. Chaperone-mediated coupling of endoplasmic reticulum and mitochondrial Ca2+ channels. J Cell Biol;175(6):901–1, 2006.

[55] De Stefani D, et al. VDAC1 selectively transfers apoptotic Ca2+ signals to mitochondria. Cell Death Differ; 19(2):267–73, 2012.

[56] Qiukai E., Xiaoyu Liu, Yunxia Liu, Wen Liu, Ji Zuo: Over-expression of GRP75 inhibits liver injury induced by oxidative damage. Acta Biochimica et Biophysica Sinica, Volume 45, Issue 2, Pages 129–134, 1 February 2013.

[57] Katrien Van Beneden, Leo A. van Grunsven, Caroline Geers, Marina Pauwels, Alexis Desmoulière, Dierik Verbeelen, Albert Geerts, Christiane Van den Branden. CRBP-I in the

renal tubulointerstitial compartment of healthy rats and rats with renal fibrosis; Nephrology Dialysis Transplantation, Volume 23, Issue 11, Pages 3464–3471, 25 May 2008.

[58] Uchio K, Tuchweber B, Manabe N, Gabbiani G, Rosenbaum J, Desmoulière A. Cellular retinol-binding protein-1 expression and modulation during in vivo and in vitro myofibroblastic differentiation of rat hepatic stellate cells and portal fibroblasts. Lab Invest. 82(5):619-28, May 2002.

[59] Jeremy S. Duffield: Macrophages and Kidney Disease: Macrophages and Immunological Inflammation of the kidney. Semin Nephrol. May 30, Vol 3, pp234–254, 2010.

[60] Tim D. Hewitson. Renal tubulointerstitial fibrosis: common but never simple. American Journal of Physiology - Renal Physiology. Vol. 296 no. 6, May 25 2009.

[61] Manushi Siddharth, Sudip K. Datta, Savita Bansal, Mohammad Mustafa, Basu D. Banerjee, Om P. Kalra, and Ashok K. Tripathi. Study on Organochlorine Pesticide Levels in Chronic Kidney Disease Patients: Association with Estimated Glomerular Filtration Rate and Oxidative Stress. J BIOCHEM MOLECULAR TOXICOLOGY Volume 26, Number 6, April 14, 2012.

[62] J Toppari, J C Larsen, P Christiansen, A Giwercman, P Grandjean, L J Guillette, Jr, B Jégou, T K Jensen, P Jouannet, N Keiding, H Leffers, J A McLachlan, O Meyer, J Müller, E Rajpert-De Meyts, T Scheike, R Sharpe, J Sumpter, and N E Skakkebaek. Male reproductive health and environmental xenoestrogens. Environ Health Perspect. 104(Suppl 4): 741–803, Aug 1996.

[63] M.H.Craig, R.W.Snow, D.le Sueur. A Climate-based Distribution Model of Malaria Transmission in Sub-Saharan Africa. Parasitology Today. Volume 15, Issue 3, Pages 105-111 March 1, 1999.

[64] Muir, D.C.G. ; Norstrom, R.J. ; Simon, M. Organochlorine contaminants in arctic marine food chains: accumulation of specific polychlorinated biphenyls and chlordane-related compounds. Environ. Sci. Technol.; (United States); Journal Volume: 22:9, September 01, 1988.

[65] Dorothy C. Sm. Pesticide residues in the total diet in Canada. Pest Management Science. March 1971.

[66] Mary S. Wolff Paolo G. Toniolo Eric W. Lee Marilyn Rivera Neil Dubin. Blood Levels of Organochlorine Residues and Risk of Breast Cancer. JNCI: Journal of the National Cancer Institute, Volume 85, Issue 8, Pages 648–652, April 21, 1993.

[67] Curtis D. Klaassen, Jie Liu, and Supratim Choudhuri. METALLOTHIONEIN: An Intracellular Protein to Protect Against Cadmium Toxicity. Annual Review of Pharmacology and Toxicology
Vol. 39:267-294. April, 1999.

[68] Ahmad I, Hamid T, Fatima M, Chand HS, Jain SK, Athar M, Raisuddin S. Induction of hepatic antioxidants in freshwater catfish (Channa punctatus Bloch) is a biomarker of papermill effluent exposure. Biochimica et Biophysica Acta 1523, 37–48. 2000.

[69] Sushil K. Sharma and Manuchair Ebadi. Metallothionein Attenuates 3-Morpholinosydnonimine (SIN-1)-Induced Oxidative Stress in Dopaminergic Neurons. Antioxidants & Redox Signaling. Volume: 5 Issue 3: July 5, 2004.

[70] JosefAbel, Nadade Ruiter. Inhibition of hydroxyl-radical-generated DNA degradation by metallothionein. Toxicology Letters. Volume 47, Issue 2, Pages 191-196, May 1989.

[71] N. Chiaverini and M. De Ley. Protective effect of metallothionein on oxidative stress-induced DNA damage. Volume 44, 2010 - Issue 6. Apr. 12, 2010.

[72] Ogra Y., Onishi S., Kajiwara A., Hara A., Suzuki K.T. Enhancement of nuclear localization of metallothionein by nitric oxide. J. Health Sci. 54:339–342; 2008.

[73] hisa Takahashi, Yasumitsu Ogra, Kazuo T. Suzuk. Nuclear trafficking of metallothionein requires oxidation of a cytosolic partner. Jurnal of Cellular Physiology. Aug. 12, 2004.

[74] Huasheng Lu, Diana Margaret Hunt, Ramapriya Ganti, Alberta Davis, Kamla Dutt, Jawed Alam, Richard C. Hunt. Metallothionein Protects Retinal Pigment Epithelial Cells Against Apoptosis and Oxidative Stress. Experimental Eye Research. Volume 74, Issue 1, Pages 83-92, January 2002.

[75] Ryuya Shimoda, William E. Achanzar, Wei Qu, Takeaki Nagamine, Hitoshi Takagi, Masatomo Mori, Michael P. Waalkes. Metallothionein Is a Potential Negative Regulator of Apoptosis. Toxicological Sciences, Volume 73, Issue 2, , Pages 294–300, June 1 2003.

[76] LuCai, Masahiko Satoh, Chiharu Tohyama, M.George Cherian. Metallothionein in radiation exposure: its induction and protective role. Toxicology. Volume 132, Issues 2–3, Pages 85-98, 15 February 1999.

[77] Cherian MG, Apostolova MD. Nuclear localization of metallothionein during cell proliferation and differentiation. Cell Mol Biol (Noisy-le-grand) ;46(2):347-56. Mar 2000.

[78] LAEMMLI, V. K. – Cleavage of structural proteins during the assembly of the head of bacteriophage T_4. Nature, 227: 680-5, 1970.

[79] Livak KJ, Schmittgen TD. Analysis of relative gene expression data using real-time quantitative PCR and the 2(-Delta Delta C(T)) Method. Methods. 25(4):402-8; Dec 2001.

[80] Chubatsu LS, Meneghini R. Metallothionein protects DNA from oxidative damage. Biochem J. 1;291 (Pt 1):193-8, Apr 1993.

[81] Vukovic V, Pheng SR, Stewart A, Vik CH, Hedley DW. Protection from radiation-induced DNA single-strand breaks by induction of nuclear metallothionein. Int J Radiat Biol. 76(6):757-62, june 2000.

[82] M. George Cherian. The Significance of the Nuclear and Cytoplasmic Localization of Metallothionein in Human Liver and Tumor Cells. *Environmental Health Perspectives*. Vol. 102, Supplement 3: Molecular Mechanisms of Metal Toxicity and Carcinogenicity; pp. 131-135, Sept 1994.

[83] Cherian MG, Apostolova MD. Nuclear localization of metallothionein during cell proliferation and differentiation. Cell Mol Biol (Noisy-le-grand). 46(2):347-56, Mar 2000.

[84] (Emilio Carpene`, Giulia Andreani, Gloria Isani Metallothionein functions and structural characteristics. ScienceDirect, Journal of Trace Elements in Medicine and Biology 21 (2007) S1, 35–39; September 10, 2007).

[85] kurunthachalam Senthil Kumar, Kurunthachalam Kannan, John p. Giesy and Shigeki Masunaga. Distribution and elimination of polychlorinated dibenzo-p-dioxins, dibenzofurans, biphenyls, and p,p′-DDE in tissues of bald eagles from the upper peninsula of michigan. Environmental Science & Technology ; vol. 36, no. 13, pages 2789-96, 2002.

[86] Ralph Gingell and Lawrence Wallcave. Species differences in the acute toxicity and tissue distribution of DDT in mice and hamsters. Toxicology and Applied Pharmacology. Volume 28, Issue 3, Pages 385-394, June 1974.

[87] Sato M, Kawakami T, Kondoh M, Takiguchi M, Kadota Y, Himeno S, Suzuki S . Development of high-fat-diet-induced obesity in female metallothionein-null mice. FASEB J. 24(7):2375-84.); Jul 2010.

[88] Nagoya-Shibata-Yasuda (NSY) Nojima K, Sugimoto K, Ueda H, Babaya N, Ikegami H, Rakugi H . Analysis of hepatic gene expression profile in a spontaneous mouse model of type 2 diabetes under a high sucrose diet. Endocr J. 60(3):261-74; 2013.

[89] Steven R. Davis and Robert J. Cousins. Metallothionein Expression in Animals: A Physiological Perspective on Function. The Jurnal of Nutrition, page 1085-1088, May 1, 2000.

[90] Neila Marouani, Dorsaf Hallegue, Mohsen Sakly, Moncef Benkhalifa, Khémais Ben Rhouma, and Olfa Tebourbi p,p'-DDT induces testicular oxidative stress-induced apoptosis in adult rats. Reprod Biol Endocrinol, May 26, 2017.

[91] Diponkar Banerjee, Satomi Onosaka and M.George Cherian. Immunohistochemical localization of metallothionein in cell nucleus and cytoplasm of rat liver and kidney. Toxicology, Volume 24, Issue 2, Pages 95-105, 1982.

[92] Ogra Y. and Suzuki KT Nuclear trafficking of metallothionein: possible mechanisms and current knowledge. Cellular and Molecular Biology (Noisy-le-Grand, France). 46(2):357-365, Mar 01, 2000.

[93] M G Cherian. he significance of the nuclear and cytoplasmic localization of metallothionein in human liver and tumor cells. Environ Health Perspect. 102(Suppl 3): 131–135; Sep 1994.

[94] Rob Moodie, David Stuckler, Carlos Monteiro, Nick Sheron, Bruce Neal, Thaksaphon Thamarangsi, Paul Lincoln, Sally Casswell of behalf of The Lancet NCD Action Group. Profits and pandemics: prevention of harmful eff ects of tobacco, alcohol, and ultra-processed food and drink industries. Lancet 381: 670–79, 2013.

[95] Christos A. Damalas and Ilias G. Eleftherohorinos. Pesticide Exposure, Safety Issues, and Risk Assessment Indicators. Int. J. Environ. Res. Public Health, Review 8(5), pages 1402-1419 May 6, 2011.

[96] Amalia Ledesma, Mario García de Lacoba, and Eduardo Rial. The mitochondrial uncoupling proteins. Genome Biol. 3(12) Nov 29, 2002.

[97] Casey L. Quinlan, Irina V. Perevoshchikova, Martin Hey-Mogensen, Adam L. Orr, and Martin D. Branda. Sites of reactive oxygen species generation by mitochondria oxidizing different substrates. Redox Biol. 1(1): pages 304–312, May 23, 2013.

[98] Pablo Muriel Role of free radicals in liver diseases. Hepatol Int. 2009 Dec; 3(4): pages 526–536. Nov 26, 2009.

[99] Marcelo J. Berardi, William M. Shih, Stephen C. Harrison & James J. Chou. Mitochondrial uncoupling protein 2 structure determined by NMR molecular fragment searching. Nature 476, pages 109–113, August 04, 2011.

[100] Amalia Ledesma, Mario García de Lacoba, and Eduardo Rial. The mitochondrial uncoupling proteins. Genome Biol. 3(12) Nov 29, 2002.

[101] Negre-Salvayre A., Hirtz, C., Carrera, G., Cazenave, R., Troly, M., Salvayre, R., Penicaud, L. &Casteilla, L.: A role for uncoupling protein-2 as a regulator of mitochondrial hydrogen peroxide generation. FASEB J. 11, 809-815, 1999.

[102] Horimoto M., Fulop P., Derdak Z., Resnick M., Wands J. R. &Baffy G.: Uncoupling protein-2 deficiency promotes oxidant stress and delays liver regeneration in mice. Hepatology39, 386-392, 2004.

[103] Andriy Fedorenko, Polina V. Lishko , Yuriy Kirichok. Mechanism of Fatty-Acid-Dependent UCP1 Uncoupling in Brown Fat Mitochondria. Cell press, Volume 151, Pages 400–413, October 12, 2012.

[104] C.-Y. Zhang, G. Baffy, P. Perret, S. Krauss, O. Peroni, D. Grujic, T. Hagen, A. J. Vidal-Puig, O. Boss, Y.-B. Kim, X. X. Zheng, M. B. Wheeler, G. I. Shulman, C. B. Chan, B. B. Lowell. Uncoupling Protein-2 negatively regulates insulin secretion and is a major link between obesity, cell dysfunction, and type 2 diabetes. Cell, Volume 105, Pages 745-755, 2001.

[105] Dominique Larrouya, Patrick Laharraguea, Georges Carrerab, Nathalie Viguerie-Bascandsa, Corinne Levi-Meyrueisc, Christophe Fleuryc, Claire Pecqueurc, MaryseNibbelinka, Mireille Andréa, Louis Casteillaa. Kupffer Cells Are a Dominant Site of Uncoupling Protein 2 Expression in Rat Liver. Volume 235, Issue 3, 760-764, June 27,1997.

[106] A Nègre-Salvayre, C Hirtz, G Carrera, R Cazenave, M Troly, R Salvayre,L Pénicaud and L Casteilla. A role for uncoupling protein-2 as a regulator of mitochondrial hydrogen peroxide generation. FASEB J 11:809-15, August 1997.

[107] Yuji Makita, Minoru Omura, Akiyo Tanaka and Chikako Kiyohara. Effects of Concurrent Exposure to Tributyltin and 1,1-Dichloro-2,2 bis (p-chlorophenyl) ethylene (p,pø-DDE) on Immature Male Wistar Rats. Basic & Clinical Pharmacology & Toxicology 2005, 97, 364–368, June 7, 2005.

[108] N. De Marco, L. Iannone, R. Carotenuto, S. Biffo, A. Vitale, C.Campanella. p27(BBP)/eIF6 acts as an anti-apoptotic factor upstream of Bcl-2 during Xenopus laevis development. Cell Death Differ., 17 , pp. 360-372, 2010.

[109] K.J. Livak, T.D. Schmittgen. Analysis of relative gene expression data using real-time quantitative PCR and the 2(-Delta Delta C(T)) Methods, 25 pp. 402, 2001.

[110] Elizabeth M Brunt and Dina G Tiniakos. Histopathology of nonalcoholic fatty liver disease. World J Gastroenterol. 2010 Nov 14; 16(42): 5286–5296. Nov 14, 2010.

[111] Pouneh S. Mofrad, Arun J. Sanyal Nonalcoholic Fatty Liver Disease. April 16, 2003.

[112] Sica R. PhD thesis. University of the studies of Naples, Federico II. (http://www.fedoa.unina.it/10406/1/PhD%20Thesis%20_%20Raffaella%20Sica.pdf) May 5, 2014.

[113] Luis A. VIDELA, Ramón RODRIGO, Myriam ORELLANA, Virginia FERNANDEZ, Gladys TAPIA, Luis QUIÑONES, Nelson VARELA, Jorge CONTRERAS, Raúl LAZARTE, Attila CSENDES, Jorge ROJAS, Fernando MALUENDA, Patricio BURDILES, Juan C. DIAZ, Gladys SMOK, Lilian THIELEMANN, Jaime PONIACHIK. Oxidative stress-related parameters in the liver of non-alcoholic fatty liver disease patients. Clinical Science, 106 (3) 261-268; Mar 01, 2004.

[114] Hartmut Jaeschke, Mitchell R. McGill, and Anup Ramachandran. Oxidant stress, mitochondria, and cell death mechanisms in drug-induced liver injury: Lessons learned from acetaminophen hepatotoxicity. REVIEW ARTICLE. Drug Metabolism Reviews, 44(1): 88–106, 2012.

[115] Cairns C. B., Walther J., Harken A. H. and Banerjee A. Mitochondrial oxidative phosphorylation efficiencies reflect physiological organ roles. Am. J. Physiol. 274: R1376-R1383, 1998.

[116] Mailloux RJ, Harper ME. Uncoupling proteins and the control of mitochondrial reactive oxygen species production. Free RadicBiol Med. Sep 15, 2011.

[117] Dominique Larrouya, Patrick Laharraguea, Georges Carrerab, Nathalie Viguerie-Bascandsa, Corinne Levi-Meyrueisc, Christophe Fleuryc, Claire Pecqueurc, MaryseNibbelinka, Mireille Andréa, Louis Casteillaa. Kupffer Cells Are a Dominant Site of Uncoupling Protein 2 Expression in Rat Liver. Volume 235, Issue 3, 760-764, June 27 1997.

[118] Francesc Villarroya, Roser Iglesias, and Marta Giralt. PPARs in the Control of Uncoupling Proteins Gene Expression. PPAR Res. Nov 28, 2006.

[119] Hannes Oberkofler, Kerstin Klein, Thomas K. Felder, Franz Krempler and Wolfgang Patsch. Role of PGC-1α in the transcriptional regulation of the human UCP2 gene in INS-1E cells. Endocrinology. As doi:10.1210/en.2005-0817, November 10, 2005.

[120] Mary P Thompson and Dongho Kim. Links between fatty acids and expression of UCP2 and UCP3 mRNAs. FEBS Letters, Volume 568, Issues 1–3, Pages 4-9, 18 June 2004.

[121] Barbara Arroyo, Jesus Olivero-Verbel and Angelica Guerrero. Direct effect of p,p'- DDT on mice liver. Brazilian Jurnal of Pharmaceutical Science. Vol52,N.2, Apr/Jun, 2016.

[122] Qian Liu, QihanWang, ChengXu, Wentao Shao, Chunlan Zhang, Hui Liu, Zhaoyan Jiang & AihuaGu. Organochloride pesticides impaired mitochondrial function in hepatocytes and aggravated disorders of fatty acid metabolism. Scientific Reports. Apr 11, 2017.

[123] Mailloux RJ1, Seifert EL, Bouillaud F, Aguer C, Collins S, Harper ME. Glutathionylation acts as a control switch for uncoupling proteins UCP2 and UCP3. J Biol Chem;286(24):21865-75, Jun 17, 2011.

[124] Ryan J. Mailloux, Erin L. Seifert, Frédéric Bouillaud, Céline Aguer, Sheila Collins, and Mary-Ellen Harper; Glutathionylation Acts as a Control Switch for Uncoupling Proteins UCP2 and UCP3. JBC Papers in Press, April 22, 2011.

[125] Nakatani T, Tsuboyama-Kasaoka N, Takahashi M, et al. Mechanism for peroxisome proliferator-activated receptor- a activator- induced up-regulation of UCP2 mRNA in rodent hepatocytes. J Biol Chem 277: 9562–9569; 2002.

[126] Villarroya F, Iglesias R, Giralt M. PPARs in the control of uncoupling proteins gene expression. PPAR Research: 74364; 2007

[127] Echtay KS, Roussel D, St-Pierre J, Jekabsons MB, Cadenas S, Stuart JA, Harper JA, Roebuck SJ, Morrison A, Pickering S, Clapham JC, Brand MD. [1]Medical Research Council Dunn Human Nutrition Unit, Hills Road, Cambridge CB2 2XY, UK. Superoxide activates mitochondrial uncoupling proteins. Nature. Jan 3;415(6867) : 96-9, 2002.

[128] Ryan J. Mailloux and Mary-Ellen Harper. The evolving role of mitochondria in metabolism Mitochondrial proticity and ROS signaling. Cell, Volume 23, Issue 9, p451–458, September 2012.

[129] Liangyou Rui. Energy Metabolism in the Liver. Compr Physiol. Author manuscript; available in PMC; June 10, 2014.

[130] William D. Carey, MD; Bertram Fleshler, MD The Liver: Biology and Pathobiology. February 18, 1983.

[131] D. M. Grant. Detoxification Pathways in the Liver. Journal of Inherited Metabolic Disease pp 421-430, (14), 1991.

[132] Cheng Ji, Neil Kaplowitz, Mo Yin Lau, Eddy Kao, Lydia M. Petrovic, and Amy S. Lee Liver-specific loss of GRP78 perturbs the global unfolded protein response and exacerbates a spectrum of acute and chronic liver diseases Hepatology. 54(1): pages 229–239, Jul 2011.

[133] Anne Platt Mc Ginn. Malaria, Mosquitoes, and DDT The toxic war against a global disease. World watch Institute. WORLD WATCH magazine. May/June, 2002.

[134] Mustapha Debboun, Stephen P. Frances, Daniel Strickman. Insect Repellents: Principles, Methods, and Uses. CRC Press, Taylor & Francis Group. 2006.

[135] (MLA style: "The Nobel Prize in Physiology or Medicine 1948". Nobelprize.org. Nobel Media AB 2014. Jul 31, 2017. <http://www.nobelprize.org/nobel_prizes/medicine/laureates/1948/>).

[136] Geisz HN, Dickhut RM, Cochran MA, Fraser WR, Ducklow HW (June 2008). "Melting glaciers: a probable source of DDT to the Antarctic marine ecosystem". Environmental Science & Technology. 42 (11): 3958–62, 2008.

[137] A. Curley, L. Fishbein, K. Gheorghiev, F. Korte, B. Paccagnella, M. Roberfroid, Y. Shirasu, E. M. B. Smith, D.C. Villeneuve. DDT and its derivatives, Environmental Health Criteria monograph No. 009, Geneva: World Health Organization, 1979, ISBN 92-4-154069-9

[138] J. M. Aislabie , N. K. Richards & H. L. Boul. Microbial degradation of DDT and its residues—A review. New Zealand Journal of Agricultural Research, Volume 40, 1997 - Issue 2, Pages 269-282; Mar 17, 2010.

[139] J. M. Aislabie, N. K. Richards & H. L. Boul: Microbial degradation of DDT and its residues—A review, Volume 40, 1997 - Issue 2, Pages 269-282 | Received 24 Jun 1996, Accepted 20 Dec 1996, Published online: 17 Mar, 2010.

[140] R.Carson: Silent spring, 1962.

[141] De Zulueta J. The end of malaria in Europe: an eradication of the disease by control measures. Parassitologia. 40 (1–2): 245–46, June 1998.

[142] World Health Organization. Indoor residual spraying. Use of indoor residual spraying for scaling up global malaria control and elimination (archived). August 2006.

[143] C.F. Curtis, Control of Malaria Vectors in Africa and Asia. Wayback Machine. October 2, 2007.

[144] Richard F. Addison and Maurice E. Zinck. PCBs Have Declined More Than DDT-Group Residues in Arctic Ringed Seals (Phoca hispida) between 1972 and 1981. Environ. Sci. Technol., Vol. 20, No. 3, 1986.

[145] Derek C. G. Mulr ,+ Ross J. Norstrom, and Mary Simon. Organochlorine Contaminants in Arctic Marine Food Chains: Accumulation of Specific Polychlorinated Biphenyls and Chlordane-Related Compounds. Environ. Sci. Technol., Vol. 22, No. 9, 1988.

[146] Jolly Jacob: A Review of the Accumulation and Distribution of Persistent Organic Pollutants in the Environment. International Journal of Bioscience, Biochemistry and Bioinformatics, Vol. 3, No. 6, November 2013.

[147] TOXICOLOGICAL PROFILE FOR DDT, DDE, and DDD: U.S. DEPARTMENT OF HEALTH AND HUMAN SERVICES Public Health Service Agency for Toxic Substances and Disease Registry September 2002.

[148] Ivan Dimauro, Timothy Pearson, Daniela Caporossi, and Malcolm J Jackson. A simple protocol for the subcellular fractionation of skeletal muscle cells and tissue. BMC Research Notes 2012 5:513; September 20, 2012.

[149] Ivan Dimauro, Timothy Pearson, Daniela Caporossi, and Malcolm J Jackson. A simple protocol for the subcellular fractionation of skeletal muscle cells and tissue. BMC Research Notes 2012 5:513; September 20, 2012.

[150] Halina Cichoż-Lach and Agata Michalak. Oxidative stress as a crucial factor in liver diseases. World J Gastroenterol. 20(25): pages 8082–8091 Jul 7, 2014.

[151] Christophe Fleury, Bernard Mignotte, Jean-Luc Vayssière. Mitochondrial reactive oxygen species in cell death signaling. Volume 84, Issues 2–3, Pages 131-141 February–March 2002.

[152] Sica R. (2015) fedOA University of Studies of Naples, Federico II: Effetti del pesticida 2,2-Bis(4-Clorofenil)-1,1-Dicloroetilene (DDE) sulla morfologia, funzionalità e dinamica mitocondriale nel testicolo e nel fegato di ratto. [PhD thesis], 31/03/2015

[153] C Garrido, L Galluzzi, M Brunet, P E Puig, C Didelot and G Kroemer. Mechanisms of cytochrome c release from mitochondria. Cell Death and Differentiation. 5 May 2006.

[154] Sica R. (2015) fedOA University of Studies of Naples, Federico II: Effetti del pesticida 2,2-Bis(4-Clorofenil)-1,1-Dicloroetilene (DDE) sulla morfologia, funzionalità e dinamica mitocondriale nel testicolo e nel fegato di ratto. [PhD thesis], 31/03/2015

[155] Jeremy S. Duffield: Macrophages and Kidney Disease: Macrophages and Immunological Inflammation of the kidney. Semin Nephrol. May 30, Vol 3, pp234–254, 2010.

[156] Anna Alisi, Guido Carpino, Felipe L. Oliveira, Nadia Panera, Valerio Nobili, and Eugenio Gaudio. The Role of Tissue Macrophage-Mediated Inflammation on NAFLD Pathogenesis and Its Clinical Implications. Mediators Inflamm. 2017.

[157] Lee AS. The ER chaperone and signaling regulator GRP78/BiP as a monitor of endoplasmic reticulum stress. Methods. 35(4): pages 373-81, Apr 2005.

[158] Pablo J Fernandez-Marcos and Johan Auwerx. Regulation of PGC-1α, a nodal regulator of mitochondrial biogenesis. The America Jurnal of Clinical Nutrition. vol. 93 no. 4, pages 884S-890S, April 2011.

[159] LeBleu VS, O'Connell JT[2], Gonzalez Herrera KN, Wikman H, Pantel K, Haigis MC, de Carvalho FM, Damascena A, Domingos Chinen LT, Rocha RM, Asara JM, Kalluri R. PGC-1α mediates mitochondrial biogenesis and oxidative phosphorylation in cancer cells to promote metastasis. Nat Cell Biol. 16(10):992-1003, Oct 2014.

[160] François R. Jornayvaz and Gerald I. Shulman: Regulation of mitochondrial biogenesis. Essays In Biochemistry. (47), pages 69-84; Jun 14, 2010.

[161] Sica R. (2015) fedOA University of Studies of Naples, Federico II: Effetti del pesticida 2,2-Bis(4-Clorofenil)-1,1-Dicloroetilene (DDE) sulla morfologia, funzionalità e dinamica mitocondriale nel testicolo e nel fegato di ratto. [PhD thesis], 31/03/2015.

[162] Shengnan Wu, Feifan Zhou, Zhenzhen Zhang, Da Xing: Mitochondrial oxidative stress causes mitochondrial fragmentation via differential modulation of mitochondrial fission–fusion proteins. The FEBS Journal, 3 February, 2011.

[163] Xiying Fan, Rajaa Hussien, George A. Brooks: H_2O_2-induced mitochondrial fragmentation in C_2C_{12} myocytes. Free Radical Biology and Medicine; Volume 49, Issue 11, Pages 1646-1654 1 December 2010.

[164]T Ahmad, K Aggarwal, B Pattnaik, S Mukherjee, T Sethi, B K Tiwari, M Kumar, A Micheal, U Mabalirajan, B Ghosh, S Sinha Roy, and A Agrawal: Computational classification of mitochondrial shapes reflects stress and redox state. Cell death & disease; Jan 17, 2013.

[165] HarmeetMalhi and Randal J.Kaufman. Endoplasmic reticulum stress in liver disease. Volume 54, Issue 4, Pages 795-809, April 2011.

[166] Robert Eskes[†], Solange Desagher, Bruno Antonsson, and Jean-Claude Martinou: Bid Induces the Oligomerization and Insertion of Bax into the Outer Mitochondrial Membrane. Molecular and Cellular Biology, 25 October 1999.

[167] Sica R. (2015) fedOA University of Studies of Naples, Federico II: Effetti del pesticida 2,2-Bis(4-Clorofenil)-1,1-Dicloroetilene (DDE) sulla morfologia, funzionalità e dinamica mitocondriale nel testicolo e nel fegato di ratto. [PhD thesis], 31/03/2015.

[168]Henning W. Zimmermann,Sebastian Seidler,Nikolaus Gassler,Jacob Nattermann,Tom Luedde,Christian Trautwein,Frank Tacke. Interleukin-8 Is Activated in Patients with Chronic Liver Diseases and Associated with Hepatic Macrophage Accumulation in Human Liver Fibrosis. PLOS, Fig3, June 22, 2011.

[169] Yonit Lavin and Miriam Merad. Macrophages: Gatekeepers of Tissue Integrity. Cancer Immunol Res. 1(4): pages 201–209, Oct 2013.

[170] Richard J. Youle1 and Alexander M. van der Bliek. Mitochondrial Fission, Fusion, and Stress. Science; 337(6098): 1062–1065, Aug 2012.

[171] Paula C.Mota , MaríliaCordeiro, Susana P.Pereira, Paulo J.Oliveira, António J.Moreno, JoãoRamalho-Santos. Differential effects of p,p′-DDE on testis and liver mitochondria:Implications for reproductive toxicology. Reproductive Toxicology. Volume 31, Issue 1, Pages 80-85, January 2011.

[172] LeonidGrinberg, EitanFibach, JohnnyAmer and DaphneAtlas. N-acetylcysteine amide, a novel cell-permeating thiol, restores cellular glutathione and protects human red blood cells from oxidative stress. Free Radical Biology and Medicine. Volume 38, Issue 1, Pages 136-145, January 1, 2005.

[173] Aldo M. J Nutr Sci Vitaminol (Tokyo). Effects of dietary levels of proteins and fats on DDT (1,1,1-trichloro-2,2-bis(p-chlorophenyl)ethane) and liver lipid metabolism. 1982.

[174] Satoh MS, Lindahl T. Role of poly(ADP-ribose) formation in DNA repair. Nature. ;356(6367):356-8, Mar 26,1992.

[175] Oliver FJ, de la Rubia G, Rolli V, Ruiz-Ruiz MC, de Murcia G, Murcia JM. Importance of poly(ADP-ribose) polymerase and its cleavage in apoptosis. Lesson from an uncleavable mutant. J Biol Chem. 11;273(50):33533-9 Dec 1998.

Papers already published and not directly correlated with my Ph.D studies.

1) **Diet impact on Mitochondrial Bioenergetics and Dynamics.**

2) **Skeletal muscle mitochondrial bioenergetics and morphology in high fat diet induced obesity and insulin resistance: Focus on dietary fat source.**

frontiers in Physiology

MINI REVIEW
published: 08 April 2015
doi: 10.3389/fphys.2015.00109

Diet impact on mitochondrial bioenergetics and dynamics

Rosalba Putti, Raffaella Sica, Vincenzo Migliaccio and Lillà Lionetti *

Department of Biology, University of Naples "Federico II", Naples, Italy

Diet induced obesity is associated with impaired mitochondrial function and dynamic behavior. Mitochondria are highly dynamic organelles and the balance in fusion/fission is strictly associated with their bioenergetics. Fusion processes are associated with the optimization of mitochondrial function, whereas fission processes are associated with the removal of damaged mitochondria. In diet-induced obesity, impaired mitochondrial function and increased fission processes were found in liver and skeletal muscle. Diverse dietary fat sources differently affect mitochondrial dynamics and bioenergetics. In contrast to saturated fatty acids, omega 3 polyunsaturated fatty acids induce fusion processes and improve mitochondrial function. Moreover, the pro-longevity effect of caloric restriction has been correlated with changes in mitochondrial dynamics leading to decreased cell oxidative injury. Noteworthy, emerging findings revealed an important role for mitochondrial dynamics within neuronal populations involved in central regulation of body energy balance. In conclusion, mitochondrial dynamic processes with their strict interconnection with mitochondrial bioenergetics are involved in energy balance and diet impact on metabolic tissues.

Keywords: mitochondrial fusion, mitochondrial fission, dietary fat, caloric restriction, energy balance

OPEN ACCESS

Edited by:
Ovidiu Constantin Baltatu, Camilo Castelo Branco University, Brazil

Reviewed by:
Giovanni Solinas, University of Gothenburg, Sweden
Luciana A. Campos, University Camilo Castelo Branco, Brazil

***Correspondence:**
Lillà Lionetti, Department of Biology, University of Naples "Federico II", Complesso Universitario Monte S. Angelo, Edificio 7, Via Cinthia, I-80126, Napoli, Italy
lilla.lionetti@unina.it

Specialty section:
This article was submitted to Integrative Physiology, a section of the journal Frontiers in Physiology

Received: *05 February 2015*
Accepted: *18 March 2015*
Published: *08 April 2015*

Citation:
Putti R, Sica R, Migliaccio V and Lionetti L (2015) Diet impact on mitochondrial bioenergetics and dynamics. Front. Physiol. 6:109. doi: 10.3389/fphys.2015.00109

Mitochondrial Dynamics and Bioenergetics

Mitochondria are referred to as the "powerhouses" of the cell due to their prominent role in ATP production and cellular metabolism regulation. Together with their energetic role, mitochondria are very dynamic organelles that continuously divide, collide and fuse with other mitochondria. Therefore, their morphology is highly variable. It can shift between small round punctuated structures or reticulum networks of elongated mitochondria as a result of the balance between fusion and fission processes. Various work has been done to analyze the mechanism of this dynamic behavior and different proteins (a group of large ATPases) have been identified as being involved (James et al., 2003; Ishihara et al., 2004, 2006; Jagasia et al., 2005; Liesa et al., 2009). In particular, the main proteins involved in mammalian mitochondrial fusion processes are mitofusin 1 and 2 (Mfn1 and 2) and autosomal dominant optic atrophy-1 (Opa1). Mitofusin is located on the outer mitochondrial membrane and plays a role in the outer membranes fusion, whereas Opa1 is located on the inner mitochondrial membrane and is involved in the inner membrane fusion process (Malka et al., 2005). In addition, Opa1 controls cristae remodeling and protects from apoptosis (Frezza et al., 2006). It should be noted that also Mfn2 has a dual role, since other than its well-known role in mitochondrial fusion (Zorzano et al., 2010), Mfn2 is also implicated in the structural and functional connection between mitochondria and the endoplasmic reticulum (ER) and it may play a role in ER stress development in conditions of metabolic stress (de Brito and Scorrano, 2008, 2009). As regards fission processes, dynamin related protein 1 (Drp1) and fission protein 1

(Fis1) are the main proteins involved. Drp1 is located mainly in the cytosol and is recruited on the outer mitochondrial membrane by Fis1 that is inserted on the outer membrane (Yoon et al., 2003; Santel and Frank, 2008). Drp1 is also involved in the regulation of apoptosis (Frank et al., 2001).

A correct balance between fusion and fission processes is important for mitochondrial bioenergetics. It has been suggested that mitochondrial fusion processes are induced in conditions in which an optimization of mitochondrial bioenergetics is required, whereas fission processes are associated with mitochondria degradation and therefore they are induced under conditions in which mitochondria are damaged (Westermann, 2012). Deficiency in proteins involved in mitochondrial fusion (Mfn2 and Opa1) reduce respiration in several cell types (Liesa et al., 2009). Mfn2 repression is associated with decreased substrate oxidation and cellular metabolism (Pich et al., 2005). Alterations in OPA1 expression also affect mitochondrial bioenergetics, for example Opa1 depletion causes a reduction in basal respiration (Chen et al., 2005). Therefore, emerging evidence suggests that the balance between mitochondrial fusion and fission processes play an important role in the regulation of mitochondrial energetics.

Several recent reviews analyzed the cellular roles of mitochondrial dynamics and the molecular mechanisms of fusion and fission (McBride et al., 2006; Detmer and Chan, 2007; Hoppins et al., 2007; Liesa et al., 2009; Westermann, 2010, 2012; Elgass et al., 2013; Zhao et al., 2013; Lackner, 2014; da Silva et al., 2014), the present review focused on the impact of diet on mitochondrial dynamic behavior and function in the main metabolic tissues, such as liver and skeletal muscle, as well as the involvement of mitochondrial dynamic processes in body energy balance regulation.

Mitochondrial Dynamics and Bioenergetics in Obesity

It is well known that mitochondrial dysfunction plays an important role in obesity related diseases, such as insulin resistance and non-alcoholic fatty liver diseases. It has also been shown that impairments of mitochondrial function are associated with changes in mitochondrial network in the main tissues involved in obesity related diseases. Indeed, in obese and insulin resistant Zucker rats, skeletal muscle is characterized by a reduced glucose uptake, insulin resistance and reduced oxygen consumption accompanied by a reduction in Mfn2 expression, mitochondrial size and in the extent of the mitochondrial network (Bach et al., 2003). Reduced Mfn2 expression was also reported in skeletal muscle of obese type 2 diabetic patients. A decreased mitochondrial proton leak and increased bioenergetics efficiency in Mfn2-depleted cells has been demonstrated (Bach et al., 2003). Therefore, it has been suggested that Mfn2 loss-of-function found in obesity conditions enhance bioenergetics efficiency and contribute to obesity development by reducing energy expenditure and increasing fat energy store (Liesa et al., 2009). In line with this suggestion, conditions characterized by increased energy expenditure (such as cold exposure, administration of β3 adrenergic agonist, chronic exercise) are associated with higher Mfn2 expression in skeletal muscle and brown adipose tissue (Cartoni et al., 2005; Soriano et al., 2006). Furthermore, an increase in mitochondrial fission proteins was reported in skeletal muscle in mice with genetically induced obesity (ob/ob) as well as in mice with high fat diet-induced obesity (Jheng et al., 2012). Mitochondrial dysfunction was associated with enhanced fission processes in liver from db/db mouse, animal model of obesity and insulin resistance (Holmström et al., 2012). All these reports suggest that a shift toward fission processes is linked to mitochondrial dysfunction in the main tissues, such as skeletal muscle and liver involved in obesity related metabolic disease. In line with this suggestion, our group recently published data on the impact of high fat diet on mitochondrial function and dynamic proteins content in rat skeletal muscle and liver. In particular, we analyzed the effect of two different fat dietary sources (saturated vs. polyunsaturated omega 3) on the above parameters (Lionetti et al., 2014).

Impact of Dietary Saturated Fatty Acids

High fat diet rich in saturated fatty acids (high lard, HL, diet) elicited hepatic fat accumulation and insulin resistance, which was parallel to impaired mitochondrial function, increased reactive oxygen species (ROS) production and a dysregulated expression profile of mitochondrial dynamics proteins (Lionetti et al., 2014). In particular, HL diet induced an increase in mitochondrial fatty acid utilization, but a decrease in $FADH_2$ linked oxygen consumption and in fatty acid induced proton leak, which caused an increase in mitochondrial energetic efficiency and an increase in ROS content. As regards to mitochondrial dynamics proteins, HL diet elicited a decrease in Mfn2 and an increase in protein involved in fission processes (Drp1 and Fis1) accompanied by the presence of numerous small round mitochondria vs. control diet, as observed by electron microscopy (**Figures 1A–C,E**) (Lionetti et al., 2014).

As regards to skeletal muscle, our results suggest that an HL diet also induced a shift toward fission as observed by electron microscopy and by immunureactivities analysis (Lionetti et al., 2013) which showed weak signal for fusion proteins and strong signals for fission proteins in rats which were fed an HL diet (Lionetti et al., 2013). These findings are in line with previous reports that Mfn2 expression is reduced in skeletal muscle of obese Zucker rats and type 2 diabetic patients (Bach et al., 2005; Hernández-Alvarez et al., 2010). In addition, it has also been suggested that Mfn2 plays a role as a regulator of *in vivo* insulin sensitivity and may be a potential target in diabetes drug development (Sebastián et al., 2012). Indeed, Mfn2 deficiency in mice produces mitochondrial dysfunction, increases oxidative stress and endoplasmic reticulum stress and activates JNK impairing insulin signaling in liver and skeletal muscle (Sebastián et al., 2012). This study suggested a role of Mfn2 in coordinating mitochondria and endoplasmic reticulum function, leading to modulation of insulin signaling *in vivo*.

Moreover, saturated fatty acids have also been reported to induce fission processes *in vitro* in differentiated C2C12 skeletal muscle cells (Jheng et al., 2012) associated with mitochondrial dysfunction. *In vivo*, as previously reported, smaller

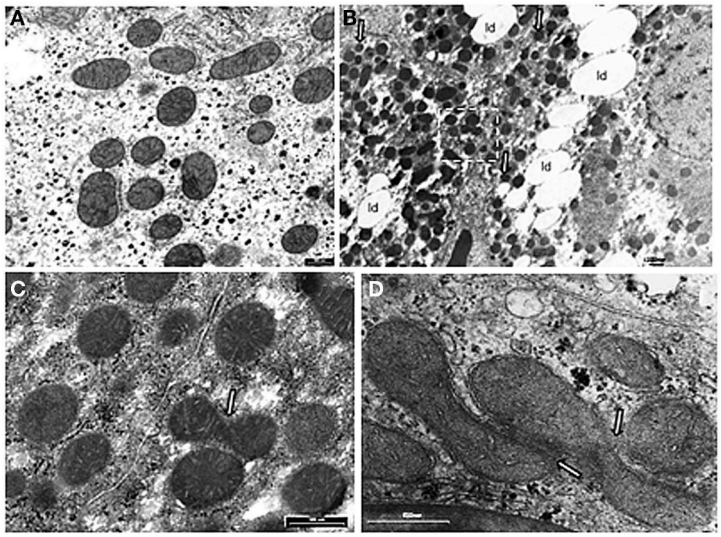

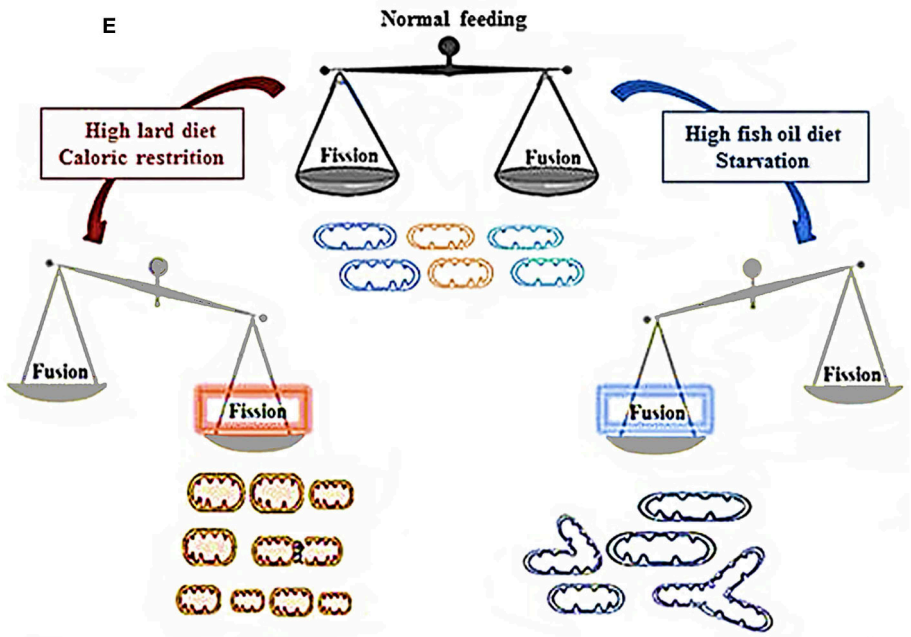

	High lard diet vs. High fish oil diet	Caloric restrition vs. Starvation
DRP1, Fis1	↑	↑
MFN2, OPA1	↓	—
ROS	↑	↓
Δψ	↑	↓
Mitochondrial dysfunction	↑	↑
Mitophagy	?	↑

FIGURE 1 | Mitochondrial morphology and dynamics. (A–D) Electron micrographs of ultrathin rat liver sections. **(A)** section of hepatocytes of rat fed a control diet. The mitochondria showed normal features with tubular, ellissoidal and round profiles. **(B)** section of hepatocyte of rat fed a HL diet. Note the abundant lipid droplet (ld) in cytosol and the prevalence of small mitochondria with round profile. **(C)** Higher magnification of insert in B showing an image suggesting a fission process (arrow). **(D)** section of hepatocyte of rat fed a HFO diet showing a cluster of mitochondria in which the fusion process is ongoing (arrows). **(E)** Diet impact on mitochondrial

(Continued)

FIGURE 1 | Continued
dynamics and function. See text for details. Shift toward fission processes has been found in response both to HLD and CR. However, in response to HLD, fission processes are associated to impairment of mitochondrial function and oxidative stress and may be useful to improve substrate intake in mitochondria or remove damaged mitochondria. On the other hand, in response to CR, mitochondrial fragmentation is associated to mitochondrial biogenesis useful to the maintenance of ATP level to meet cellular energetic needs. In addition, during CR, oxidative stress is reduced and mitochondrial fission may contribute to remove damaged mitochondria by mitophagy explaining the prolongevity effect of CR. Noteworthy, in condition of a more stressed nutrient deprivation, such as cell starvation, it has been reported an increase in mitochondrial fusion processes with elongated mitochondria that were spared by mitochondrial degradation and contributed to increase ATP production to face energetic needs. Fusion processes were found to be increased also in condition of HFO diet, where they contributed to an increase in mitochondrial substrate oxidation and to avoid lipid accumulation and oxidative stress. HLD, high fat diet rich in lard; HFO, high fat diet rich in fish oil; $\Delta\psi$, mitochondrial membrane potential; ROS, reactive oxygen species; CR, caloric restriction ⬆= increase, ⬇= decrease; −= no changes.

mitochondria and increased mitochondrial fission machinery have been described in the skeletal muscle of mice with genetic obesity and those with diet-induced obesity (Jheng et al., 2012). Moreover, inhibition of mitochondrial fission improved the muscle insulin signaling and systemic insulin sensitivity of obese mice (Civitarese and Ravussin, 2008).

Mitochondrial fragmentation and increased fission processes in association with ROS formation have also been reported after treatment with high glucose (HG) in both a rat liver cell-line and myoblasts (Yu et al., 2006). Such fragmentation has been suggested to provide metabolically active organelles with increased total surface area that would increase accessibility of metabolic substrate to carrier proteins (Yu et al., 2006). Therefore, it can also be suggested that HL diet induced-mitochondrial fragmentation might be an adaptive cellular response to increase mitochondrial intake and oxidation of surplus of dietary fatty acids, which would result in elevated ROS production (Lionetti et al., 2014).

Impact of Omega 3 Polyunsaturated Fatty Acids

Different sources of dietary fats have been suggested to have different effects on mitochondrial function and dynamic behavior. In fact, in contrast to the effect of saturated fatty acids, omega 3 polyunsaturated fatty acids have been reported to improve mitochondrial function, reduce ROS production, and promote mitochondrial fusion both *in vitro* and *in vivo* experiments. In an *in vitro* steatotic hepatocyte model both eicosapentaenoic and docosahexaenoic acids increased the expression of Mfn2 and the ATP levels, and decreased oxidative stress (Zhang et al., 2011). On the other hand, in Mfn2-depleted steatotic hepatocytes, omega 3 PUFA did not induce the previously described effects (Zhang et al., 2011).

These data obtained *in vitro* were in line with our data showing improvement of mitochondrial function, reduced ROS production and induction of hepatic mitochondrial fusion through fish oil i*n vivo* (Lionetti et al., 2014). Indeed, the comparison of the effect of high fat diet rich in fish oil (HFO diet) and HL diet in rats showed that HFO diet led to less lipid accumulation in liver and higher fatty acid utilization. We also observed in HFO diet fed rats a mild mitochondrial uncoupling due to enhanced expression of uncoupling protein 2. These decreases in mitochondrial efficiency might contribute to increased fatty acid utilization and reduce ROS production. In HFO diet fed rats, a shift toward fusion was found with concomitant increases in Mfn2 and Opa1 as well as decreases in Drp1 and Fis1, in line with an increased number of tubular mitochondria observed by electron microscopy compared to HL diet (**Figures 1D,E**). This fusion phenotype was in accordance with reduced weight gain found in HFO diet vs. HL diet fed rats. With the limitation that the cause-consequence relationship between the leaner phenotype of HFO diet vs. HL diet fed rats and mitochondrial dynamics is not known, it can be suggested that the specific dietary fatty acid composition may play a role in obesity and hepatic steatosis development as well as in mitochondrial bioenergetics and dynamics (Lionetti et al., 2014).

Similar results were found in skeletal muscles of rats fed HFO diet, where, compared to HL diet, reduced fission processes and increased fusion events were suggested by immuoreactivity analysis and electron microscopy (Lionetti et al., 2013). Indeed, skeletal muscle sections from HFO fed rats showed a greater number of immunoreactive fibers for Mfn2 and Opa1 protein as well as weaker immunostaining for Drp1 and Fis1 compared to sections from HL fed rats. The shift toward fusion events in HFO fed rats was associated with the improvement of obesity and systemic and skeletal muscle insulin sensibility (Lionetti et al., 2013).

Differential effects of saturated and unsaturated fatty acids on mitochondrial morphology and dynamics were reported *in vitro* in C2C12 skeletal muscle cells. The results showed that treatment with saturated fatty acids induced mitochondrial fragmentations, whereas unsaturated and polyunsaturated fatty acids protected against palmitate-induced mitochondrial fission (Jheng et al., 2012).

Starvation, Caloric Restriction and Mitochondrial Dynamics

Opposite mitochondrial dynamics behavior has been reported in two different conditions of nutrient deficiency, such as starvation (Rambold et al., 2011) and caloric restriction (CR) (Khraiwesh et al., 2013).

Mitochondrial elongation is a reversible response to nutrient deprivation in many cell culture types (Rambold et al., 2011). It depends on the type of nutrient depleted. Indeed, either glucose or serum elimination increased mitochondrial fragmentation, whereas mitochondrial fusion was induced by a nitrogen-source deficiency (either glutamine or amino acids). However, a combination of nutrient depletions induced a further mitochondrial elongation, suggesting that mitochondrial fusion can be modulated according to type and severity of starvation. Starvation-induced mitochondrial fusion depends on Mfn1 and Opa1 and is mediated by decreased DRP1 fission activity and by preventing Drp1 localization to mitochondria (**Figure 1E**). Mitochondrial fusion has a protective function, leading to an exchange of

mitochondrial DNA and delaying apoptosis (Chen et al., 2010; Rambold et al., 2011). In fact, mitochondrial elongation might be useful to protect mitochondria from mitophagy. In accordance, during the initial period of starvation cytoplasmic components are degraded, whereas mitochondria become substrate much later (Kristensen et al., 2008), because mitochondria spared from degradation may contribute to maximize cellular energy production to sustain cell during nutrient deprivation (Rambold et al., 2011). Accordingly, mitochondrial fusion has been associated with increase in ATP production during stress and starvation (Gomes et al., 2011) producing beneficial effects for cells under conditions of low nutrient supply. Interestingly, it has been demonstrated that mitochondria provide membrane to autophagosomes during starvation (Hailey et al., 2010) and it can be also suggested that sparing mitochondria may be useful to permit them to serve as an autophagosome membrane source in nutrient depletion conditions.

On the other hand, in a study performed to evaluate dynamic mitochondrial behavior in an animal model of CR (mice submitted to 40% CR for 6 months), proteins related to mitochondrial fission (Fis1 and mitochondrial Drp1) increased, but no changes were detected in proteins involved in mitochondrial fusion (Mfn1/Mfn2, and Opa1) (Khraiwesh et al., 2013) (**Figure 1E**). A significant increase in the number of mitochondria per cells as well as in parameters related to mitochondrial biogenesis was also found in CR conditions (Nisoli et al., 2005; López-Lluch et al., 2006). Given that fission is the postulated mechanism for mitochondrial proliferation (Scheffler, 2007), the increase in Fis1 and Drp1 proteins support the idea of increased mitochondrial biogenesis in CR. Moreover, in a model of *in vitro* CR, the greater number of mitochondria was linked to reduced oxygen consumption and membrane potential (López-Lluch et al., 2006). As it has been demonstrated that ROS production by electron leakage increases at high membrane potential (Lambert and Merry, 2004), the decreased membrane potential found in CR conditions is in agreement with the lower ROS production associated with CR. Noteworthy, the levels of ATP production were no different in CR conditions vs. control (Khraiwesh et al., 2013). In effect, CR induced an increase in the number of mitochondria capable to maintain critical ATP levels in conditions of decreased oxidative stress. It is well known that CR attenuates age-dependent oxidative damage and it is correlated with an extension of lifespan in animals as well as with prevention of cancer and diabetes (Sohal and Weindruch, 1996; Colman et al., 2009). It has been suggested that the increase in fission proteins found in CR may be useful in removing damaged mitochondria and to support the prolongevity effect of CR (López-Lluch et al., 2008; Khraiwesh et al., 2013). This suggestion seems to be in contrast with the report that unopposed mitochondrial fission in absence of mitochondrial fusion in the Δmgm1 mutants of S. cerevisiae (yeast Mgm1 is the ortholog of mammalian Opa1) leads to severe lifespan shortening (Scheckhuber et al., 2011). However, it should be noted that the different correlation found between mitochondrial fission processes and lifespan may be due to the different experimental model.

Mitochondrial Dynamics in Regulation of Energy Balance

It is well known that in mammals the NPY/Agrp and POMC neurons within the arcuate nucleus of the hypothalamus regulate hunger and satiety. Recent works suggested that mitochondrial dynamics play an important role in these two neuronal populations, and that Mfn1 and Mfn2 are involved (reviewed in Nasrallah and Horvath, 2014). During positive energy balance (high fat diet exposure) in mice, mitochondrial fusion increased in orexigenic NPY/Agrp neurons to enable elevated neuronal activity and maximize storage of excess energy in fat (Dietrich et al., 2013). The electric activity of NPY/Agrp neurons was impaired when mitochondrial fusion mechanism was altered by cell-selectively knocking down MFN1 or Mfn2. The decreased activity of Agrp neurons was correlated with resistance to fat gain during high fat diet in Agrp-specific Mfn1 or Mfn2 knockout mice (Dietrich et al., 2013). Conversely in anorexigenic pro-opiomelanocortin POMC neurons, Mfn2 selective deletion causes severe obesity and leptin resistance (Schneeberger et al., 2013) probably by mediating ER stress-induced leptin resistance. In fact, ER stress plays a role in the development of obesity and leptin resistance (Zhang et al., 2008; Lionetti et al., 2009; Ozcan et al., 2009; Mollica et al., 2011) and genetic loss of Mfn2 generates ER stress (Sebastián et al., 2012). Indeed, Mfn2 plays an important role in the structural and functional communication between mitochondria and ER (de Brito and Scorrano, 2008). Schneeberger et al. (2013) showed that specific ablation of Mfn2 in POMC neurones causes a decrease in mitochondrial respiratory capacity and an increase in oxidative stress as well as loss of mitochondria-ER contacts, ER stress-induced leptin resistance, hyperphagia, reduced energy expenditure and obesity. Moreover, in diet induced obese mice, it was shown a decrease in mitochondrial network complexity and in mitochondria-ER association due to a reduction in Mfn2 expression in the hypothalamus which precedes the onset of obesity. On the other hand, Mfn2 overexpression ameliorates the diet induced obese phenotype (Schneeberger et al., 2013).

In all, these data suggested that mitochondrial dynamics, namely Mfn1 and Mfn2, in NPY/Agrp and POMC neurons may play a role in the central regulation of energy balance and in etiology of diet induced obesity.

Concluding Remarks

Mitochondrial function varies in accordance to cellular energetic needs and to nutrient supply. Noteworthy, a number of recent works have been focused on the importance of mitochondrial dynamic behavior in terms of fusion and fission processes in determining mitochondrial functionality in diverse diet conditions as well as in the central regulation of energy balance. Therefore, mitochondrial dynamic behavior contributes to bioenergetics physiological adaptation in response to the nutritional status (**Figure 1E**).

References

Bach, D., Naon, D., Pich, S., Soriano, F. X., Vega, N., Rieusset, J., et al. (2005). Expression of Mfn2, the Charcot-Marie-Tooth neuropathy type 2A gene, in human skeletal muscle: effects of type 2 diabetes, obesity, weight loss, and the regulatory role of tumor necrosis factor alpha and interleukin-6. *Diabetes* 54, 2685–2693. doi: 10.2337/diabetes.54.9.2685

Bach, D., Pich, S., Soriano, F. X., Vega, N., Baumgartner, B., Oriola, J., et al. (2003). Mitofusin-2 determines mitochondrial network architecture and mitochondrial metabolism. A novel regulatory mechanism altered in obesity. *J. Biol. Chem.* 278, 17190–17197. doi: 10.1074/jbc.M212754200

Cartoni, R., Leger, B., Hock, M. B., Praz, M., Crettenand, A., Pich, S., et al. (2005). Mitofusins 1/2 and ERRalpha expression are increased in human skeletal muscle after physical exercise. *J. Physiol.* 567, 349–358. doi: 10.1113/jphysiol.2005.092031

Chen, H., Chomyn, A., and Chan, D. C. (2005). Disruption of fusion results in mitochondrial heterogeneity and dysfunction. *J. Biol. Chem.* 280, 26185–26192. doi: 10.1074/jbc.M503062200

Chen, H., Vermulst, M., Wang, Y. E., Chomyn, A., Prolla, T. A., McCaffery, J. M., et al. (2010). Mitochondrial fusion is required for mtDNA stability in skeletal muscle and tolerance of mtDNA mutations. *Cell* 141, 280–289. doi: 10.1016/j.cell.2010.02.026

Civitarese, A. E., and Ravussin, E. (2008). Mitochondrial energetics and insulin resistance. *Endocrinology* 149, 950–954. doi: 10.1210/en.2007-1444

Colman, R. J., Anderson, R. M., Johnson, S. C., Kastman, E. K., Kosmatka, K. J., Beasley, T. M., et al. (2009). Caloric restriction delays disease onset and mortality in rhesus monkeys. *Science* 325, 201–204. doi: 10.1126/science.1173635

da Silva, A. F., Mariotti, F. R., Máximo, V., and Campello, S. (2014). Mitochondria dynamism: of shape, transport and cell migration. *Cell. Mol. Life Sci.* 71, 2313–2324. doi: 10.1007/s00018-014-1557-8

de Brito, O. M., and Scorrano, L. (2008). Mitofusin 2 tethers endoplasmic reticulum to mitochondria. *Nature* 456, 605–610. doi: 10.1038/nature07534

de Brito, O. M., and Scorrano, L. (2009). Mitofusin-2 regulates mitochondrial and endoplasmic reticulum morphology and tethering: the role of Ras. *Mitochondrion* 9, 222–226. doi: 10.1016/j.mito.2009.02.005

Detmer, S. A., and Chan, D. C. (2007). Functions and dysfunctions of mitochondrial dynamics. *Nat. Rev. Mol. Cell Biol.* 8, 870–879. doi: 10.1038/nrm2275

Dietrich, M. O., Liu, Z. W., and Horvath, T. L. (2013). Mitochondrial dynamics controlled by mitofusins regulate Agrp neuronal activity and diet-induced obesity. *Cell* 155, 188–199. doi: 10.1016/j.cell.2013.09.004

Elgass, K., Pakay, J., Ryan, M. T., and Palmer, C. S. (2013). Recent advances into the understanding of mitochondrial fission. *Biochim. Biophys. Acta* 1833, 150–161. doi: 10.1016/j.bbamcr.2012.05.002

Frank, S., Gaume, B., Bergmann-Leitner, E. S., Leitner, W. W., Robert, E. G., Catez, F., et al. (2001). The role of dynamin-related protein 1, a mediator of mitochondrial fission, in apoptosis. *Dev. Cell* 1, 515–525. doi: 10.1016/S1534-5807(01)00055-7

Frezza, C., Cipolat, S., Martins de Brito, O., Micaroni, M., Beznoussenko, G. V., Rudka, T., et al. (2006). OPA1 controls apoptotic cristae remodeling independently from mitochondrial fusion. *Cell* 126, 177–189. doi: 10.1016/j.cell.2006.06.025

Gomes, L. C., Benedetto, G. D., and Scorrano, L. (2011). During autophagy mitochondria elongate, are spared from degradation and sustain cell viability. *Nat. Cell. Biol.* 13, 589–598. doi: 10.1038/ncb2220

Hailey, D. W., Rambold, A. S., Satpute-Krishnan, P., Mitra, K., Sougrat, R., Kim, P. K., et al. (2010). Mitochondria supply membranes for autophagosome biogenesis during starvation. *Cell* 141, 656–667. doi: 10.1016/j.cell.2010.04.009

Hernández-Alvarez, M. I., Thabit, H., Burns, N., Shah, S., Brema, I., Hatunic, M., et al. (2010). Subjects with early-onset type 2 diabetes show defective activation of the skeletal muscle PGC-1α/Mitofusin-2 regulatory pathway in response to physical activity. *Diabetes Care* 33, 645–651. doi: 10.2337/dc09-1305

Holmström, M. H., Iglesias-Gutierrez, E., Zierath, J. R., and Garcia-Roves, P. M. (2012). Tissue-specific control of mitochondrial respiration in obesity-related insulin resistance and diabetes. *Am. J. Physiol. Endocrinol. Metab.* 302, E731–E739. doi: 10.1152/ajpendo.00159.2011

Hoppins, S., Lackner, L., and Nunnari, J. (2007). The machines that divide and fuse mitochondria. *Annu. Rev. Biochem.* 76, 751–780. doi: 10.1146/annurev.biochem.76.071905.090048

Ishihara, N., Eura, Y., and Mihara, K. (2004). Mitofusin 1 and 2 play distinct roles in mitochondrial fusion reactions via GTPase activity. *J. Cell Sci.* 117, 6535–6546. doi: 10.1242/jcs.01565

Ishihara, N., Fujita, Y., Oka, T., and Mihara, K. (2006). Regulation of mitochondrial morphology through proteolytic cleavage of OPA1. *EMBO J.* 25, 2966–2977. doi: 10.1038/sj.emboj.7601184

Jagasia, R., Grote, P., Westermann, B., and Conradt, B. (2005). DRP-1-mediated mitochondrial fragmentation during EGL-1-induced cell death in C. elegans. *Nature*433, 754–760. doi: 10.1038/nature03316

James, D. I., Parone, P. A., Mattenberger, Y., and Martinou, J. C. (2003). hFis1, a novel component of the mammalian mitochondrial fission machinery. *J. Biol. Chem.* 278, 36373–36379. doi: 10.1074/jbc.M303758200

Jheng, H. F., Tsai, P. J., Guo, S. M., Kuo, L. H., Chang, C. S., Su, I. J., et al. (2012). Mitochondrial fission contributes to mitochondrial dysfunction and insulin resistance in skeletal muscle. *Mol. Cell. Biol.* 32, 309–319. doi: 10.1128/MCB.05603-11

Khraiwesh, H., Lopez-Dominguez, J. A., Lopez-Lluch, G., Navas, P., de Cabo, R., Ramsey, J. J., et al. (2013). Alterations of ultrastructural and fission/fusion markers in hepatocyte mitochondria from mice following calorie restriction with different dietary fats. *J. Gerontol. A Biol. Sci. Med. Sci.* 68, 1023–1034 doi: 10.1093/gerona/glt006

Kristensen, A. R., Schandorff, S., Høyer-Hansen, M., Nielsen, M. O., Jäättelä, M., Dengjel, J., et al. (2008). Ordered organelle degradation during starvation-induced autophagy. *Mol. Cell. Proteomics* 7, 2419–2428. doi: 10.1074/mcp.M800184-MCP200

Lackner, L. L. (2014). Shaping the dynamic mitochondrial network. *BMC Biol.* 12:35. doi: 10.1186/1741-7007-12-35

Lambert, A. J., and Merry, B. J. (2004). Effect of caloric restriction on mitochondrial reactive oxygen species production and bioenergetics: reversal by insulin. *Am. J. Physiol. Regul. Integr. Comp. Physiol.* 286, R71–R79. doi: 10.1152/ajpregu.00341.2003

Liesa, M., Palacín, M., and Zorzano, A. (2009). Mitochondrial dynamics in mammalian health and disease. *Physiol. Rev.* 89, 799–845. doi: 10.1152/physrev.00030.2008

Lionetti, L., Mollica, M. P., Donizzetti, I., Gifuni, G., Sica, R., Pignalosa, A., et al. (2014). High-lard and high-fish-oil diets differ in their effects on function and dynamic behaviour of rat hepatic mitochondria. *PLoS ONE* 9:e92753. doi: 10.1371/journal.pone.0092753

Lionetti, L., Mollica, M. P., Lombardi, A., Cavaliere, G., Gifuni, G., and Barletta, A. (2009). From chronic overnutrition to insulin resistance: the role of fat-storing capacity and inflammation. *Nutr. Metab. Cardiovasc. Dis.* 19, 146–152. doi: 10.1016/j.numecd.2008.10.010

Lionetti, L., Sica, R., Mollica, M. P., and Putti, R. (2013). High-lard and high-fish oil diets differ in their effects on insulin resistance development, mitochondrial morphology and dynamic behaviour in rat skeletal muscle. *Food Nutr. Sci.* 4, 105–112. doi: 10.4236/fns.2013.49A1017

López-Lluch, G., Hunt, N., Jones, B., Zhu, M., Jamieson, H., Hilmer, S., et al. (2006). Age-related accumulation Calorie restriction induces mitochondrial biogenesis and bioenergetic efficiency. *Proc. Natl. Acad. Sci. U.S.A.* 103, 1768–1773. doi: 10.1073/pnas.0510452103

López-Lluch, G., Irusta, P. M., Navas, P., and de Cabo, R. (2008). Mitochondrial biogenesis and healthy aging. *Exp. Gerontol.* 43, 813–819. doi: 10.1016/j.exger.2008.06.014

Malka, F., Guillery, O., Cifuentes-Diaz, C., Guillou, E., Belenguer, P., and Lombes, A. R., et al. (2005). Separate fusion of outer and inner mitochondrial membranes. *EMBO Rep.* 6, 853–859. doi: 10.1038/sj.embor.7400488

McBride, H. M., Neuspiel, M., and Wasiak, S. (2006). Mitochondria: more than just a powerhouse. *Curr. Biol.* 16, R551–R560. doi: 10.1016/j.cub.2006.06.054

Mollica, M. P., Lionetti, L., Putti, R., Cavaliere, G., Gaita, M., and Barletta, A. (2011). From chronic overfeeding to hepatic injury: role of endoplasmic reticulum stress and inflammation. *Nutr. Metab. Cardiovasc. Dis.* 21, 222–230. doi: 10.1016/j.numecd.2010.10.012

Nasrallah, C. M., and Horvath, T. L. (2014). Mitochondrial dynamics in the central regulation of metabolism. *Nat. Rev. Endocrinol.* 10, 650–658. doi: 10.1038/nrendo.2014.160

Nisoli, E., Tonello, C., Cardile, A., Cozzi, V., Bracale, R., Tedesco, L., et al. (2005). Calorie restriction promotes mitochondrial biogenesis by inducing the expression of eNOS. *Science* 310, 314–317. doi: 10.1126/science.1117728

Ozcan, L., Ergin, A. S., Lu, A., Chung, J., Sarkar, S., Nie, D., et al. (2009). Endoplasmic reticulum stress plays a central role in development of leptin resistance. *Cell Metab.* 9, 35–51. doi: 10.1016/j.cmet.2008.12.004

Pich, S., Bach, D., Briones, P., Liesa, M., Camps, M., Testar, X., et al. (2005). The Charcot-Marie-Tooth type 2A gene product, Mfn2, up-regulates fuel oxidation through expression of OXPHOS system. *Hum. Mol. Genet.* 14, 1405–1415. doi: 10.1093/hmg/ddi149

Rambold, A. S., Kostelecky, B., Elia, N., and Lippincott-Schwartz, J. (2011). Tubular network formation protects mitochondria from autophagosomal degradation during nutrient starvation. *Proc. Natl. Acad. Sci. U.S.A.* 108, 10190–10195. doi: 10.1073/pnas.1107402108

Santel, A., and Frank, S. (2008). Shaping mitochondria: the complex posttranslational regulation of the mitochondrial fission protein DRP1. *IUBMB Life* 60, 448–455. doi: 10.1002/iub.71

Scheckhuber, C. Q., Wanger, R. A., Mignat, C. A., and Osiewacz, H. D. (2011). Unopposed mitochondrial fission leads to severe lifespan shortening. *Cell Cycle* 10, 3105–3110. doi: 10.4161/cc.10.18.17196

Scheffler, I. E. (2007). "Structure and morphology. Integration into the cell," in *Mitochondria, 2nd Edn* (Hoboken, NJ: John Wiley & Sons, Inc.), 18–59. doi: 10.1002/9780470191774.ch3

Schneeberger, M., Dietrich, M. O., Sebastián, D., Imbernón, M., Castaño, C., Garcia, A., et al. (2013). Mitofusin 2 in POMC neurons connects ER stress with leptin resistance and energy imbalance. *Cell* 155, 172–187. doi: 10.1016/j.cell.2013.09.003

Sebastián, D., Hernández-Alvarez, M. I., Segalés, J., Sorianello, E., Muñoz, J. P., Sala, D., et al. (2012). Mitofusin 2 (Mfn2) links mitochondrial and endoplasmic reticulum function with insulin signaling and is essential for normal glucose homeostasis. *Proc. Natl. Acad. Sci. U.S.A.* 109, 5523–5528.

Sohal, R. S., and Weindruch, R. (1996). Oxidative stress, caloric restriction, and aging. *Science* 273, 59–63 doi: 10.1126/science.273.5271.59

Soriano, F. X., Liesa, M., Bach, D., Chan, D. C., Palacin, M., and Zorzano, A. (2006). Evidence for a mitochondrial regulatory pathway defined by peroxisome proliferator-activated receptor-gamma coactivator-1 alpha, estrogen-related receptor-alpha, mitofusin 2. *Diabetes* 55, 1783–1791. doi: 10.2337/db05-0509

Westermann, B. (2010). Mitochondrial fusion and fission in cell life and death. *Nat. Rev. Mol. Cell Biol.* 11, 872–884. doi: 10.1038/nrm3013

Westermann, B. (2012). Bioenergetic role of mitochondrial fusion and fission. *Biochim. Biophys. Acta* 1817, 1833–1838. doi: 10.1016/j.bbabio.2012.02.033

Yoon, Y., Krueger, E. W., Oswald, B. J., and McNiven, M. A. (2003). The mitochondrial protein hFis1 regulates mitochondrial fission in mammalian cells through an interaction with the dynamin-like protein DLP1. *Mol. Cell. Biol.* 23, 5409–5420. doi: 10.1128/MCB.23.15.5409-5420.2003

Yu, T., Robotham, J. L., and Yoon, Y. (2006). Increased production of reactive oxygen species in hyperglycemic conditions requires dynamic change of mitochondrial morphology. *Proc. Natl. Acad. Sci. U.S.A.* 103, 2653–2658. doi: 10.1073/pnas.0511154103

Zhang, X., Zhang, G., Zhang, H., Karin, M., Bai, H., and Cai, D. (2008). Hypothalamic IKKbeta/NF-kappaB and ER stress link overnutrition to energy imbalance and obesity. *Cell* 135, 61–73. doi: 10.1016/j.cell.2008.07.043

Zhang, Y., Jiang, L., Hu, W., Zheng, Q., and Xiang, W. (2011). Mitochondrial dysfunction during *in vitro* hepatocyte steatosis is reversed by omega-3 fatty acid-induced up-regulation of mitofusin 2. *Metabolism* 60, 767–777. doi: 10.1016/j.metabol.2010.07.026

Zhao, J., Lendahl, U., and Nistér, M. (2013). Regulation of mitochondrial dynamics: convergences and divergences between yeast and vertebrates. *Cell. Mol. Life Sci.* 70, 951–976. doi: 10.1007/s00018-012-1066-6

Zorzano, A., Liesa, M., Sebastián, D., Segalés, J., and Palacín, M. (2010). Mitochondrial fusion proteins: dual regulators of morphology and metabolism. *Semin. Cell. Dev. Biol.* 21, 566–574. doi: 10.1016/j.semcdb.2010.01.002

Conflict of Interest Statement: The authors declare that the research was conducted in the absence of any commercial or financial relationships that could be construed as a potential conflict of interest.

frontiers in Physiology

MINI REVIEW
published: 20 January 2016
doi: 10.3389/fphys.2015.00426

Skeletal Muscle Mitochondrial Bioenergetics and Morphology in High Fat Diet Induced Obesity and Insulin Resistance: Focus on Dietary Fat Source

*Rosalba Putti, Vincenzo Migliaccio, Raffaella Sica and Lillà Lionetti **

Department of Biology, University of Naples "Federico II," Naples, Italy

It has been suggested that skeletal muscle mitochondria play a key role in high fat (HF) diet induced insulin resistance (IR). Two opposite views are debated on mechanisms by which mitochondrial function could be involved in skeletal muscle IR. In one theory, mitochondrial dysfunction is suggested to cause intramyocellular lipid accumulation leading to IR. In the second theory, excess fuel within mitochondria in the absence of increased energy demand stimulates mitochondrial oxidant production and emission, ultimately leading to the development of IR. Noteworthy, mitochondrial bioenergetics is strictly associated with the maintenance of normal mitochondrial morphology by maintaining the balance between the fusion and fission processes. A shift toward mitochondrial fission with reduction of fusion protein, mainly mitofusin 2, has been associated with reduced insulin sensitivity and inflammation in obesity and IR development. However, dietary fat source during chronic overfeeding differently affects mitochondrial morphology. Saturated fatty acids induce skeletal muscle IR and inflammation associated with fission phenotype, whereas ω-3 polyunsaturated fatty acids improve skeletal muscle insulin sensitivity and inflammation, associated with a shift toward mitochondrial fusion phenotype. The present minireview focuses on mitochondrial bioenergetics and morphology in skeletal muscle IR, with particular attention to the effect of different dietary fat sources on skeletal muscle mitochondria morphology and fusion/fission balance.

Keywords: mitochondrial fusion, mitochondrial fission, lard, fish oil, omega-3 fatty acids

OPEN ACCESS

Edited by:
Gilles Gouspillou, Université du Québec à Montréal, Canada

Reviewed by:
Giovanni Solinas, University of Gothenburg, Sweden
Brennan Smith, McMaster University, Canada

****Correspondence:***
Lillà Lionetti
lilla.lionetti@unina.it

Specialty section:
This article was submitted to Striated Muscle Physiology, a section of the journal Frontiers in Physiology

Received: *31 July 2015*
Accepted: *27 December 2015*
Published: *20 January 2016*

Citation:
Putti R, Migliaccio V, Sica R and Lionetti L (2016) Skeletal Muscle Mitochondrial Bioenergetics and Morphology in High Fat Diet Induced Obesity and Insulin Resistance: Focus on Dietary Fat Source. Front. Physiol. 6:426. doi: 10.3389/fphys.2015.00426

INTRODUCTION

Skeletal muscle seems to play a central role in whole body insulin resistance (IR) and metabolic syndrome associated with high fat (HF) feeding, obesity and aging (see Corpeleijn et al., 2009; DeFronzo and Tripathy, 2009; Lark et al., 2012).

Some evidence suggested that cytosolic ectopic accumulation of fatty acids (FA) metabolites, such as diacylglycerols (DAG) and/or Ceramides, (Yu et al., 2002; Adams et al., 2004), underlies IR development in skeletal muscle (lipotoxicity theory) (reviewed in Lark et al., 2012). Numerous evidence has also suggested a link between elevated systemic and tissue inflammation with IR

(inflammatory theory) (see Shenk et al., 2008; Lark et al., 2012). The effectors of IR in HF diet-induced inflammation are suggested to involve hyperactivation of stress-sensitive Ser/Thr kinases, such as JNK and IKKβ, which in turn inhibits insulin receptor/IRS1 axis. Several mechanisms were proposed to explain the link between inflammation and IR: endoplasmic reticulum (ER) stress (Ozcan et al., 2004; Lionetti et al., 2009; Mollica et al., 2011), oxidative stress (Lark et al., 2012), signaling through inflammation-associated receptors, such as TLR4 signaling (Uysal et al., 1997; Shi et al., 2006), and partitioning/activation of c-SRC (a key mediator of JNK activation) by saturated FA (Holzer et al., 2011; **Figure 1A**).

In recent years, different reviews focused on mechanism(s) by which mitochondrial bioenergetics (Fisher-Wellman and Neufer, 2012; Lark et al., 2012; Muoio and Neufer, 2012; Holloszy, 2013) and morphology (Liesa and Shirihai, 2013; Montgomery and Turner, 2015) may be linked to the etiology of IR in skeletal muscle. In the present review, the challenging debate on the involvement of mitochondrial dysfunction in IR will be briefly reviewed. Then, the main aim of the review will be to underline the importance of including mitochondrial morphology/dynamics and dietary fat source in the debate on skeletal muscle mitochondria involvement in IR etiology and to highlight the need of further research studies to clarify the involved mechanism(s).

SKELETAL MUSCLE MITOCHONDRIAL BIOENERGETICS AND IR

Two leading theories on mechanisms underlying skeletal muscle IR onset focus on mitochondria, although with opposite views (**Figure 1B**). In one theory, mitochondrial dysfunction is suggested to cause intramyocellular lipid accumulation leading to IR (Kelley et al., 1999; Lowell and Shulman, 2005; reviewed in Civitarese and Ravussin, 2008; Montgomery and Turner, 2015). In this case, the strategies to accelerate flux through β-oxidation should improve insulin sensitivity. In the second theory, excess fuel within mitochondria in the absence of increased energy demand stimulates mitochondrial oxidant production and emission, ultimately leading to the development of IR (Fisher-Wellman and Neufer, 2012; **Figure 1B**). In this case, elevated flux through β-oxidation without added energy demand is viewed as an underlying cause of IR disease (Muoio and Neufer, 2012).

Several studies have revealed a reduction in skeletal mitochondrial mass in obesity and type 2 diabetes (Kelley et al., 2002; Morino et al., 2005; Ritov et al., 2005), decreased ATP synthesis in insulin resistant offspring of patients with type 2 diabetes (Petersen et al., 2004, 2005) and decreased maximal respiration rates in skeletal muscle isolated mitochondria from type 2 diabetics (Mogensen et al., 2007). Moreover, with the limitation that gene expression is not a direct assessment of function itself, HF diet has been shown to coordinately down-regulate genes required for mitochondrial oxidative phosphorylation in human and rodents skeletal muscle (Sparks et al., 2005). Interestingly, in skeletal muscle from obese or diabetic patients, decreased activity of electron transport chain and reduced number of mitochondria have been mainly reported in skeletal muscle mitochondria located beneath the sarcolemmal membrane (SS mitochondria) (Ritov et al., 2005). SS mitochondria also displayed lower respiratory capacities in presence of succinate as substrates in adult rats exhibiting HF diet-induced IR (Lionetti et al., 2007). The two mitochondrial subpopulations (SS and intermyiofibrillar, IMF) are differentiated not only by the different localization but also by the different functions (Cogswell et al., 1993; Mollica et al., 2006): SS mitochondria could be more affected by the impairing effect of saturated FA due to their localization beneath the sarcolemmal membrane.

However, although correlative studies seem to implicate mitochondrial dysfunction and impaired β-oxidation as predisposing risk factors for IR, still uncertain is whether diminished fat oxidation reflects a cause or a late stage consequence of the disease process (reviewed in Muoio, 2010). In fact, obese/diabetic humans never use their mitochondrial capacity for lipid oxidation; therefore, a marginal decline in oxidative potential has little relevance in causing lipotoxicity and IR in sedentary individuals. Moreover, it has been suggested that early stages of obesity and IR are accompanied by increased, rather than reduced β-oxidation (Muoio, 2010). These findings question the concept that mitochondrial dysfunction is a primary cause of IR (Hoeks et al., 2010, 2011), as also underscored by the study of Bonnard et al. (2008), showing mitochondrial dysfunction in skeletal muscle after 16 weeks, but not after 4 weeks HF feeding, while muscle IR was observed after both 4 and 16 weeks of HF feeding. In addition, mitochondrial deficiency, severe enough to impair fat oxidation in resting muscle, cause an increase, not a decrease, in insulin action (reviewed in Holloszy, 2013). Altogether, these studies suggest that deficiency of mitochondria in muscle does not cause IR (reviewed in Holloszy, 2013).

An alternative mechanism to explain the connection between mitochondria and IR focused on reactive oxygen species (ROS) production (reviewed in Muoio and Neufer, 2012; Holloszy, 2013). Lefort et al. (2010) showed normal oxidative capacity, decreased mitochondrial mass and high rates of ROS production in mitochondria isolated from skeletal muscle of obese insulin resistant individuals. Moreover, FA overload within the mitochondria results in the accumulation of partially oxidized acyl-carnitines, increased mitochondrial hydrogen peroxide (H_2O_2) emission and a shift to a more oxidized intracellular redox environment (Anderson et al., 2009; reviewed in Lark et al., 2012). H_2O_2 emission may induce IR by directly targeting protein involved in the glucose uptake process. On the other hand, given the sensitivity of cellular phosphatase to redox state, it has been suggested that elevated mitochondrial H_2O_2 production may decrease phosphatase tone in cells, increasing the inhibition state of insulin signaling proteins by stress-sensitive kinases (reviewed in Lark et al., 2012).

Although the primary role of skeletal muscle mitochondrial dysfunction in the pathogenesis of IR and type 2 diabetes is under debate (Hoeks et al., 2010, 2011; Holloszy,

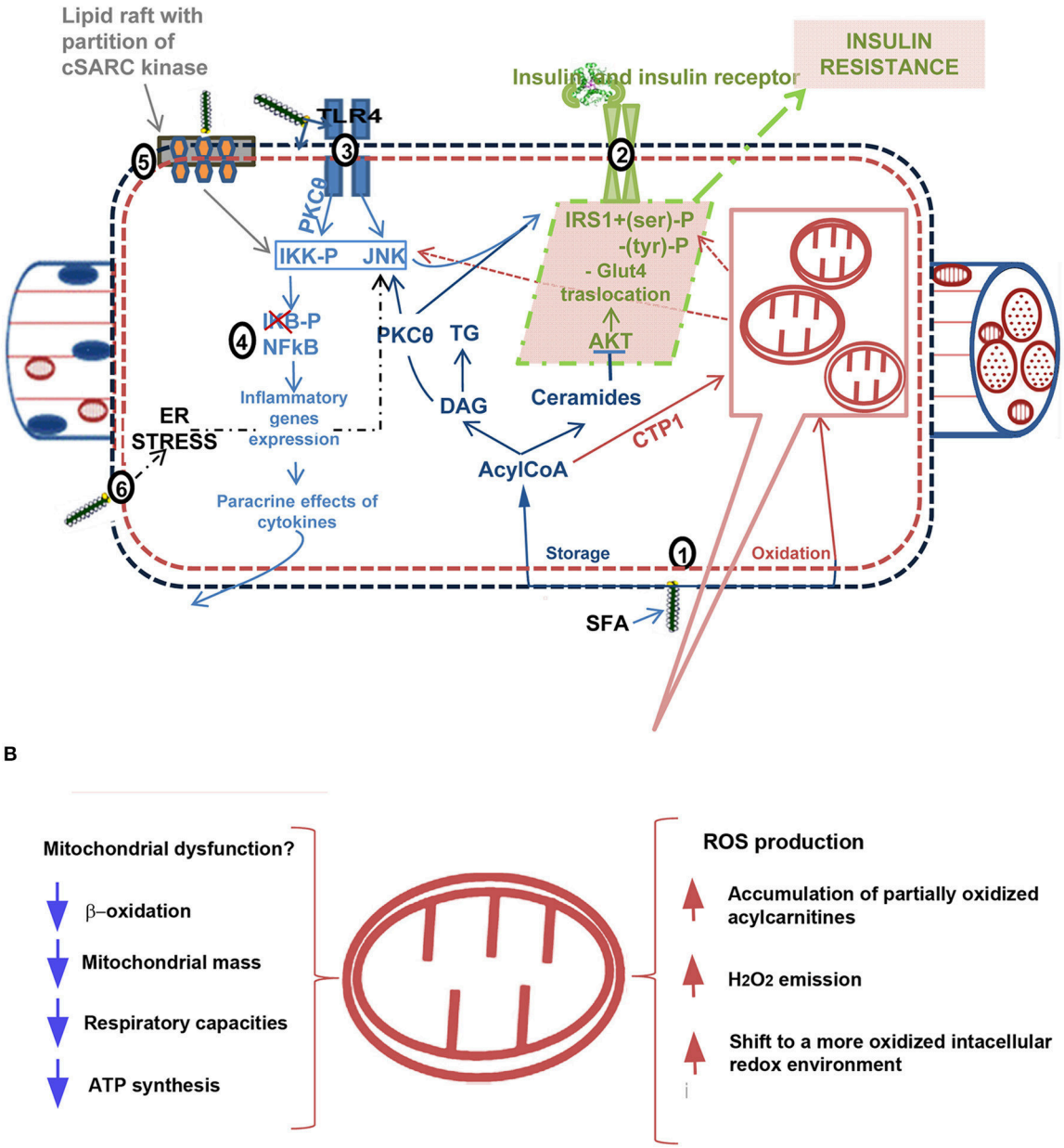

FIGURE 1 | Mechanism linking excess fatty acids to insulin resistance in skeletal muscle. (A): (1) Excess free fatty acids (FFAs) are esterified in AcylCoAs, substrates involved in both synthetic and oxidative pathways. In the synthetic pathway, they are either stored as Triacylglycerols (TG) in lipid droplets or accumulated in metabolites (DAGs, Ceramides) that act as signaling molecules and may interfere with normal cellular signaling. DAGs are associated with membrane translocation and activation of Protein kinase C theta (PKC-θ), increased IRS1 serine/threonine phosphorylation and decreased insulin-stimulated IRS1 tyrosine phosphorylation, whereas Ceramides impair insulin action by inhibiting protein kinase PKB/AKT (dark blue). In the oxidative pathway, AcylCoAs are imported into the mitochondria by carnitine palmitoyltransferase-1 (CPT-1) shuttle and degraded via β-oxidation (in purple). (2) Insulin signaling pathway impaired by excess FFA (in green). Among FFAs, saturated FAs (SFAs) stimulate the activation of several inflammatory pathways. (3) Receptor-mediated mechanisms, as those of Toll like receptors 2/4 (TLR 2/4), activate serine kinases inhibitor kappaB kinase (IKK) and c-JUN NH_2-terminal kinase (JNK). The activation of PKCθ also contributes to IKK and JNK activation. Altogether, these kinases catalyze IRS1 serine phosphorylation and lead to a reduction of insulin-induced IRS1 tyrosine phosphorylation, impairing insulin action. Moreover, IKK/NFkB axis (4) triggers expression of inflammatory genes with cytokines production (e.g., Tumor necrosis factor, TNFα), which in turn activate intracellular pathways promoting insulin resistance development (in light blue). (5) SFAs enter the cellular membranes and incorporate into them reducing membrane fluidity and

(Continued)

FIGURE 1 | Continued
creating or expanding subdomains rich in cholesterol and sphingolipids (lipid raft). They induce clustering and activation of cytosolic cSRC. cSRC activity is required for JNK1 activation and inhibition of insulin signaling (in grey). (6) Endoplasmic reticulum stress (ER stress), induced by lipotoxicity, contributes to activate inflammatory pathways and impair insulin signaling. **(B)**: Putative role of mitochondria in development of IR. Mitochondrial dysfunction in presence of excess FFAs leads to intramyocellular lipid accumulation due to impaired β-oxidation. Decreased mitochondrial mass, respiratory capacities and ATP synthesis have been found in obesity and diabetes. Alternatively, excess FFA within mitochondria in the absence of increased energy demand stimulates oxidative stress with high rates of ROS production and H_2O_2 emission and a shift to a more oxidized intracellular redox environment, ultimately leading to the development of IR.

2013), it is generally accepted that in this disease a mitochondrial defect occurs, possibly secondary to a fat intake increase.

MITOCHONDRIAL MORPHOLOGY AND SKELETAL MUSCLE IR

It is well known that mitochondrial morphology is highly variable, ranging between long tubular mitochondria and short circular ones and it is maintained through a dynamic balance between fusion and fission processes (Westermann, 2010, 2012), which allow mitochondria to redistribute in a cell, exchange contents and repair damaged mitochondria. These two opposing processes are finely regulated by mitochondrial fusion proteins mitofusins 1 and 2 (Mfn1 and Mfn2), and optic atrophy gene 1 (OPA1) (Cipolat et al., 2004; Palmer et al., 2011) and by mitochondrial fission protein dynamin-related protein 1 (DRP1) and fission protein 1 (Fis1) (Nunnari et al., 2002; Liesa et al., 2009).

Several pieces of evidence suggested that mitochondrial dynamic behavior play a key role in mitochondrial health, bioenergetics function, quality control, and cell viability. Notably, disruption of mitochondrial dynamics has been found in IR and type 2 diabetes (Bach et al., 2003, 2005; Yu et al., 2006; Liesa and Shirihai, 2013).

The group of Zorzano showed that decreased expression of Mfn2 and altered expression of OPA1 participated in obesity and type 2 diabetes development in both patients and rodent models (Bach et al., 2003; Zorzano et al., 2009a,b, 2010; Hernández-Alvarez et al., 2010; Quirós et al., 2012). In obese Zucker rats, skeletal muscle mitochondrial network was reduced by 25% associated with a repression of Mfn2 (Bach et al., 2003). In addition, skeletal muscle of obese subjects and type 2 diabetic patients also showed a reduced expression of Mfn2 mRNA and Mfn2 protein compared to lean subjects (Bach et al., 2003, 2005). Mfn2 repression was detected in the skeletal muscles of both obese and non-obese type 2 diabetic patients (Bach et al., 2005). Notably, the expression of one of the mitochondrial proteases involved in OPA1 processing, presenilin-associated rhomboid-like (PARL), was also reduced in diabetic animals. In humans, a positive linear correlation between PARL mRNA levels and insulin sensitivity has been reported (Walder et al., 2005). These data suggest multiple alterations in mitochondrial fusion in IR. However, reduction of Mfn2 expression together with decreased mitochondrial size in skeletal muscle in obesity and type 2 diabetes states allow proposing a relevant role for Mfn2 in IR (Civitarese and Ravussin, 2008; Zorzano et al., 2009a,b). In agreement with this suggestion, a positive correlation between Mfn2 expression in skeletal muscle and insulin sensitivity has been reported (Bach et al., 2005). It is of interest that the involvement of Mfns in diet-induced obesity via the regulation of leptin resistance and systemic energy metabolism was also revealed (Dietrich et al., 2013; Schneeberger et al., 2013; reviewed in Putti et al., 2015). Moreover, it has been suggested that there is an association between increased mitochondrial fission, mitochondrial bioenergetics and fat induced-IR in skeletal muscle (Jheng et al., 2012). Indeed, in differentiated C2C12 muscle cells mitochondrial fragmentation and increased mitochondrion associated-DRP1 and Fis1 was induced by excess palmitate and this fission phenotype was associated with increased oxidative stress, loss of ATP production and reduced insulin-stimulated glucose uptake. These authors also found smaller and shorter mitochondria and increased mitochondrial fission machinery in the skeletal muscle of mice with genetic or diet-induced obesity. Furthermore, inhibition of mitochondrial fission improved muscle insulin signaling and systemic insulin sensitivity in obese mice (Jheng et al., 2012).

A shift toward fission was also found in skeletal muscle of HF diet (HFD)-induced obese mice by Liu et al. (2014). Notably, these authors also faced the question of whether mitochondrial dynamics exists in skeletal muscle *in vivo*. It should be considered that mitochondria in skeletal muscle are rigidly located between bundles of myofilaments in a highly regular "crystal like" pattern (Vendelin et al., 2005) and therefore, their motility and dynamics may be very restricted. Liu et al. (2014) confirmed that mitochondria are dynamic organelles in skeletal muscle *in vivo*, by demonstrating that they exchange contents within the whole mitochondrial population through nanotunneling-mediated mitochondrial fusion. In this way, mitochondria can bypass the restriction of myofilament and exchange mitochondrial matrix contents even if they are distant. This dynamic communication among mitochondria in skeletal muscle may protect from injury by preventing the accumulation of detrimental metabolites. Liu et al. (2014) also showed that this dynamic behavior was inhibited in skeletal muscle of HFD–induced obese mice associated with decreased Mfn2 and increased Fis1 and DRP1 expression compared to normal diet fed mice. This impaired mitochondrial fusion in skeletal muscle of HFD-induced obese mice was accompanied with damaged mitochondrial respiratory function and decreased ATP content. Therefore, the authors suggest that mitochondrial dynamics play an important role in regulating mitochondrial function, including respiration rate and ATP production (Liu et al., 2014).

DIETARY FAT SOURCE DIFFERENTLY AFFECT SKELETAL MUSCLE IR AND MITOCHONDRIAL MORPHOLOGY

It has been suggested that diverse dietary fat sources have different effects on obesity and associated diseases development. Saturated FA are well known to induce both obesity and related disease, whereas omega 3 polyunsaturated FA (ω-3 PUFA) from fish oil have been shown in many studies to protect against these metabolic diseases (Xin et al., 2008; Gonzalez-Periz et al., 2009; Abete et al., 2011). The effect of ω-3 PUFA on metabolic disease has been extensively studied during the past three decades since the first studies such as the one by Storlien et al. (1987) showing that fish oil prevents IR induced by high-fat feeding in rats. Further studies confirmed that ω-3 PUFA had an anti-obesity effect and enhanced insulin sensitivity and glucose homeostasis in rodent models of IR: the replacement of a small proportion of the diet with ω-3 PUFAs from fish oil completely prevents the development of skeletal muscle IR (Storlien et al., 1991; Fryer et al., 1995). Recent studies hypothesized that ω-3 PUFAs protect glucose tolerance, in part by preventing the accumulation of bioactive lipid mediators that interfere with the insulin signaling pathway (Lanza et al., 2013). Lanza et al. (2013) evaluated the influence of dietary ω-3 PUFAs on mitochondrial physiology and muscle lipid metabolites in the context of 10 weeks high-fat feeding in mice. They found a lower content of long-chain Acyl-CoAs and Ceramides in the presence of fish oil, whereas mitochondrial oxidative capacity was similarly increased with or without fish oil. Several studies have also indicated that ω-3 PUFAs possess anti-inflammatory properties that prevent and reverse the development of IR in mice which are fed a high-fat diet in an adiponectin-dependent manner (Kalupahana et al., 2010, 2011). On the other hand, unsaturated FA prevent c-Src membrane partitioning and activation and block JNK activation with consequent beneficial effects on insulin sensitivity (Holzer et al., 2011). Considering the anti-inflammatory properties of ω-3 PUFAs, in a recent study, we compared the effects of chronic high-fish oil and high-lard diets on obesity-related inflammation by evaluating serum and tissue adipokine levels and histological features in insulin-sensitive tissues (white adipose tissue, liver and skeletal muscle) (Lionetti et al., 2014b). We showed that the replacement of lard (saturated FA) with fish oil (ω-3 PUFAs) in chronic high-fat feeding attenuated the development of systemic and tissue inflammation. Indeed, compared with a high-lard diet, a high-fish oil diet resulted in a lower degree of systemic inflammation and IR that were associated with a lower ectopic lipid depot, inflammation degree and IR in the skeletal muscle (Lionetti et al., 2014b). In a further study on the same experimental design, we confirmed that the replacement of lard with fish oil in HF diet had preventive effects on obesity and systemic inflammation and IR development as well as we showed a fusion mitochondrial phenotype in association with the improvement of IR in skeletal muscle (Lionetti et al., 2013). As for preventive effects on obesity, body weight gain after 6 weeks of HF diet was lower in fish oil fed rats compared to lard fed rats. As for skeletal muscle IR, we showed that high-lard diet induced a defect in the skeletal muscle insulin signaling pathway with a lower immune-reactivity to IRS1 and pIRS (Tyr632), in agreement with other authors (Yaspelkis et al., 2009; Yuzefovych et al., 2013). On the other hand, a high fish oil diet elicited IRS1 and pIRS (Tyr632) immune-reactivity similar to a control diet, in agreement with ameliorated systemic insulin sensitivity (Lionetti et al., 2013). We cannot exclude the possibility that the fish oil protective effect was due to indirect effects of differences on adiposity. We also showed that the beneficial effects of fish oil feeding on skeletal muscle IR development was associated with changes in protein involved in mitochondrial dynamic behavior, with a greater number of immunoreactive fibers for Mfn2 and OPA1 proteins, as well as a weaker immunostaining for DRP1 and Fis1 compared to high lard feeding. Skeletal muscle electron microscopy observations also suggested a prominent presence of fission events in high-lard diet fed rats, and fusion events in high-fish oil diet fed rats (Lionetti et al., 2013).

The finding on the effects of different dietary FA on skeletal muscle mitochondrial fusion/fission proteins may be associated with effects on inflammatory processes involved in IR development. Indeed, Bach et al. (2005) suggested that TNF-α inhibits Mfn2 gene expression in cells in culture, suggesting that inflammatory parameters may play a regulatory role on Mfn2. In agreement, we showed that pro-inflammatory dietary saturated FA reduced Mfn2 expression and induced fission phenotype in skeletal muscle (Lionetti et al., 2013). On the other hand, the anti-inflammatory effect of dietary ω-3 PUFAs was associated with no reduction in skeletal muscle Mfn2 content and a tendency to mitochondrial fusion. This shift toward fusion may be an adaptive mechanism to counteract cellular stress induced by chronic HF diet, by allowing functional mitochondria to complement dysfunctional mitochondria. In accordance, myocytes cultured with docosahexaenoic acid exhibited a higher mitochondrial mass with a higher proportion of large and elongated mitochondria with downregulation of fission genes DRP1 and Fis1 (Casanova et al., 2014).

The pro-fusion effect of ω-3 PUFAs dietary fat on skeletal muscle mitochondria is in agreement with the results found in liver mitochondria, where a shift toward mitochondrial fusion phenotype was also suggested (Zhang et al., 2011; Lionetti et al., 2014a).

The mechanism underlying fish oil/ω-3 PUFAs mitochondrial fusion stimulation may involve receptor-mediated signaling and/or lipid membrane composition, among other factors. Indeed, ω-3 PUFAs are incorporated into cellular membranes and may affect lipid-protein interactions as well as membrane fluidity, and therefore the function of embedded proteins. Recently, it has been suggested a role for ω-3 PUFAs in reorganizing the composition of the mitochondrial membrane, while promoting improvements in ADP sensitivity, determined as mitochondrial responses during ADP titration (Herbst et al., 2014). Moreover, it is well known that saturated FA incorporation reduces membrane fluidity, whereas PUFA do not have such effect (Clamp et al., 1997; Stulnig et al., 2001; Holzer et al., 2011). Further studies are needed to elucidate these mechanisms.

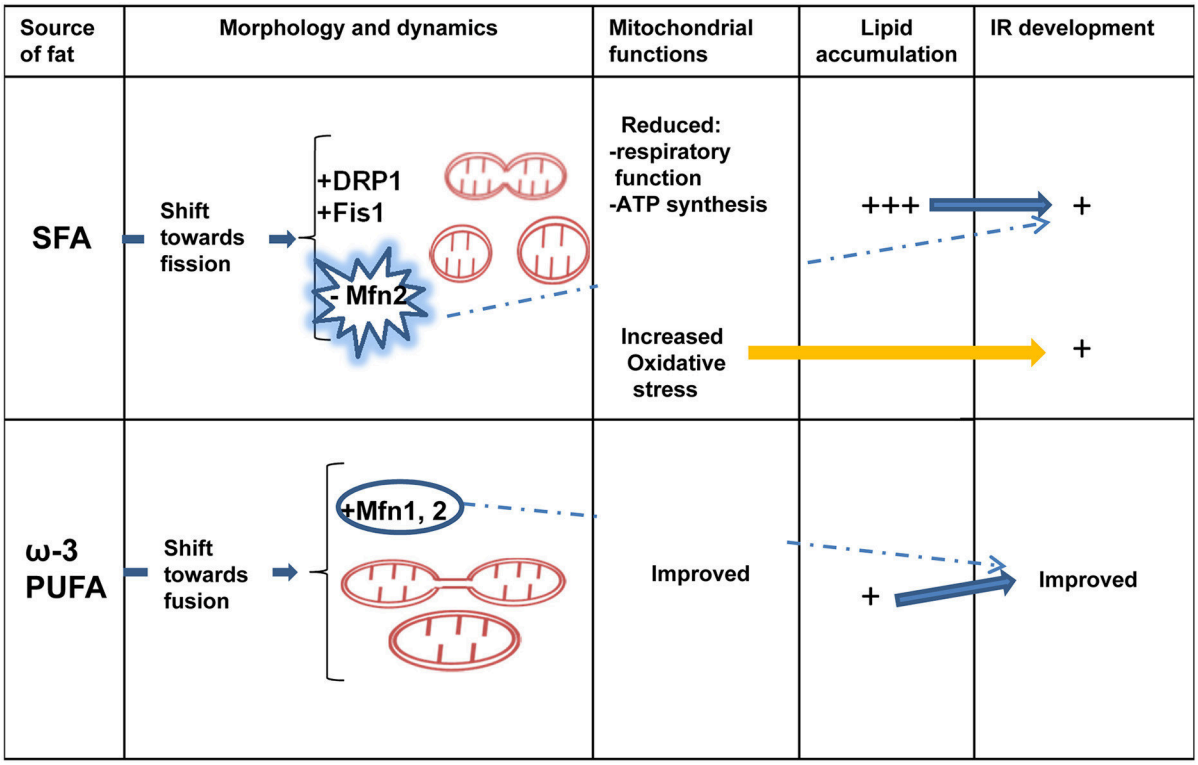

FIGURE 2 | Dietary fat source, mitochondrial dynamics and skeletal muscle IR. Diverse dietary fat sources induce different effects on mitochondrial morphology/dynamics and IR development in skeletal muscle. Saturated fatty acids (SFA) elicit a shift toward fission processes (decreased Mfn2 and increased Fis1 and DRP1 expression) associated with reduced mitochondrial function, increased oxidative stress, lipid accumulation and IR development. Ω-3 polyunsaturated fatty acids (PUFAs) induce Mfn2 expression and fusion processes associated with less lipid accumulation and improved IR. IR, insulin resistance; Mfn2, mitofusin 2; DRP1, dynamin-related protein 1; Fis1, fission protein 1.

CONCLUSIONS

Recent evidence highlighted an association between mitochondrial morphology and IR development in skeletal muscle. Few works on different dietary fat source started to underline the different effect of saturated and ω-3 PUFAs on skeletal muscle IR and mitochondrial protein involved in dynamics behavior, suggesting an association between beneficial protective effect of ω-3 PUFAs toward IR development and mitochondrial fusion phenotype (**Figure 2**). However, it is important to underline that most of the data present in literature on skeletal muscle mitochondrial morphology and IR are from associational studies. Therefore, there is an urgent requirement for *in vivo* mechanistic studies to confirm the associational relationship between mitochondrial morphology/dynamics and IR development.

REFERENCES

Abete, I., Goyenechea, E., Zulet, M. A., and Martínez, J. A. (2011). Obesity and metabolic syndrome: potential benefit from specific nutritional components. *Nutr. Metab. Cardiovasc. Dis.* 21, B1–B15. doi: 10.1016/j.numecd.2011.05.001

Adams, J. M. II, Pratipanawatr, T., Berria, R., Wang, E., DeFronzo, R. A., Sullards, M. C., et al. (2004). Ceramide content is increased in skeletal muscle from obese insulin-resistant humans. *Diabetes* 53, 25–31. doi: 10.2337/diabetes.53.1.25

Anderson, E. J., Lustig, M. E., Boyle, K. E., Woodlief, T. L., Kane, D. A., Lin, C. T., et al. (2009). Mitochondrial H_2O_2 emission and cellular redox state link excess fat intake to insulin resistance in both rodents and humans. *J. Clin. Invest.* 119, 573–581. doi: 10.1172/JCI37048

Bach, D., Naon, D., Pich, S., Soriano, F. X., Vega, N., Rieusset, J., et al. (2005). Expression of Mfn2, the Charcot-Marie-Tooth neuropathy type 2A gene, in human skeletal muscle: effects of type 2 diabetes, obesity, weight loss, and the regulatory role of tumor necrosis factor alpha and interleukin-6. *Diabetes* 54, 2685–2693. doi: 10.2337/diabetes.54.9.2685

Bach, D., Pich, S., Soriano, F. X., Vega, N., Baumgartner, B., Oriola, J., et al. (2003). Mitofusin-2 determines mitochondrial network architecture and mitochondrial metabolism. A novel regulatory mechanism altered in obesity. *J. Biol. Chem.* 278, 17190–17197. doi: 10.1074/jbc.M212754200

Bonnard, C., Durand, A., Peyrol, S., Chanseaume, E., Chauvin, M. A., Morio, B., et al. (2008). Mitochondrial dysfunction results from oxidative stress in the skeletal muscle of diet-induced insulin-resistant mice. *J. Clin. Invest.* 118, 789–800. doi: 10.1172/jci32601

Casanova, E., Baselga-Escudero, L., Ribas-Latre, A., Arola-Arnal, A., Bladé, C., Arola, L., et al. (2014). Epigallocatechin gallate counteracts oxidative stress in docosahexaenoxic acid-treated myocytes. *Biochim. Biophys. Acta* 1837, 783–791. doi: 10.1016/j.bbabio.2014.01.014

Cipolat, S., Martins de Brito, O., Dal Zilio, B., and Scorrano, L. (2004). OPA1 requires mitofusin 1 to promote mitochondrial fusion. *Proc. Natl. Acad. Sci. U.S.A.* 101, 15927–15932. doi: 10.1073/pnas.0407043101

Civitarese, A. E., and Ravussin, E. (2008). Mitochondrial energetics and insulin resistance. *Endocrinology* 149, 950–954. doi: 10.1210/en.2007-1444

Clamp, A. G., Ladha, S., Clark, D. C., Grimble, R. F., and Lund, E. K. (1997). The influence of dietary lipids on the composition and membrane fluidity of rat hepatocyte plasma membrane. *Lipids* 32, 179–184. doi: 10.1007/s11745-997-0022-3

Cogswell, A. M., Stevens, R. J., and Hood, D. A. (1993). Properties of skeletal muscle mitochondria isolated from subsarcolemmal and intermyofibrillar regions. *Am. J. Physiol.* 264, C383–C389.

Corpeleijn, E., Saris, W. H., and Blaak, E. E. (2009). Metabolic flexibility in the development of insulin resistance and type 2 diabetes: effects of lifestyle. *Obes. Rev.* 10, 178–193. doi: 10.1111/j.1467-789X.2008.00544.x

DeFronzo, R. A., and Tripathy, D. (2009). Skeletal muscle insulin resistance is the primary defect in type 2 diabetes. *Diabetes Care* 32, S157–S163. doi: 10.2337/dc09-S302

Dietrich, M. O., Liu, Z. W., and Horvath, T. L. (2013). Mitochondrial dynamics controlled by mitofusins regulate Agrp neuronal activity and diet-induced obesity. *Cell* 155, 188–199. doi: 10.1016/j.cell.2013.09.004

Fisher-Wellman, K. H., and Neufer, P. D. (2012). Linking mitochondrial bioenergetics to insulin resistance via redox biology. *Trends Endocrinol. Metab.* 23, 142–153. doi: 10.1016/j.tem.2011.12.008

Fryer, L. G. D., Orfali, K. A., Holness, M. J., Saggerson, E. D., and Sugden, M. C. (1995). The long-term regulation of skeletal muscle pyruvate dehydrogenase kinase by dietary lipid is dependent on fatty acid composition. *Eur. J. Biochem.* 229, 741–748. doi: 10.1111/j.1432-1033.1995.tb20522.x

Gonzalez-Periz, A., Horrillo, R., Ferre, N., Gronert, K., Dong, B., Morán-Salvador, E., et al. (2009). Obesity-induced insulin resistance and hepatic steatosis are alleviated by omega-3 fatty acids: a role for resolvins and protectins. *FASEB J.* 23, 1946–1957. doi: 10.1096/fj.08-125674

Herbst, E. A. F., Paglialunga, S., Gerling, C., Whitfield, J., Mukai, K., Chabowski, A., et al. (2014). Omega-3 supplementation alters mitochondrial membrane composition and respiration kinetics in human skeletal muscle. *J. Physiol.* 592, 1341–1352. doi: 10.1113/jphysiol.2013.267336

Hernández-Alvarez, M. I., Thabit, H., Burns, N., Shah, S., Brema, I., Hatunic, M., et al. (2010). Subjects with early-onset type 2 diabetes show defective activation of the skeletal muscle PGC-1{alpha}/Mitofusin-2 regulatory pathway in response to physical activity. *Diabetes Care* 33, 645–651. doi: 10.2337/dc09-1305

Hoeks, J., van Herpen, N. A., Mensink, M., Moonen-Kornips, E., van Beurden, D., Hesselink, M. K., et al. (2010). Prolonged fasting identifies skeletal muscle mitochondrial dysfunction as consequence rather than cause of human insulin resistance. *Diabetes* 59, 2117–2125. doi: 10.2337/db10-0519

Hoeks, J., Wilde, J. D., Hulshof, M. F., Berg, S. A., Schaart, G., Dijk, K. W., et al. (2011). High fat diet-induced changes in mouse muscle mitochondrial phospholipids do not impair mitochondrial respiration despite insulin resistance. *PLoS ONE* 6:e27274. doi: 10.1371/journal.pone.0027274

Holloszy, J. O. (2013). "Deficiency" of mitochondria in muscle does not cause insulin resistance. *Diabetes* 62, 1036–1040. doi: 10.2337/db12-1107

Holzer, R. G., Park, E. J., Li, N., Tran, H., Chen, M., Choi, C., et al. (2011). Saturated fatty acids induce c-Src clustering within membrane subdomains, leading to JNK activation. *Cell* 147, 173–184. doi: 10.1016/j.cell.2011.08.034

Jheng, H. F., Tsai, P. J., Guo, S. M., Kuo, L. H., Chang, C. S., Su, I. J., et al. (2012). Mitochondrial fission contributes to mitochondrial dysfunction and insulin resistance in skeletal muscle. *Mol. Cell. Biol.* 32, 309–319. doi: 10.1128/MCB.05603-11

Kalupahana, N. S., Claycombe, K. J., and Moustaid-Moussa, N. (2011). (n-3) Fatty acids alleviate adipose tissue inflammation and insulin resistance: mechanistic insights. *Adv. Nutr.* 2, 304–316. doi: 10.3945/an.111.000505

Kalupahana, N. S., Claycombe, K., Newman, S., Stewart, T., Siriwardhana, N., Matthan, N., et al. (2010). Eicosapentaenoic acid prevents and reverses insulin resistance in high-fat diet-induced obese mice via modulation of adipose tissue inflammation. *J. Nutr.* 140, 1915–1922. doi: 10.3945/jn.110.125732

Kelley, D. E., Goodpaster, B., Wing, R. R., and Simoneau, J. A. (1999). Skeletal muscle fatty acid metabolism in association with insulin resistance, obesity and weight loss. *Am. J. Physiol.* 277, E1130–E1141.

Kelley, D. E., He, J., Menshikova, E. V., and Ritov, V. B. (2002). Dysfunction of mitochondria in human skeletal muscle in type 2 diabetes. *Diabetes* 51, 2944–2950. doi: 10.2337/diabetes.51.10.2944

Lanza, I. R., Blachnio-Zabielska, A., Johson, M. L., Schimke, J. M., Jakaitis, D. R., Lebrasseur, N. K., et al. (2013). Influence of fish oil on skeletal muscle mitochondrial energetics and lipid metabolites during high-fat diet. *Am. J. Physiol. Endocrinol. Metab.* 304, E1391–E1403. doi: 10.1152/ajpendo.00584.2012

Lark, D. S., Fisher-Wellman, K. H., and Neufer, P. D. (2012). High-fat load: mechanism(s) of insulin resistance in skeletal muscle. *Int. J. Obes.* 2, S31–S36. doi: 10.1038/ijosup.2012.20

Lefort, N., Glancy, B., Bowen, B., Willis, W. T., Bailowitz, Z., De Filippis, E. A., et al. (2010). Increased reactive oxygen species production and lower abundance of complex I subunits and carnitine palmitoyltransferase 1B protein despite normal mitochondrial respiration in insulin-resistant human skeletal muscle. *Diabetes* 59, 2444–2452. doi: 10.2337/db10-0174

Liesa, M., Palacín, M., and Zorzano, A. (2009). Mitochondrial dynamics in mammalian health and disease. *Physiol. Rev.* 89, 799–845. doi: 10.1152/physrev.00030.2008

Liesa, M., and Shirihai, O. S. (2013). Mitochondrial dynamics in the regulation of nutrient utilization and energy expenditure. *Cell Metab.* 17, 491–506. doi: 10.1016/j.cmet.2013.03.002

Lionetti, L., Mollica, M. P., Crescenzo, R., D'Andrea, E., Ferraro, M., Bianco, F., et al. (2007). Skeletal muscle subsarcolemmal mitochondrial dysfunction in high-fat fed rats exhibiting impaired glucose homeostasis. *Int. J. Obes.* 31, 1596–1604. doi: 10.1038/sj.ijo.0803636

Lionetti, L., Mollica, M. P., Donizzetti, I., Gifuni, G., Sica, R., Pignalosa, A., et al. (2014a). High-lard and high-fish-oil diets differ in their effects on function and dynamic behavior of rat hepatic mitochondria. *PLoS ONE* 9:e92753. doi: 10.1371/journal.pone.0092753

Lionetti, L., Mollica, M. P., Lombardi, A., Cavaliere, G., Gifuni, G., and Barletta, A. (2009). From chronic overnutrition to insulin resistance: the role of fat-storing capacity and inflammation. *Nutr. Metab. Cardiovasc. Dis.* 19, 146–152. doi: 10.1016/j.numecd.2008.10.010

Lionetti, L., Mollica, M. P., Sica, R., Donizzetti, I., Gifuni, G., and Pignalosa, A. (2014b). Differential effects of high-fish oil and high-lard diets on cells and cytokines involved in the inflammatory process in rat insulin-sensitive tissues. *Int. J. Mol. Sci.* 15, 3040–3063. doi: 10.3390/ijms15023040

Lionetti, L., Sica, R., Mollica, M. P., and Putti, R. (2013). High-lard and high-fish oil diets differ in their effects on insulin resistance development, mitochondrial morphology and dynamic behavior in rat skeletal muscle. *Food Nutr. Sci.* 4, 105–112. doi: 10.4236/fns.2013.49A1017

Liu, R., Jin, P., Yu, L., Wang, Y., Han, L., Shi, T., et al. (2014). Impaired mitochondrial dynamics and bioenergetics in diabetic skeletal muscle. *PLoS ONE* 9:e92810. doi: 10.1371/journal.pone.0092810

Lowell, B. B., and Shulman, G. I. (2005). Mitochondrial dysfunction and type 2 diabetes. *Science* 307, 384–387. doi: 10.1126/science.1104343

Mogensen, M., Sahlin, K., Fernström, M., Glintborg, D., Vind, B. F., Beck-Nielsen, H., et al. (2007). Mitochondrial respiration is decreased in skeletal muscle of patients with type 2 diabetes. *Diabetes* 56, 1592–1599. doi: 10.2337/db06-0981

Mollica, M. P., Lionetti, L., Crescenzo, R., D'Andrea, E., Ferraro, M., Liverini, G., et al. (2006). Heterogeneous bioenergetic behavior of subsarcolemmal and intermyofibrillar mitochondria in fed and fasted rats. *Cell. Mol. Life Sci.* 63, 358–366. doi: 10.1007/s00018-005-5443-2

Mollica, M. P., Lionetti, L., Putti, R., Cavaliere, G., Gaita, M., and Barletta, A. (2011). From chronic overfeeding to hepatic injury: role of endoplasmic reticulum stress and inflammation. *Nutr. Metab. Cardiovasc. Dis.* 21, 222–230. doi: 10.1016/j.numecd.2010.10.012

Montgomery, M. K., and Turner, N. (2015). Mitochondrial dysfunction and insulin resistance: an update. *Endocr. Connect.* 4, R1–R15. doi: 10.1530/EC-14-0092

Morino, K., Petersen, K. F., Dufour, S., Befroy, D., Frattini, J., Shatzkes, N., et al. (2005). Reduced mitochondrial density and increased IRS-1 serine phosphorylation in muscle of insulin-resistant offspring of type 2 diabetic parents. *J. Clin. Invest.* 115, 3587–3593. doi: 10.1172/JCI25151

Muoio, D. M. (2010). Intramuscolar triacylglycerol and insulin resistance: guilty as charged or wrongly accused? *Biochim. Biophys. Acta* 1801, 281–288. doi: 10.1016/j.bbalip.2009.11.007

Muoio, D. M., and Neufer, P. D. (2012). Lipid-induced mitochondrial stress and insulin resistance. *Cell Met*. 15, 595–605. doi: 10.1016/j.cmet.2012.04.010

Nunnari, J., Wong, E. D., Meeusen, S., and Wagner, J. A. (2002). Studying the behavior of mitochondria. *Methods Enzymol*. 351, 381–393. doi: 10.1016/S0076-6879(02)51859-0

Ozcan, U., Cao, Q., Yilmaz, E., Lee, A. H., Iwakoshi, N. N., Ozdelen, E., et al. (2004). Endoplasmic reticulum stress links obesity, insulin action, and type 2 diabetes. *Science* 306, 457–456. doi: 10.1126/science.1103160

Palmer, C. S., Osellame, L. D., Stojanovski, D., and Ryan, M. T. (2011). The regulation of mitochondrial morphology: intricate mechanisms and dynamic machinery. *Cell Sign*. 23, 1534–1545. doi: 10.1016/j.cellsig.2011.05.021

Petersen, K. F., Dufour, S., Befroy, D., Garcia, R., and Shulman, G. I. (2004). Impaired mitochondrial activity in the insulin-resistant offspring of patients with type 2 diabetes. *N. Engl. J. Med*. 350, 664–671. doi: 10.1056/NEJMoa031314

Petersen, K. F., Dufour, S., and Shulman, G. I. (2005). Decreased insulin-stimulated ATP synthesis and phosphate transport in muscle of insulin-resistant offspring of type 2 diabetic parents. *PLoS Med*. 2:e233. doi: 10.1371/journal.pmed.0020233

Putti, R., Sica, R., Migliaccio, V., and Lionetti, L. (2015). Diet impact on mitochondrial bioenergetics and dynamics. *Front Physiol*. 6:109. doi: 10.3389/fphys.2015.00109

Quirós, P. M., Ramsay, A. J., Sala, D., Fernández-Vizarra, E., Rodríguez, F., Peinado, J. R., et al. (2012). Loss of mitochondrial protease OMA1 alters processing of the GTPase OPA1 and causes obesity and defective thermogenesis in mice. *EMBO J*. 31, 2117–2133. doi: 10.1038/emboj.2012.70

Ritov, V. B., Menshikova, E. V., He, J., Ferrell, R. E., Goodpaster, B. H., and Kelley, D. E. (2005). Deficiency of subsarcolemmal mitochondria in obesity and type 2 diabetes. *Diabetes* 54, 8–14. doi: 10.2337/diabetes.54.1.8

Schneeberger, M., Dietrich, M. O., Sebástian, D., Imbernón, M., Castaño, C., Garcia, A., et al. (2013). Mitofusin 2 in POMC neurons connects ER stress with leptin resistance and energy imbalance. *Cell* 155, 172–187. doi: 10.1016/j.cell.2013.09.003

Shenk, S., Saberi, M., and Olefsky, J. M. (2008). Insulin sensitiivyt: modulation by nutrients and inflammation. *J. Clin. Invest*. 118, 2992–3002. doi: 10.1172/JCI34260

Shi, H., Kokoeva, M. V., Inouye, K., Tzameli, I., Yin, H., and Flier, J. S. (2006). TLR4 links innate immunity and fatty acid-induced insulin resistance. *J. Clin. Invest*. 116, 3015–3025. doi: 10.1172/JCI28898

Sparks, L. M., Xie, H., Koza, R. A., Mynatt, R., Hulver, M. W., Bray, G. A., et al. (2005). A high-fat diet coordinately downregulates genes required for mitochondrial oxidative phosphorylation in skeletal muscle. *Diabetes* 54, 1926–1933. doi: 10.2337/diabetes.54.7.1926

Storlien, L. H., Jenkins, A. B., Chisholm, D. J., Pascoe, W. S., Khouri, S., and Kraegen, E. W. (1991). Influence of dietary fat composition on development of insulin resistance in rats: relationship to muscle triglyceride and ω-3 fatty acids in muscle phospholipid. *Diabetes* 40, 280–289. doi: 10.2337/diab.40.2.280

Storlien, L. H., Kraegen, E. W., Chisholm, D. J., Ford, G. L., Bruce, D. G., and Pascoe, W. S. (1987).Fish oil prevents insulin resistance induced by high-fat feeding in rats. *Science* 237, 885–888. doi: 10.1126/science.3303333

Stulnig, T. M., Huber, J., Leitinger, N., Imre, E. M., Angelisova, P., Nowotny, P., et al. (2001). Polyunsaturated eicosapentaenoic acid displaces proteins from membrane rafts by altering raft lipid composition. *J. Biol. Chem*. 276, 37335–37340. doi: 10.1074/jbc.M106193200

Uysal, K. T., Wiesbrock, S. M., Marino, M. W., and Hotamisligil, G. S. (1997). Protection from obesity-induced insulin resistance in mice lacking TNF-alpha function. *Nature* 389, 610–614. doi: 10.1038/39335

Vendelin, M., Beraud, N., Guerrero, K., Andrienko, T., Kuznetsov, A. V., Olivares, J., et al. (2005). Mitochondrial regular arrangement in muscle cells: a "crystal-like" pattern. *Am. J. Physiol. Cell Physiol*. 288, C757–C767. doi: 10.1152/ajpcell.00281.2004

Walder, K., Kerr-Bayles, L., Civitarese, A., Jowett, J., Curran, J., Elliott, K., et al. (2005). The mitochondrial rhomboid protease PSARL is a new candidate gene for type 2 diabetes. *Diabetologia* 48, 459–468. doi: 10.1007/s00125-005-1675-9

Westermann, B. (2010). Mitochondrial fusion and fission in cell life and death. *Nat. Rev. Mol. Cell Biol*. 11, 872–884. doi: 10.1038/nrm3013

Westermann, B. (2012). Bioenergetic role of mitochondrial fusion and fission. *Biochim. Biophys. Acta* 1817, 1833–1838. doi: 10.1016/j.bbabio.2012.02.033

Xin, Y. N., Xuan, S. Y., Zhang, J. H., Zheng, M. H., and Guan, H. S. (2008). Omega-3 polyunsaturated fatty acids: a specific liver drug for non-alcoholic fatty liver disease (NAFLD). *Med. Hypotheses*. 71, 820–821. doi: 10.1016/j.mehy.2008.07.008

Yaspelkis, B. B. III, Kvasha, I. A., and Figuero, T. Y. (2009). High-fat feeding increases insulin receptor and IRS-1 coimmunoprecipitation with SOCS-3, Ikkα/B phos- phorylation and decreases PI-3 kinase activity in muscle. *Am. J. Physiol. Regul. Integr. Comp. Physiol*. 296, R1709–R1715. doi: 10.1152/ajpregu.00117.2009

Yu, C., Chen, Y., Cline, G. W., Zhang, D., Zong, H., Wang, Y., et al. (2002). Mechanism by which fatty acids inhibit insulin activation of insulin receptor substrate-1 (IRS-1)-associated phosphatidylinositol 3-kinase activity in muscle. *J. Biol. Chem*. 277, 50230–50236. doi: 10.1074/jbc.M200958200

Yu, T., Robotham, J. L., and Yoon, Y. (2006). Increased production of reactive oxygen species in hyperglycemic conditions requires dynamic change of mitochondrial morphology. *Proc. Natl. Acad. Sci. U.S.A*. 103, 2653–2658. doi: 10.1073/pnas.0511154103

Yuzefovych, L. V., Musiyenko, S. I., Wilson, G. L., and Rachek, L. I. (2013). Mitochondrial DNA damage and dysfunction, and oxidative stress are associated with endoplasmic reticulum stress, protein degradation and apoptosis in high fat diet-induced insulin resistance mice. *PLoS ONE* 8:e54059. doi: 10.1371/journal.pone.0054059

Zhang, Y., Jiang, L., Hu, W., Zheng, Q., and Xiang, W. (2011). Mitochondrial dysfunction during *in vitro* hepatocyte steatosis is reversed by omega-3 fatty acid-induced up-regulation of mitofusin 2. *Metabolism* 60, 767–775. doi: 10.1016/j.metabol.2010.07.026

Zorzano, A., Hernández-Alvarez, M. I., Palacín, M., and Mingrone, G. (2010). Alterations in the mitochondrial regulatory pathways constituted by the nuclear co-factors PGC-1alpha or PGC-1beta and mitofusin 2 in skeletal muscle in type 2 diabetes. *Biochim. Biophys. Acta* 1797, 1028–1033. doi: 10.1016/j.bbabio.2010.02.017

Zorzano, A., Liesa, M., and Palacín, M. (2009a). Mitochondrial dynamics as a bridge between mitochondrial dysfunction and insulin resistance. *Arch. Physiol. Biochem*. 115, 1–12. doi: 10.1080/13813450802676335

Zorzano, A., Liesa, M., and Palacin, M. (2009b). Role of mitochondrial dynamics proteins in the pathophysiology of obesity and type 2 diabetes. *Int. J. Biochem. Cell. Biol*. 41, 1846–1854. doi: 10.1016/j.biocel.2009.02.004

Conflict of Interest Statement: The authors declare that the research was conducted in the absence of any commercial or financial relationships that could be construed as a potential conflict of interest.